STUDY THE POTENTIAL OF SOLAR, WIND AND MICRO-HYDRO POWER FOR RURAL ELECTRIFICATION:

A CASE OF MAGNA LEGE BUNA VILLAGE

By

Nuri Jemal Aman

A Thesis Submitted to the Department of Thermal and Aerospace Engineering

School of Mechanical, Chemical & Materials Engineering

Office of Graduate Studies

Adama Science and Technology University

February 2021

Adama, Ethiopia

Study the Potential of Solar, Wind and Micro-Hydro Power for Rural Ectrification-:

A Case of Magna Lege Buna Village

By

Nuri Jemal Aman

Advisor: Dr. Addisu Bekele

A Thesis Submitted to the Department of Thermal and Aerospace Engineering

School of Mechanical, Chemical and Materials Engineering

Office of Graduate Studies

Adama Science and Technology University

February 2021

Adama, Ethiopia

DECLARATION

I hereby declare that this M.Sc. thesis entitled "STUDY THE POTENTIAL OF SOLAR, WIND AND MICRO-HYDRO POWER FOR RURAL ELECTRIFICATION-: A CASE OF MAGNA LEGE BUNA VILLAGE" in partial fulfillment of the requirements for the award degree of Master of Sciences in Thermal Engineering is an authentic record of my work under the supervision of Dr. Addisu Bekele, Associate Professor of Thermal Engineering, Adama Science and Technology University.

The matter embedded in this thesis has not been submitted for the award of a degree or diploma in any other university. All relevant resource information used in this paper has been duly acknowledged.

Nuri Jemal Aman____	__________________	_____________
Candidate	Signature	Date

This is to certify that the above statement made by the candidate is correct to the best of my knowledge and belief. This thesis has been submitted for examination with my approval.

_____Dr. Addisu Bekele____	__________________	______________
Advisor	Signature	Date

APPROVAL OF BOARD OF EXAMINERS

We, undersigned, members of the board of examiners of the final open defense by **Nuri Jemal Aman** have read and evaluated his thesis entitled **"Study the Potential of Solar, Wind and Micro-Hydro Power for Rural Ectrification-: A Case of Magna Lege Buna Village"** and examined the candidate. This is, therefore, to certify that the thesis has been accepted in partial fulfillment of the degree of Master of Science in Thermal Engineering

____________________	____________	____________
Name of student	Signature	Date
____________________	____________	____________
Advisor	Signature	Date
____________________	____________	____________
External Examiner	Signature	Date
____________________	____________	____________
Internal Examiner	Signature	Date
____________________	____________	____________
Chair Person	Signature	Date
____________________	____________	____________
Studies Head of Department	Signature	Date
____________________	____________	____________
School Dean	Signature	Date
____________________	____________	____________
Post Graduate Dean	Signature	Date

ACKNOWLEDGEMENTS

First and foremost, I take this opportunity to give glory to the almighty God without whom the completion of this work would have been impossible. Next, my deepest heartfelt gratitude goes to my advisor Dr. Addisu Bekele for his generosity and kindness throughout my thesis work. The thesis would not have been accomplished without his readiness to help, constructive comments, and very valuable suggestions. He has been a constant source of inspiration throughout my study period.

Again I would like to thank Dr. Dawit Gudeta and Dr. Gezahegn Habtamu for sharing their academic experience, knowledge, and guidance during my Master's study as well as during my thesis work. I would like to appreciate all staff of the Thermal and Aerospace Engineering department, and administrative workers of the faculty for support and cooperation during this thesis.

Last but not least, my special thanks to my family, colleagues, friends especially Abdul Kerim Aman, and my brothers (Temam) and my aunt who helped me in numerous ways to make this thesis a success.

ABSTRACT

Ethiopia is a country with highly increasing population numbers from day to day and the current population number is around 110 million people. From this total population, about 85% are living in rural remote areas, where there are no accesses to the central grid system or not covered by grid extension to date. Until today only About 2% of these areas are accessible to electricity. Specifically, as other Ethiopians, people of Magna Lege Buna village with site's location is 7° 58' 28" N latitude and 39° 40' 36" E longitudes uses nonrenewable energy for every daily activity (cooking, milling, lighting, etc.) even though this village is rich with many rivers and high solar intensity and wind forces that can produce a huge amount of energy.

The work was begun by visiting the site, collecting data and analyzing those data with the help of HOMER software, sizing of different components, investigating the power-producing potential of solar, wind, and micro-hydro turbine of the desired site, energy demand of the village, finding feasible and suitable hybridization for electrification of the site under study. The annual average potential of solar energy of the site is 6.3 k$kWh/m^2/day$, average wind speed at the required hub height of 50m is 5.46 m/s and unganged run off of river has a flow rate 0.21 m^3/s and net head height of 13.99 m. For energy yield estimation, a three-bladed wind turbine of 800kW rated power with a rotor diameter of 48m from Enercon, 335W rating power of solar panel with 21% efficiencies of mono crystalline from sun power and Cross flow of 20 kW shaft output and the turbine will be coupled with a three phases synchronous generator to produce electrical energy about 17.32 kW was chosen..

The overall simulation results indicate that the proposed off-grid hybrid system of solar, wind, and micro-hydro with battery storage would be a feasible solution for electric power generation of a remote village with 740 households with an average of six family members per household and another community service such as the clinic, school, mosque, churches, mill flour, and water pump. The electricity, produced from these hybrid systems will replace conventional energy sources like wood, animal dung and kerosene.

Key words: Renewable enegy potential; Hybridization; Primary and defferable load; Run of river; HOMER; Optimization and Simulation.

TABLE OF CONTENTS

CONTENTS PAGE

LIST OF FIGURE

LIST OF TABLE

ACRONYMS AND ABBREVIATIONS

PV	Photovoltaic
MHP	Micro-hydropower
H	Head in meters (m)
Q	Flow rate in meter cube per second (m^3/s)
HOMER	Hybrid optimization model for Renewable Energy
GPS	Global Position surface
NASA	National Aeronautics and Space Administration
EEP	Ethiopia Electric Power
MoWIE	Ministry of Water, Irrigation, and Energy
EPCO	Ethiopian Electric Power Corporation
A	Cross-sectional Area
AC	alternating current
DC	Direct Current
MHS	Micro-hydropower system
STC	Standard test condition
P_{peak}	peak power of the PV array under Standard test condition (kW)
SHP	Small hydropower
I_{STC}	incident solar radiation under Standard test condition (kW/m^2)
η_{PV}	The efficiency of the PV array (decimal)
A_{array}	Area of the PV array (m^2)
P_W	Wind speed extracted power
P_t	Wind turbine extracted power
$I_{d\beta}$	Hourly diffused radiation on the tilted surface

$I_{b\beta}$	Hourly beam radiation on the tilted surface
H	Monthly Average daily global solar radiation on horizontal Surface
Ho	Average daily extraterrestrial solar radiation on horizontal Surface
HAWT	Horizontal Axis Wind Turbine
VAWT	Vertical Axis Wind Turbine
WMO	World Meteorological Organization
CFL	Compact Fluorescent Lamp
DOD	Depth of discharge
NMSA	National Metrological Service Agency
AMS	Adama meteorological station
D	Rotor Diameter
Gsc	Solar constant with a value of 1367 (W/m^2)
NPC	Net Present Cost
UEAP	Universal Electricity Access Program
f_{pv}	derating factor [%]
GT	Solar radiation incident on the PV array in the current time step
$\bar{G}$	Incident radiation at standard test conditions (kW/m^2)
G	Solar radiation striking the PV array (kW/m^2)
SOC	State of charge

CHAPTER ONE

INTRODUCTION

1.1 Background of the Study

Ethiopia is among the least developed countries on the globe with total access to electricity not exceeding 16%. This means that about 85% of the population lives in places where access to electricity is less than 2%. One such place, which is the subject of this study, is the Arsi, Chole district having a total population of 111,831 within 20 villages (CSA 2005 National statics archived). About 17 villages (corresponding to 92,000 people) which make the task of their electrification nonrenewable energy systems such as Kerosene for lighting, diesel for milling and pumping, biomass for cooking, and dry cells for radio are being used in the non-electrified villages. Nothing has been done so far in developing renewable energy resources, such as small-scale hydro, solar, and wind energy in these districts.

Reliable access to electricity is a basic precondition for improving people's lives in rural areas, for enhanced healthcare, education, and growth within local economies. At present, more than 80% of people in Ethiopia do not have access to electricity in their homes. Almost all of these people live in rural areas; most have scant prospects of gaining access to electricity soon. The Ethiopian Government has tried to connect this rural location by using the national grid extension for the last two decades. However, still, the current electricity access is below 50% and the real connection is less than 14%. In this scenario, the rural people who have very low load demand with the dispersed settlement will not get electricity soon. Off-grid electricity is currently used for lighting, charging mobile phones, and the provision of electric power to rural health centers, schools, and water pumping systems, among other uses, and has seen remarkable growth in the past five years (Hilawe *et al.*, 2017). With efficient, reliable and cost-effective renewable energy resources, off-grid supply can be used as an alternative to the power supplied by a diesel generator for rural electrification. However, due to the intermittency nature of renewable resources, the use of any particular renewable energy resource-based system may lead to component over-sizing and unnecessary operational and lifecycle costs. Such limitations can be overcome by combining one or more renewable energy resources in a form of a hybrid system. Hybrid systems improve load factors and save maintenance and replacement costs, as the renewable resource components complement each other.

For an optimal combination of different renewables, various types of hybrid systems and methods of techno-economic analysis are used. Excel-based, linear programming, artificial intelligence LINGO and HOMER are the most commonly used methods of hybrid system optimization techniques (Girma, 2016).

1.2 Problem of the Statement.

Even though Ethiopia has several renewable energy sources such as solar, wind, hydro and biomass energy, until today many Ethiopian people especially those living in the rural area are not electrified. However, Reliable access to electricity is a basic precondition for improving people's living in rural and urban areas, for enhanced health care and education and growth within local economies. Specifically, peoples in Arsi zone, Chole Woreda, Magna Lege Buna village are using non-renewable energy sources such as kerosene, firewood, cow dung, and petroleum fuels for lighting, cooking, crop milling, cell phone charging, etc., which have the problem of daily increasing in price and negative environmental effect because of deforestation, carbon monoxide emission (pollution) and soil erosion.

This is the reason why most of the people in Magna Lege Buna village are looking after the government supports for the problem of food shortage and other social services. However, if these communities are supplied with modern electricity from renewable energy resources that available freely around them, their life will be improved and the environment will be protected from damage and this is the basic idea of this thesis. Rural households not only have limited access to modern energy sources at reasonable rates but also incur high expenditure on traditional fuel sources, which exacerbates their lack of affordability concerning household fuels. The village understudy is 95km far away from extended grid; so further grid extension is not advantageous for electrifying that village and the only solution at moment is using renewable energy resources.

1.3 Objective of the Study

1.3.1 General Objective

The general objective of this research is to study the hybrid renewable energy potential to fulfill the energy demand of Magna Lege Buna village.

1.3.2 Specific Objective of the Paper

The specific objective of this thesis is:

- ✓ Accessing the electricity demand of Magna Lege Buna village
- ✓ Accessing the availability and potential of renewable energy resources
- ✓ Studying a possible hybrid system for the potential of renewable energy sources to fulfill the energy demand of the village
- ✓ Performing a comparative study between the available energy system and designing a system by using a tool (HOMER)

1.4 Significances of the Study

The significance of this thesis is basically to solve the problem of peoples who are living in a rural remote area that is no access to electricity supply until today to get more reliable and clean energy for household needs such as primarily lightning, Radio, mobile charging, TV and another service load in better quality. Specifically, to solve the problem of Magna Lege Buna village community who directly utilize nonrenewable energy for their daily life activities. From this study, the rural area of Chole Woreda of Magna Lege Buna village will be electrified and the living standard of the community may change. The problem such as deforestation, soil erosion, and air pollution will be reduced. Finally, the living standard of each household may shift from a traditional electric system (kerosene for lighting) to a modified lighting system such as using solar and wind energy. It also serves as a design input or design option for both governmental and non-governmental organization which is working on rural electrification where the resource is available.

1.5 Scope and Limitation

1.5.1 Scope of the Study

The scope of this study is to know the potential of renewable energy such as solar, wind, and micro-hydropower and the demand for electricity for the selected sample site village and to undergo the comparative study between different renewable energy sources especially solar, hydro, and wind energy. During the study of solar, wind, and micro-hydro power for rural electrification different tasks such as collecting and analyzing relevant data and information to examine the power generating capacity of each renewable energy source necessary measures that configure a system to accommodate the current and near-future electrical energy demand for the village.

1.5.2 Limitation of the Study

Reaching electrical energy for final utilization may require the knowledge of three departments (mechanical, electoral, and surveyor engineering). Besides this, it also may need about finial analysis for the total investment of the project. During performing on this thesis, there is no deep analysis of the civil structure and some of the electrical components because there is no deep knowledge of those sub-specialized departments. Besides this there is no measured daily or monthly water flow rate of the river understudy to perform analysis on power-producing potential of the river throughout the year. In this case; obviously, there is a limitation on this thesis for final utilization of energy

1.6 Research Question

The output of this study is going to answer the following questions

- What is the energy demand of the community of that Village?
- What is the availability RE and does these energy sources fulfill the demand for energy for the village?
- What is the power generating capacity and efficiency of each RE sources in the selected village?
- What is the appropriate system design that can meet the power/energy demand of that Village?
- what is your suggestion of energy load is suitable (single off-grid or integrated energy system)?

CHAPTER TWO

LITERATURE REVIEW

2.1 Introduction about Renewable Energy Resources

2.1.1 Hydropower Generation Principles

Hydro Power generation from water depends upon a combination of head and flow. Both must be available to produce electricity. Water is diverted from a stream into a pipeline, where it is directed downhill and through the turbine (flow). The vertical drop (head) creates pressure at the bottom end of the pipeline. The pressurized water emerging from the end of the pipe creates the force that drives the turbine. The turbine turns the generator rotor which then converts this mechanical energy into electrical energy as the turbine shaft rotates the generator. Electrical power output will always be slightly less than waterpower input due to turbine and system inefficiencies. Water pressure or Head created by the difference in elevation between the water intake and the turbine. Head can be expressed as vertical distance (feet or meters), or as pressure, such as pounds per square inch (psi). Net head is the pressure available at the turbine when water is flowing, which will always be less than the pressure when the water flow is turned off (static head), due to the friction between the water and the pipe. Pipeline diameter also affects the net head. Flow is the quantity of water available and is expressed as 'volume per unit of time', such as gallons per minute (g/m), cubic meters per second (m^3/s), or liters per second (l/s). Power generation from water depends upon a combination of head and flow. In nature, energy cannot be created or destroyed, but its form can change. In generating electricity, no new energy is created. One form of energy is converted to another form of energy, which means the potential energy of flowing water is converted into kinetic energy as it travels through the penstock from the upper level to the lower level of the ground.

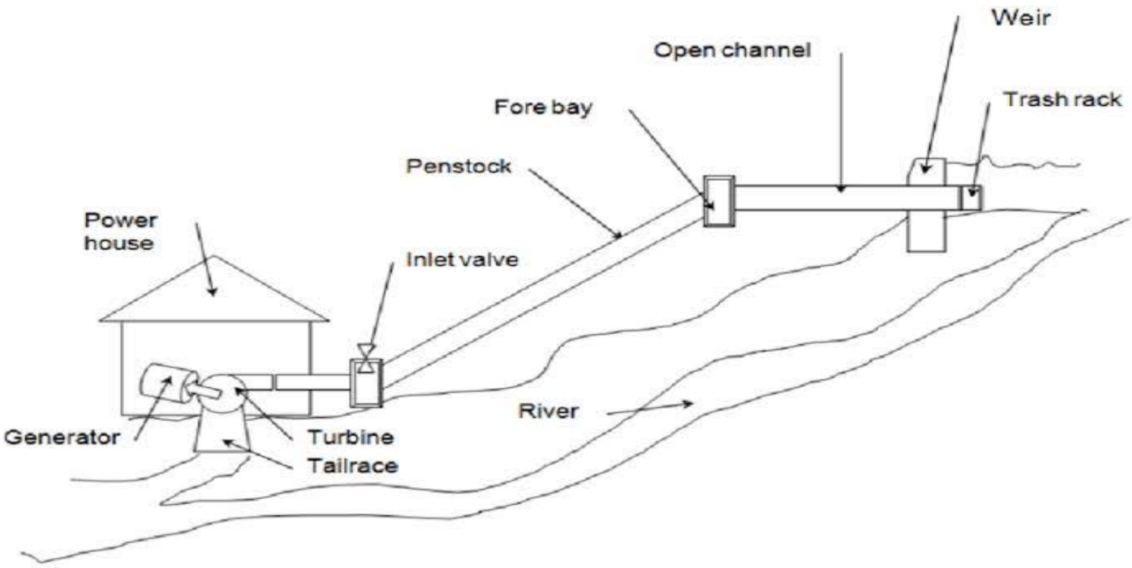

Figure 2. 1 Schematic diagram of micro-hydro-electric power plant (Nasir, 2013)

2.1.2 Classification of Hydropower Plant

Hydropower Plants can be classified based on the type of Operational feature, by demand of Electrical power, by installed capacity, available head at the inlet, discharge through the vanes, and specific speed.

a) ***Classification of Hydropower by Operational Feature***

In studying the subject of hydropower engineering, it is important to understand the different types of Hydropower plant development. The flowing classification system is used in this text:

- **Run-of-river developments**. A dam with a short penstock (supply pipe) directs the water to the turbines, using the natural flow of the river with very little alteration to the terrain stream channel at the site and little impoundment of the water.

- **Diversion and canal developments**. The water is diverted from the natural channel into s canal or a leg penstock, thus changing the flow of the water in the stream for a considerable distance.

- **Storage regulation developments**. An extensive impoundment at the power plant or reservoirs upstream of the power plant permits changing the flow of the river by storing water during high–flow periods to augment the water available during the low-flow periods, supplying the energy demand more efficiently. The word storage is used for long-time impounding of water to meet the seasonal fluctuation in water, availability, and the fluctuations in energy demand. While the word *bondage* refers to the short-time (daily) impounding of water to meet the short-time changes of energy demand (Eder *et al*. 2015).

 Pumped Storage Developments. Water is pumped from a lower reservoir to a higher reservoir using inexpensive dump power during periods of low energy demand. The water is then run down through the turbines to produce power to meet peak demand (Eder *et al.* 2015).

b) Classification of hydropower by installed capacity

Classification of hydropower according to installed capacity is different from different scholars. However, here with the most common classification source hydropower engineering lecture notes in AAIT (Bhattarai, 2005).

a) **Large Conventional Hydropower plants:** although no official definition exists for the capacity range of large hydroelectric power stations, facilities from over a few hundred megawatts to more than 10GW are generally considered large hydroelectric facilities.

b) **Small Conventional Hydropower plants**: - the definition of a small-hydro project varies but a generating capacity of up to 10MW is generally accepted as the upper limit of what can be termed small-hydro. This may be stretched to 25 MW and 30MW in Canada and the United State

Micro-hydro: Micro-hydro is a term used for hydroelectric power installations that typically produce up to 100KW of power.

Pico: - hydro is a term used for hydroelectric power generation of under 5KW. It is useful in small, remote communities that require only a small amount of electricity for example, to power one or two fluorescent bulbs and TV or radio for a few homes.

Table 2. 1 Hydropower plant classification by installed capacity (ESHA, 2004).

S/N	Types of plant	Installed capacity	Consumer
1	Pico hydro	Less than 5KW	Mostly single households
2	Micro-hydro	5KW-100KW	Usually provided power for a small community or rural industry in remote areas far away from the grid
3	Mini-hydro	100KW - 1MW	Ether standalone schemes or more often feeding into the grid
4	Small-hydro	1MW - 15MW	Usually feeding into the grid
5	Medium-hydro	15MW - 100MW	Feeding grid
6	Large-hydro	More than 100MW	Feeding into the large electricity grid

2.1.3 Mini Hydro Power Plants in Ethiopia

The available potential of mini-scale hydropower in the country has hardly been exploited so far due to the government's focus on large-scale hydropower development to meet the energy demand of the country.

Table 2. 2 Mini hydropower plant in Ethiopia (Altinbilek, 2005).

Name & location	Head (m)	Type of scheme	Installed capacity (kW)	Commission year	Current status
Yadot,Bale zone	23	ROR	350	1991	Operational
Welga,weliso town	16	ROR	162	1965	Not Operational
Sotosomere ,jima town	30	ROR	147	1954	Not Operational
Hulka, Ambo town	40	ROR	150	1954	Not Operational
Deneba,Buno Bedele	14	ROR	123	1967	Not Operational
Gelemite,Dembi dollo	42	ROR	195	1966	Not Operational
Chemoge, Debre	55	ROR	195	1962	Not Operational

Markos					
Debre Berhan		ROR	130	1955	Not Operational
Jibo, Harar Zone		ROR	420		Not Operational
Total capacity			1872		
Operational			350		
Not operational			1522		

2.1.4 General Principle of Micro Hydro Power system (MHS)

Micro hydropower plants are designed to generate electrical or mechanical power based on the demand for energy of the surrounding locality. In a typical MHS (Micro-hydropower System) the water from the source is diverted by weir through an opening intake into a canal (Fox, 2004). A settling basin might sometimes be used to sediment the foreign particles from the water. The canal is designed along the contours of the landscape available to preserve the elevation of the diverted water. The water then enters the fore-bay tank and passes through the penstock pipes which are connected at a lower elevation level to the turbine. The turning shaft of the turbine is then used to operate and generate electricity (Simoes, 2004). This type of MHS (Micro-hydropower System) is designed to supply the load directly, as it does not use the battery as storage. This is the most common system that can be found in normal use and is most suitable for off-grid sites and remote standalone sites.

A micro-hydropower system is a small system in the range of 5-100 KW. The simplest micro-hydro power plant is based on a run-of-river design, which means it does not have water storage capability. It will produce power only when water is running or it might have relatively small water storage capability. Micro-hydropower is an interesting prospect for providing electricity for rural communities (Mahai, 2007).

2.1.5 Hydro Power Turbine Classification

Hydraulic head is a key site-specific factor affecting the turbine type selection, equipment, and construction costs of an MHP. It is noted that the suggested water head ranges are not rigid but are merely a means of categorizing sites. Hence, a set of representative reference models should have developed for different head ranges and corresponding turbine types:

- Low head (2-25m): axial flow (AF) Kaplan/propeller, cross-flow, Francis
- Medium head (25-70m): conventional Kaplan/propeller, Francis
- High head (>70 m): Francis, Turgo, Pelton

Table 2. 3 Classification of micro-hydro turbines based on head, flow rate, and power output (ESHA, 2004).

Classification	Turbine Name	Head Range (m)	Flow Range $\left(m^3/_s\right)$	Power output (kW)
Impulse	Pelton	50-1000	0.2-3	50-15000
	Turgo	30-200	0.2-5	20-5000
	Cross Flow	2-50	0.01-2	0.1-600
Reaction	Kaplan	3-40	3-20	50-5000
	Propeller	3-40	3-20	50-500
	Francis Radial Flow	40-200	1-20	500-15000
	Francis mixed Flow	10-40	0.7-10	100-5000

2.2 Solar Energy for Rural Electrification.

The sun is the ultimate energy sources of all alive on eatht and the sources of most renewable energy. Solar energy can be used to generate electricity directly with the use of photovoltaic modules. PV technology is now spreading into terrestrial applications ranging from powering remotes sites to feeding utility grids around the world.

Photovoltaic Cells: The solar cell is the elementary building block of photovoltaic technology. Solar cells are made of semiconductor materials, such as silicon. Several solar cells are electrically connected and mounted in a single support structure or frame is called a ‘photovoltaic module’. Modules are designed to supply electricity at a certain voltage, such as a common 12-volt system. Several modules can be wired together to form an array. Photovoltaic arrays produce direct-current electricity. They can be connected in both series and parallel electrical arrangements to produce any required voltage and current combination.

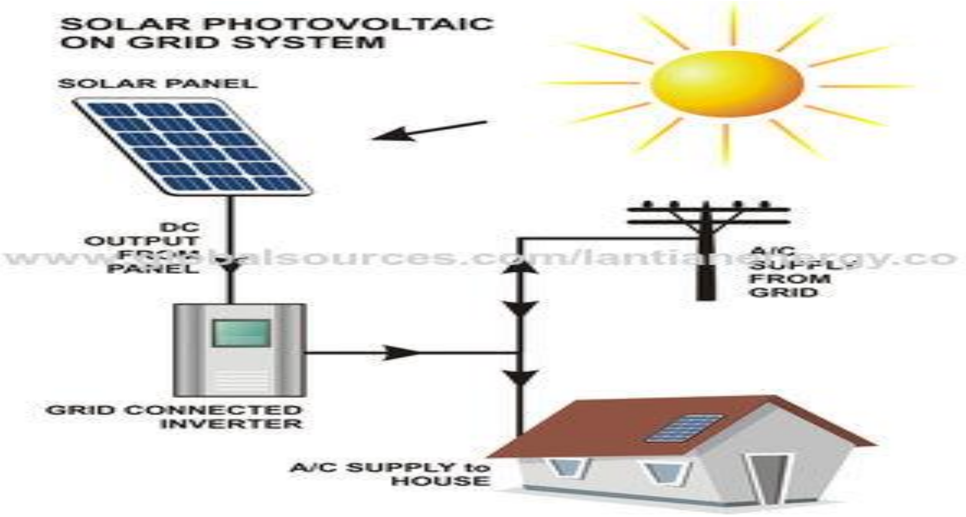

Figure 2. 2 Electric powers from solar energy (Kacira *et al.*,2004).

2.2.1 Components of Solar PV System

PV systems have the following main components that work together to produce electricity for electrification. Solar panel, battery, charge regulator, and inverter performing the different tasks as assigned by the manufacturer. System sizing for each of this components are discussed in the next chapter five of this thesis.

Solar panels to produce electricity solar panels are made from a semiconductor material that converts sunlight into electrical energy and the most common material used as a semiconductor during the solar cell manufacturing process is silicon. Even though the main function of the PV panel is to convert sunlight into electrical energy it does not convert all energy it receives into useful energy in steady it absorbed by the panel as heat. This may result in the increased working temperature of the panel which may consequently cause an efficiency drop of the PV panel system. Hence there is an efficiency drop of 0.5 percent due to an increase in operating temperature.

Type of PV panel

There are three main different types of solar panels available on the market based on the manufacturing process, appearance, cost, and installation process. Monocrystalline, Polycrystalline, and thin-film solar panel. Each type of PV panel has its unique advantage and disadvantage and the solar panel which best suited for installation is depend upon factory specification for the property and desired system characteristics.

a) **Mono-crystalline solar panels**

A solar panel with a black cell appearance is most likely a mono-crystalline panel. These cells appear black because of how light interacts with the pure silicon crystal. While the solar cells themselves are black, mono-crystalline solar panels have a variety of colors for their back sheets and frames.

b) **Poly-crystalline solar panel**s

Unlike mono-crystalline solar cells, poly-crystalline solar cells tend to have a bluish hue to them due to the light reflecting off the silicon fragments in the cell in a different way than it reflects off a pure monocrystalline silicon wafer. Similar to mono-crystalline, poly-crystalline panels have different colors for back sheets and frames. Most often, the frames of poly-crystalline panels are silver, and the back sheets are either silver or white.

c) **Thin-film solar panel**s

As their name suggests, thin-film panels are often slimmer than other panel types. This is because the cells within the panels are roughly 350 times thinner than the crystalline wafers used in mono-crystalline and poly-crystalline solar panels. There are adhesive thin-film solar panels that lie as-close-as-possible to the surface of a roof, but there are more durable thin-film panels that have frames up to 50 millimeters thick. As far as color goes, thin-film solar panels can come in both blue and black hues, depending on what they're made from. glass or stainless steel substrates. As the semiconductor layers are so thin, the costs of raw material are much lower than the capital equipment and processing costs.

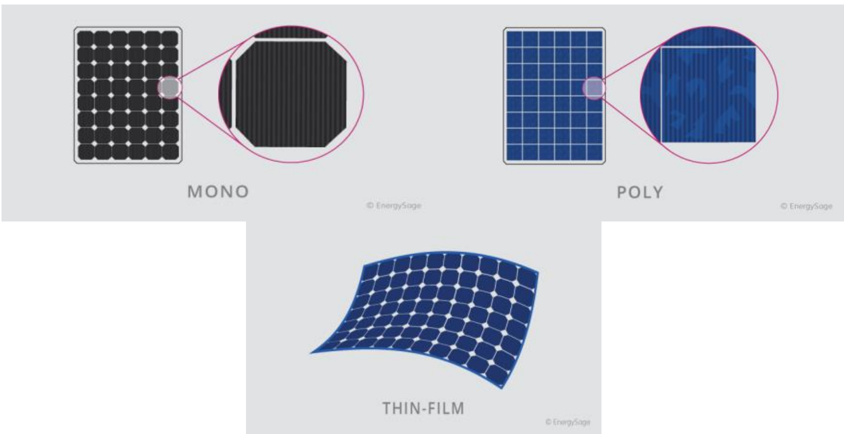

Figure 2. 3 Thin-film crystalline solar cell appearances (Becker *et al*., 2013).

Apart from aesthetic differences, the most obvious difference amongst PV cell technologies is in their conversion efficiency, as summarized in table 2.4. For example, a thin-film amorphous silicon PV array will need to close twice the space of a crystalline silicon PV array because its module efficiency is halved, for the same nominal capacity under Standard Test Conditions (STC) rating.

Table 2. 4 Efficiency of the solar cell (Becker *et al.*, 2013)

Type of PV module	**Module efficiency**
mono-crystalline	17-23%
Poly-crystalline	14-16 %
Thin-film –crystalline	12- 17 %

The above table 2.4 indicates the range of efficiency of different types of PV modules and Mon crystalline modules are the most efficient and thin-film crystalline is the least efficient while poly is in the mid-range of efficiency.

2.3 Introduction about Wind Speed Power Production

The wind is simple air in motion. It is caused by the uneven heating of the earth's surface by the sun. Since the earth's surface is made of very different types of land and water, it absorbs the sun's heat at different rates. During the day, the air above the land heats up more quickly than the air over water. The warm air over the land expands and rises, and the heavier, cooler air rushes in to take its place, creating winds. At night, the winds are reversed because the air cools more rapidly over land than over water. In the same way, the large atmospheric winds that circle the earth are created because the land near the earth's equator is heated more by the sun than the land near the North and South Poles.

Power has been extracted from the wind over hundreds of years with historic designs, known as Windmills, constructed from wood, cloth, and stone to pump water or grind corn. Historic designs, typically large, heavy, and inefficient, were replaced in the 19th century by fossil fuel engines and the implementation of a nationally distributed power network. A greater understanding of aerodynamics and advances in materials, particularly polymers, has led to the return of wind energy extraction in the latter half of the 20th century. Wind power devices are now used to produce electricity and are commonly termed wind turbines. Now a day wind power generation refers to the technology of converting the kinetic energy of moving air (wind) into electrical power through a wind turbine. The installation produces electricity by collecting and transforming wind power into rotational mechanical energy to derive the generating units.

2.3.1 Classification of Wind Turbine

Depending on the orientation of the shaft and position rotational axis of the wind, two distinctly different design configurations are available for a wind turbine, the horizontal axis configuration is known as horizontal axis wind turbine (HAWT) and the vertical axis configuration is known as vertical axis wind turbine (VAWT) correspondingly. A turbine with a shaft-mounted horizontally parallel to the ground is known as a horizontal axis wind turbine or (HAWT). A vertical axis wind turbine (VAWT) has its shaft normal to the ground. Among the two configurations, horizontal axis wind turbines are the most commercial applications in the wind energy world.

a) Horizontal Axis Wind turbine (HWAT)

The common wind turbine with a horizontal axis or Propeller Type is simple in principle, but the design of the complete system, especially a large one that will produce electric power economically, is complex. Not only must individual components, such as rotor, generator, tower, be as efficient as possible, but this component must function effectively in combination. This type of wind turbine currently dominates the wind turbine application.

Merits of Horizontal Axis wind Turbine

- Horizontal axis wind turbine has low cut-in wind speed and easy furling.
- Horizontal axis wind turbine has a relatively high-power coefficient than that of vertical axis wind turbine.
- The main benefit of HAWTs is the good aerodynamics efficiency and versatility of application.

The demerits of the Horizontal Axis wind Turbine

- Require the tailor yaw drive to orient the turbines towards wind direction.
- The Generator and gearbox of this type of wind turbine situated over the tower which makes its design more complex and expensive. This is the main disadva

b) Vertical Axis Wind Turbine (VAWT)

The axis of rotation of the vertical axis wind turbine (VAWT) is vertical to the ground contrasting the horizontal counterpart and almost perpendicular to the wind direction. These types of wind turbines have very low starting torque and this may be a critical issue for a certain application. The VAWT can take the wind from any direction. Hence complicated yaw devices can be disregarded. The vertical axis rotors have the great advantage of not having to be turned in to the wind stream as the wind direction changes because their operation is independent of wind direction, vertical axis machine is called anemones (from Greek words meaning "all wind") (Ahmad *et al.,* 2018). There are many advantages associated with the vertical axis wind turbine

Among those advantages, some of them are listed below

- Since its one-directional no need for a yaw mechanism
- Wind generator and gearbox can be placed at the ground
- Generator and gearbox installation and maintenance is simple since located at the ground

Even if the vertical axis wind turbines have an advantage which was listed above, it has also some disadvantages and listed below.

- Normally require a guy wire attached to the top for support.
- difficult to control the output power simply in high wind speed by changing the blade pitch this also plays a vital role for not to be more applicable to the world right now.
- Wind speeds are very low close to the ground level
- The machine is not self-starting since you may use the generator as a motor drawing current from the grid to start the machine).
- The overall efficiency of the vertical axis wind turbine machines is less than in the case of a horizontal.

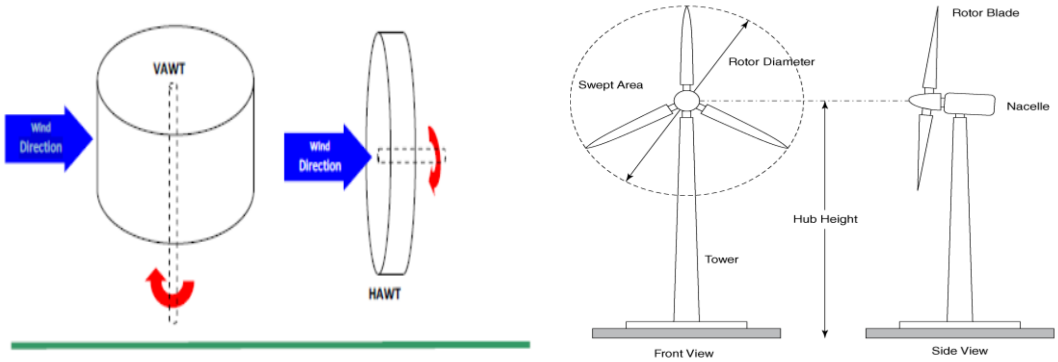

Figure 2. 4 Horizontal and vertical rotor orientation of the wind turbine (Schubel and Crossley. 2012 (*Hodge.2017*).

2.3.2 Wind Turbine Components

The major components of a commercial wind turbine are the rotor and its blades, hub assembly, main shaft, gearbox system, transmission, yaw mechanism, over-speed protection, nacelle, electric generator, and sensor and yaw drive, Power regulation and controlling equipment, and the tower of the system. These main components are the foundation, tower, nacelle, and rotor which consist of the three blades and central hub. The nacelle sits at the top of the tower and contains the gearbox, shafts, and generator of a wind turbine. The tower is the base structure that supports and elevates a wind turbine rotor and nacelle (Ahmad *et al.*, 2018).

2.3.3 Working Principlels of Wind Turbine

The working principle of wind turbine is simply when a wind blow across the blade (rotor) pressure difference is created between upwind and downwind side of the blade. This pressure gradient resulting lifting force, which causes the blade to rotate. while the blade is connected to slow motion main shaft. Through numbers of gears this slow rotation of main shaft is connected to high rotation of output shaft which is connected to generator. This is where mechanical rotational motion is converted to electrical output. The generator used in this thesis is Synchronous generator which produces AC current and electricity generated by generator is optimized by step up in the power electronics system to reach the required output voltage needed to supply the power grid.

Figure 2. 5 Typical configurations of a modern large scale wind turbine (www.turnpixel.com).

2.4 Work Done by the Previous Researcher

Several pieces of research have been conducted in remote area electrification by hybrid off-grid power generation all over the world and in Ethiopia. Different scholars used different Technology options and approaches to evaluate the various configurations of renewable energy resources, such as solar energy, wind energy, small hydropower, and hybrid configurations. Here few of them are selected and reviewed in the paragraph below

Temirat (2007) work on comparative analysis of solar PV, Micro hydropower, and wind turbine power generation for two rural villages are Dillamo village in Amara regional state and Gode village in Somalia regional state. The study indicates that three and two renewable energy identified for Dillamo and Gode village respectively. The result shows that solar radiation and wind speed of the Gode site have the potential of 6.23 $kWh/m^2/day$ and 5.93m/s respectively.

Berihun (2013) presented a case study of a rural area in Ethiopia entitled "Modeling and Simulating of a Micro Hydro-Wind hybrid power generation system for rural areas of Ethiopia" by using HOMER software. The objective of the study was to develop a hybrid system cost competitive to supply energy for remote villages for a model community of 660 households with one primary school two churches one mosque and one health center. He concluded the micro-hydro system is the most economical and can only satisfy the energy demand of the village and technically feasible option. However, if he includes solar resources in the hybrid configuration, his hybrid system may be cost-effective regarding his title.

Girma (2016) study the Hybrid renewable energy design for rural electrification in Ethiopia for electrification of a remote village called Dembile which, is located around 80km from Arbaminch town. This village consists of 200 households with an average of five family members per household and the energy demand of the village according to the study is 279 kWh/day and 64 kW peak power. The result shows that monthly average solar radiation of the site occurs in the month February with average radiation of 6 $kWh/m^2/day$ and the minimum radiation available in July and wind speed of the selected village is very low and it ranges from 3m/s to 4.5 m/s with a monthly average of 3.91m/s.

Getachow and Getnet (2011) researched a Feasibility study of a small-scale Hydro/PV/Wind hybrid system for off-grid rural electrification at Dejen district which is located in Amara regional state. When performing research solar, hydro, and wind power potentials available at Dejen district are calculated and optimal hybrid combinations are proposed for electrification of the district inhabited by 10,500 families (average of six members per family). A total of six hydropower potential have been identified.

Abdullah *et al. (*2010*)* had been analyzed Rural electrification programmers in Kenya and Policy conclusions from a valuation study in the case of Kenya, which provides the focus for this study, replacing the dominant traditional forms of energy with modern ones such as electricity creates social, economic and health-related benefits, particularly for rural households which depend solely on traditional fuels. In conclusion, rural electrification programs in developing countries face socio-economic and political barriers, with a key factor that is impeding their development being the inability of rural households to connect to electricity services.

Olayinka *et al.* (2010) develop small hydropower (SHP) development in Nigeria and propose that Energy is a very important ingredient for development and a powerful engine of social and economic opportunity in that no country can manage to develop beyond a subsistence economy without having at least minimum access to energy services for the larger proportion of its population. Studies have indicated a strong correlation between energy consumption and economic growth; access to modern energy services directly contribute to economic growth and poverty reduction via the creation of wealth. China for example has moved 300 million of its people out of poverty since 1990 through increased access to energy.

Getnet ***et al. (2017)*** work on the design and modeling of hybrid PV-micro hydro power generation case study Jimma zone. Access to modern energy, especially in rural, remote areas would help significantly to reduce poverty, to get better health care and education, to facilitate modern communication and information systems. Further, it will reduce city migration and depletion of fossil fuel resources and deforestation as well as pollutant gas emission to the environment. The development of renewable energy based on locally available resources should play a key role in this regard. Ethiopia has huge renewable energy (micro-hydro power, solar, biomass, and wind energy) potential that has been attempted for rural electrification.

Lahimar et al. (2012) carried out research and development aspects of Pico-hydro power Pico-hydro refers to the smallest scale in a hydropower plant. This paper summarizes that to meet the substantial electricity demand worldwide, Pico-hydro has been proven to be the most cost-effective option for the electrification of remote communities because of its affordability, simplicity, low unit cost, low electricity tariff, power continuity, income generation, no environmental impact, locally manufactured and managed, and easy to install, operate, and maintain. As such, Pico-hydro is becoming an attractive prospect in satisfying the basic electricity needs of remote communities.

VanMacro et al. (2014) develop Mini-scale hydropower development for rural electrification in South Africa. The objective of the study is to enhance the uptake of micro-hydro technology, making local stakeholders (private sector, financial sector, government entities, etc. aware of the opportunities that this technology brings, and the coordinated efforts required for its successful re-implementation. The project will prove that, under the current legislative and policy framework, mini-hydropower technology can provide ‘grid-quality’ electricity to rural communities.

Gebreyohannes ***et al.*** **(2009)** performed a case study of rural areas in Ethiopia entitled “Modeling and simulation of Mini/Wind Hybrid Power Generation System for rural Area of Ethiopia” by using HOMER software. He aimed to develop a hybrid power supply system cost competitive to supply power for remote villages for a model community of 660 households, one primary school, two churches, one mosque, and one health center. From the study two options Wind/mini hydro hybrid system and mini-hydro only system by comparing the cost of energy to select the cost-competitive for the remote village.

Saheb-Koussa ***et al.*** **(2017)** in their study, deal with the design of the hybrid system. Techno-economic optimizations of two renewable sources that are photovoltaic and wind with diesel and battery storage have been obtained. They aimed to find a suitable standalone hybrid system that will provide the energy supply of remote areas with minimum COE. This paper has been selected because it has the same target as the one that the researcher has in his thesis work.

Mehmet et al. (2016) perform research on mini-hydropower for sustainable energy development in Turkey and according to their studies energy is considered to be a key factor in the generation of wealth, social development, and improved quality of life in all developed and developing countries in the world. These energy sources are primary, domestic, clean inexhaustible sources. Hydroelectric power in Turkey accounts for about 30% of electricity supply in renewable energy sources with additional potential for growth. Hydropower technology largely relies on its plant design and characteristics including the location of water intake, penstock, head size, water flows, and the turbine types. Those are the factors that affect the efficiency and maximum power output of the turbine

Kusre et al. (2009) perform an assessment of hydropower potential using GIS and hydrological modeling technique in the Kopili River basin in Assam (India) Hydropower is a clean, renewable and reliable energy source that serves national environmental and energy policy objectives. The energy associated with this flowing water is known as kinetic energy that is released through the friction of flowing water with the rocks and the sediment in the river beds. From their paper of research, they concluded that traditionally the water resources assessment is made using historically observed discharged data at the outlet of the watershed. Such assessments were site-specific and would generally ignore some other potential sites within the watershed resulting in the poor motivation of the water resources project.

Adigüzel ***et al. (2002)*** Moreover, because of the considerable amount of financial requirements and insufficient financial sources of the national budget, together with the strong opposition of environmentalist, civil organizations, large scale hydropower projects cannot be completed in the planned construction period generally, which leads to use of SHP in developing countries with its low investment cost, short construction period, and environmentally friendly nature. Comprising these features, mini-hydro power has been getting attention in both developed and developing countries.

Wube (2016) Performs analysis on the Design and Analysis of Mini Hydro Power for Rural Electrification and according to his study reliable access to electricity is a basic precondition for improving people's lives in rural and urban areas, for enhanced health care and education, and growth within local economies. At present, more than 1.5 billion people worldwide do not have access to electricity in their homes (Kari Sørnes, 2010). A mini hydropower scheme requires both water flow and a drop in height called ahead to produce useful power. The research aims to generate electric power from Mini Rivers and waterfalls could generate electricity to energize many off-grid rural areas in Ethiopia.

2.5 Literature Summary and Gap

Using renewable energy for rural electrification is not a new technology because for a century different researchers use either solar, wind, hydro, biogas, and other renewable resources for different applications throughout the world and as well in our country Ethiopia. Even if many researcher studies about the using of renewable energy for rural electrification and way of optimization of the hybrid system, the study must be carried out based on different load demands and application, location of the studies as well as on climatic data's. Standalone renewable energy had been used for various applications in a rural areas, but the problem is using this energy separately may not provide continuous and sufficient energy for the user. This is the reason that for example during June the intensity of solar radiation is weak and during the summer season since no enough rain, the water capacity to drive the turbine wheel may have decreased. This implies that the standalone use of renewable energy sources may not provide enough energy for consumers. So the solution to this problem is integrating them.

Every hybrid power system has to be designed based on site available climatic condition data, number of households, service center, and consumer load profile. Nothing has been done so far in developing the renewable energy resources, such as small-scale hydro, solar, and wind energy for different application in these district area and even very limited study has been undertaken for this village for limited resources.

CHAPTER THREE

METHODOLOGY AND DATA COLLECTION

3.1 Methodology

This section explains about the objective approaching mechanisms such as reviewing Literature review, selection of the site for study, identification of data sources and data collection method, sampling techniques, analysis of collected data, interpretation of the analyzed data, result and conclusion and finally about the recommendation for the future workers. Theoretical and numerical approaches were used as a methodology in this study. The numerical (theoretical) approach uses a governing equation in each analysis of components. The HOMER (Hybrid Optimization Model for Electrical Renewable) is used in this study as the modeling and simulation software for optimization and sensitivity analysis of the system. This software was developed by the US National Renewable Energy Laboratory (NREL).

3.2 Description of the Study Area

Oromia region is one of the largest regional states in the federal administration system of Ethiopia. It borders the Somalia region to the east, Amara region, the Afar region and the Benishangul-gumuz region to the north, Kenya to the south, and Gambela region and south nation, nationalities and peoples region to the west. A study was conducted in one of nine administrative zones and the zone is known as Arsi zone more specifically study area is well known by its name Magna Lege Buna village which is found in the Arsi zone of Chole Woreda.

Magna Lege Buna village is one of the rural villages in the Arsi Zone Chole Woreda district Oromia region of Ethiopia that does not have access to electricity and is isolated from the national grid system. Study area geographically located in 7° 58' 28" N latitude, 39° 40' 36" E longitudes and Altitude: 1546.00m/5072.18ft. The field data which includes the population data, number of households, and their daily activities related to energy consumption are collected by visiting the selected village through interview and basic questionnaire steps. According to population data collected from "Chole agricultural office and Chole Health Center", which is found in the nearby kebele, most of the data taken from them, especially number household of the village is 740 with six families per housed and total number population is about 4,440 and the community under study, which equipped with one primary school, two Mosques, and one health post in the village.

Magna Lege Buna, Chole, Arsi, Ethiopia

Latitude: 7° 58' 28" North

Longitude: 39° 40' 36" East

Altitude: 1546.00m/5072.18ft

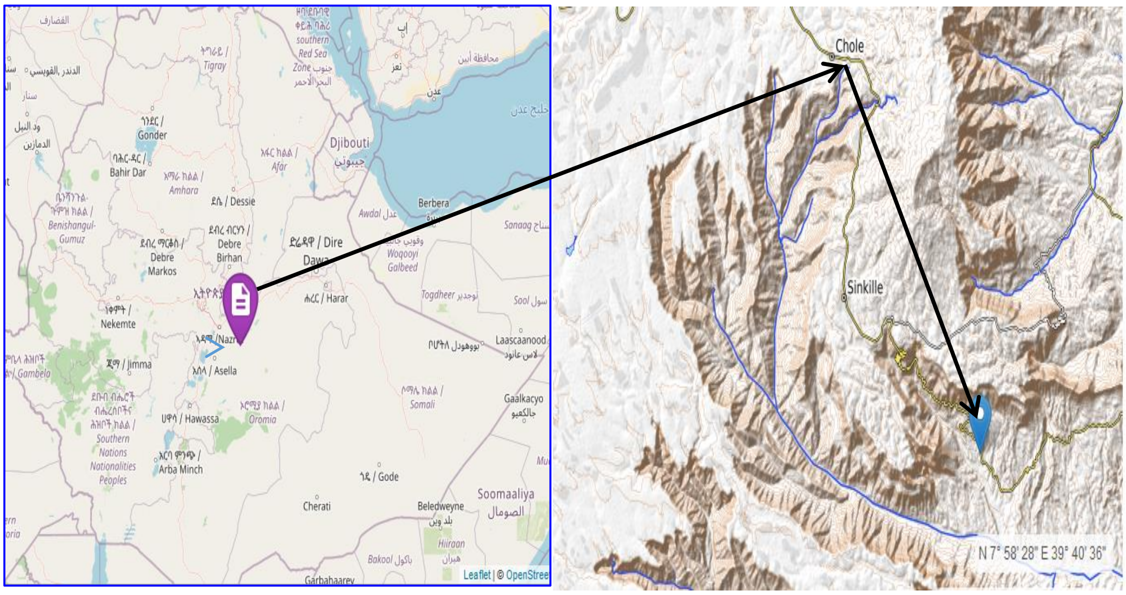

Figure 3. 1 Location map of the project area (Sources. Google Map)

3.3 Data Collection Techniques and Data Sources

To fulfill this research data is gathered from both primary and secondary sources of data.

Primary sources of data are data directly obtained by the researcher herself by conducting a field survey. During the field survey, the primary data necessary for this study are the available head of ungagged run of river and flow rate of the river, the number of religious institutes and type of community services, such as school, health post, and small-scale industries. The gross head is measured by 72HGPS, with an accuracy of 3.4m, whereas the number of schools, clinic, mosque, churches, and community services is collected from Chole Woreda Administration, Chole Woreda agricultural office, Chole Woreda Education office, and the local people live near to the selected River. Accordingly, the primary data collected are listed below in Table 3.1.

The gross head is the vertical distance that the waterfalls through in giving up its potential energy (i.e. between the upper and lower water surface levels) Field measurements of the gross head are usually carried out using surveying techniques. GPS tool is used in this project. In short data type and their sources can be indicated in the following brief and short table.

Table 3. 1 Collected data type and their respective sources (site understudy).

Data type		**Specification**	**Sources of data**
Primary data	Hydrological data	Ungagged discharge	From the site of the study
		Head of the river	
Secondary data	A load of village	Number of households	Chole Woreda Admiration office
		Number of schools	Chole Woreda Education bureau
		Number of health post	Chole Woreda Healthy center
		FTC numbers	Chole Woreda agricultural office
		Mosque and churches	Religious institute numbers
	Solar data	Sunshine hour	NMAE from Adama station
		Clearness index	Calculated
		Solar radiation	Calculated
	Wind data	Wind speed	NMAE from Adama station
		Wind direction	NMAE from Adama station

Table 3. 2 Secondarry data collected from the site of study (source. Chole Woreda administration)

No	**Kebele**	**Village**	**Number of Public and Public service**		**Quantity**	**Specification**
1	Chole	Magna Lege Buna	Households		740	-----------------
			School	Primary	2	Gado billa primary school
				Secondary	1	Magna Lege Buna secondary school
			Healthy extension		2	
			Mosque		4	Bilal,Najash, Alnur etc mosque
			Church		2	Arsema church
			Agricultural office and FTC		2	

			Flour mill		2	H/Jamalo & Dawud flour mill
			Water pump		1	
			Razor House		10	------------------
2		Magna Oda Adi	Households		610	
			School	Primary	1	
				Secondary	-	
			Healthy extension		1	
			Mosque		5	
			Church		-	
			Agriculture office and FTC		2	
			Flour mill		2	
3		Magna Derartu	Households		656	
			School	Primary	1	
				Secondary	2	
			Healthy extension		1	
			Mosque		5	
			Church		2	
			Agricultural office		2	
			Flour mill		1	
4	Chole	Magna Werqi	Households		520	
			school	Primary	1	
				Secondary	-	
			Healthy extension		1	
			Mosque		2	
			Church		-	
			Agricultural office		-	
			Flour Mill			
5		Magna	Households		698	
			School	Primary	1	

		Adare		Secondary	-	
			Healthy extension		1	
			Mosque		2	
			Church		1	
			Agricultural office		2	
			Flour mill		1	

3.4 Resource Assessment of the Village

3.4.1 Micro-hydropower Resource Assessment of the Village

a) Head Measurement

Though there are different methods for head measurement, in this project a GPS (Global Positioning Systems) and traditional Rope measurements tool were used. Two waterfalls with a height of 35 and 15m respectively contribute almost more than one-fifth of the head of the water head.

Figure 3. 2 Micro-hydropower recourses in Magna Lege Buna village

b) Flow/ discharge measurement method for the un-gauged run-off river

For un-gauged river without flow rate data, like the one in this study, manual measurement of flow rate using different methods is a requirement. Among those flow rate measuring methods, the velocity area method is used in this thesis (Nasir. 2013).

Velocity–area method

The river under measurement of the velocity-area method should have a uniform flow, usually level ground, and a well-defined area at the point of measurement.

a. Mean Velocity Measurement

Since it is an un-gauged run-of-river, the material used for float is a leaf of a piece of 'Bergamo' for velocity measurement (Tewidell and Tony Weir, 2006). The float material was supposed to travel for 5m in length. The number of trials and the corresponding result is shown in Table 3.3. Since the flow speed is zero on the bottom of the stream (because of viscous friction), the mean speed will be slightly less than the speed of the float, on the top surface. To estimate the average flow speed (V_{mean}), the above value must be multiplied by a correction factor, which may vary between (0.6) and (0.85), depending on the watercourse depth and their bottom and river bank roughness (0.75 is a well-accepted value). For a rectangular cross-section, it has been found that (Nasir. 2013).

$$V_{mean} = 0.75 \times U_s \text{---(3.1)}$$

Where U_s, can be measured by simply placing afloat, e.g. a leaf, on the surface and measuring the time it takes to go a certain distance along the stream. For best results, the measurement should be made where the stream is a reasonably straight and uniform cross-section.

Table 3. 3 Velocity of flow measurement for the un-gauged river to cross the 6m line (mesuared value during survey on May 17,2020)

No of trial	1	2	3	4	5	6	7	8	9	10	11	12	13
Time is taken in Min.	1:05	0:55	0:45	1:03	0:42	0:35	1:10	1:04	1:06	0:43	0:46	0:48	0:45

No of trial	14	15	16	17	18	19	20	21	22	23	24	25	26
Time taken in Min.	0:40	0:37	0:41	1:09	1:02	0:52	0:50	0:55	0:56	0:53	0:46	0:48	0:53

$U_s = \frac{\Delta S}{\Delta t}$ --(3.2)

Where U_s mean float velocity

ΔS distance of river which floats flow

Δt average of the time change

So this raw data indicate that $\Delta S = 6m$, $\Delta t = 51.88s$ and $U_s = 0.1156\, m/s$

b. Measuring the cross-sectional area of the stream

The linear dimension of the cross-section for the river where the velocity measurement using a float is taken as the average value of 2.80m. The number of the complete cross-section measurement is two and the averaged result is taken.

c. Cross- Section: Measurement of depth

To compute the cross-sectional area of the stream under a velocity –area method measurement, the cross-sectional area shall be uniformly divided into a series of the trapezoid (Nasir, 2013). Measuring by marked rules as illustrated in figure 3.3.

Table 3. 4 Cross-section measurement with an interval of 20cm (May 17, 2020)

Depth measurement interval at every 20 cm.	1	20	40	60	80	100	120	140	160
Measurement 1	28	70	86	88	96	95	98	96	96
Measurement 2	28	76	93	85	95	98	96	95	93

Depth measurement interval at every 20 cm.	180	200	220	240	260	280
Measurement 1	94	90	89	77	68	39
Measurement 2	90	94	85	75	64	34

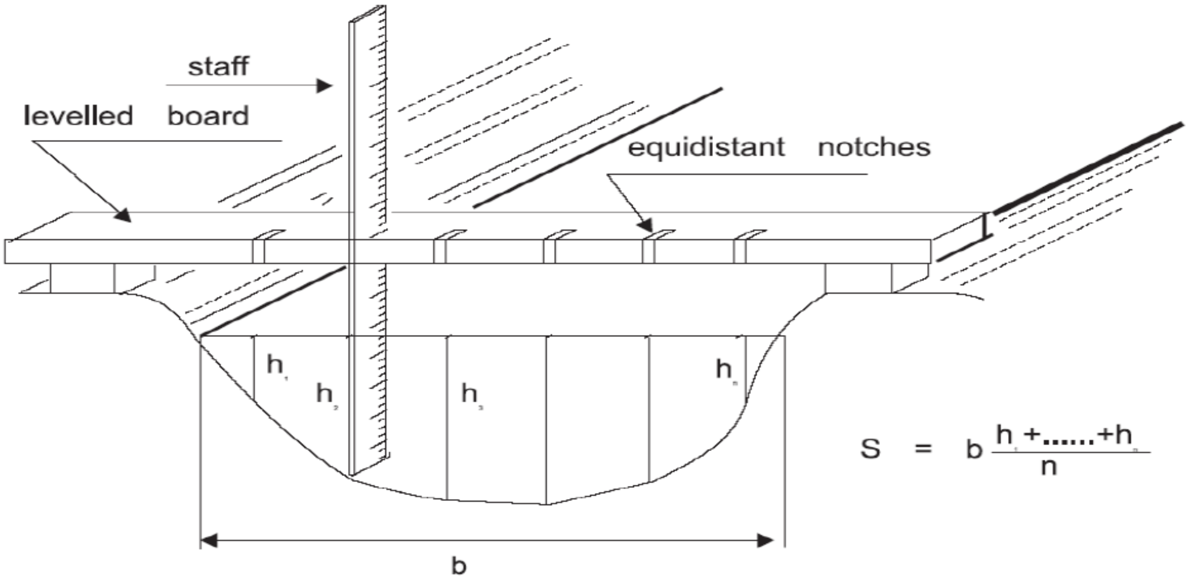

Figure 3. 3 Measuring the cross-sectional area (Nasir. 2013).

The area covered by the run of the river is the product of the average width and depth of the river.

$A_r = \frac{(a+b)}{2} \times \frac{h_1+h_2+h_3+h_4+\cdots+h_n}{n}$---(3.3)

Where $a =$ width of the river at the upper surface (m) and $a = 3\ m$.

$b =$ Width of the river at the bottom surface (m) and $b = 2.6\ m$.

$\frac{h_1+h_2+h_3+h_4+\cdots+h_n}{n} =$ Average height of water in the river (m)

$$A_1 = 2.8m\frac{13.285\text{m}}{15} = 2.48\ m^2$$ and

$$A_2 = 2.8m\frac{12.84m}{15} = 2.39\ m^2$$

$$A = \frac{A_1+A_2}{2} = \frac{2.48\ m^2+2.39\ m^2}{2} = 2.435m^2$$ then,

$$Q = A \times V_{mean}$$

$$Q = 2.431m^2 \times 0.0867\, m/s \approx 0.21\, m^3/s$$

The secondary data. The secondary data that may use are reference books and international journal those collected by someone else (maybe the researcher) for another purpose. For this thesis, the secondary datum that is collected is the solar sunshine duration data, wind speed and direction data, and temperature of the site under study from Adama meteorological station.

3.4.2 Solar Resource Assessment of the Village

The Ethiopian Meteorological Service collects only the average sunshine hours of the country and the solar radiation is calculated from the average sunshine hours. This is due to the malfunctioning of the equipment used to measure solar radiation.

Table 3. 5 The actual average duration of sunshine hours (n) of Chole village

Year	2010	2011	2012	2013	2014	2015	2016	2017	2018	2019	Ave.
Jan	7.6	9.9	9.8	9.2	9.65	9.8	6.9	10.1	9.3	10.2	9.2
Feb	5.3	9.5	9.8	9.8	8.7	10.2	9.1	7.9	8.6	9.6	8.8
Mar	6.4	8.5	9.5	8.4	7.7	8.5	8.5	9.1	6.3	9.3	8.2
Apr	7.3	6.8	6.5	8.2	8.3	7.9	5.7	8.3	6.2	7.6	7.2
May	6.9	6.5	8.8	7.6	8.6	8.1	8.3	7.8	6.8	7.2	7.6
Jun	7.8	6.8	6.5	7.5	7.9	6.8	7.2	8.1	5.3	6.7	7.4
Jul	5.3	9.8	6.7	5.8	6.2	8.3	6.9	4.7	4.9	6.8	6.5
Aug	7.6	8.3	6.5	6.4	7.1	8.7	7.2	6.1	6.9	5.5	6.9
Sep	7.6	7.3	6.9	7.4	6.8	7.8	6.9	6.6	7.9	6.6	7.1
Oct	6.7	10.1	7.6	6.7	7.5	6.4	7.6	6.9	6.35	7.4	7.4
Nov	8.1	9.8	8.7	7.3	7.5	7.8	8.7	8.4	7.2	6.3	7.9
Dec	8.9	9.8	8.9	8.6	9.4	8.2	9.4	9.9	8.2	8.3	8.9

Table 3. 6 Ten years average Sunshine hour duration of the site understudy

Months	Jan	Feb	Mar	App	May	Jun	Jul	Aug.	Sep	Oct	Now	Dec
Ave.	9.2	8.8	8.2	7.2	7.6	7.4	6.5	6.9	7.1	7.4	7.9	8.9

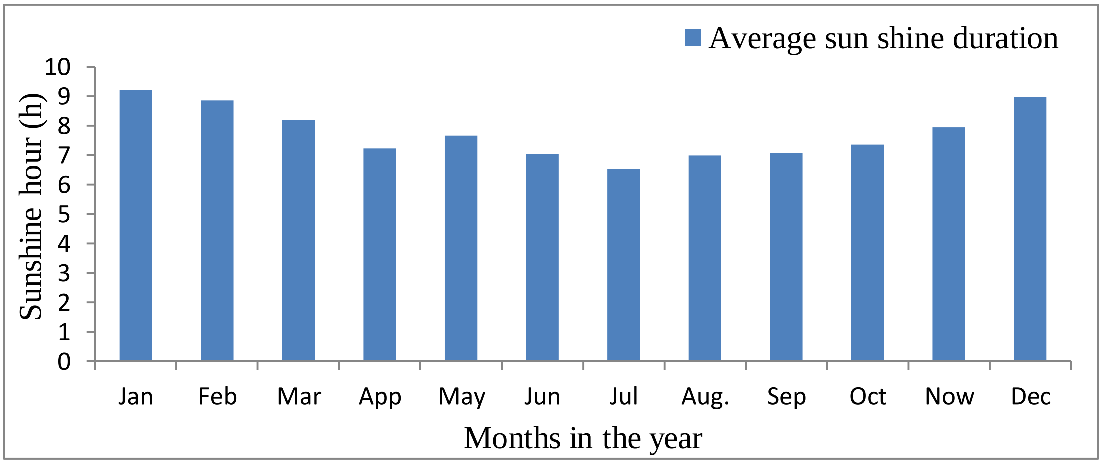

Figure 3. 4 Monthly average sunshine hours for Magna Lege Buna village

3.4.3 Wind Resource Assessment of the Site of the Village

Wind resource is the most important element in determining the performance of a given turbine at the site. The power extracted from moving wind energy is directly proportional to the cube of its velocity, meaning that doubling the wind velocity increases the available energy by a factor of eight. Wind resource itself varies with year, seasons, time of day, elevation above ground, and form of terrain. The wind speed data of the study site have been taken from a nearby metrological station (Adama station) which is measured at 10-meter height.

Table 3. 7 Average wind speed of the village at 10m

Month	Jan	Feb	Mar	Apr	Ma	Jun	July	Aug	Sep	Oct	No	Dec
2010	2.65	2.45	3.09	3.15	3.65	4.14	3.99	4.56	5.23	4.12	3.98	3.71
2011	3.11	3.32	3.17	4.32	5.45	3.76	4.23	3.76	2.34	3.08	2.89	3.61
2012	3.78	4.22	4.76	5.62	4.5	4.23	3.56	5.34	4.86	3.67	6.32	2.15
2013	2.98	2.79	4.65	3.89	3.69	2.89	4.66	4.9	4.98	3.54	5.23	3.12
2014	3.67	2.11	2.16	3.76	3.71	3.33	5.03	4.34	5.23	4.52	3.77	4.43
2015	3.12	5.23	5.18	2.98	4.04	5.21	5.34	4.45	3.98	4.55	3.78	3.94
2016	4.01	4.05	3.56	4.32	4.23	4.11	4.76	2.98	4.32	4.52	4.32	2.86
2017	3.89	3.45	3.09	4.01	3.23	4.01	4.06	2.06	4.32	5.24	4.47	4.32
2018	2.99	2.84	3.06	3.54	3.03	3.64	3.44	3.87	3.05	5.07	5.43	4.05
2019	2.00	2.25	2.65	1.53	3.5	2.45	3.87	3.05	4.22	4.24	5.45	3.76
Av. (2010-2019)	3.65	3.23	3.14	3.72	3.57	4.37	4.89	4.37	3.56	3.76	3.87	3.59

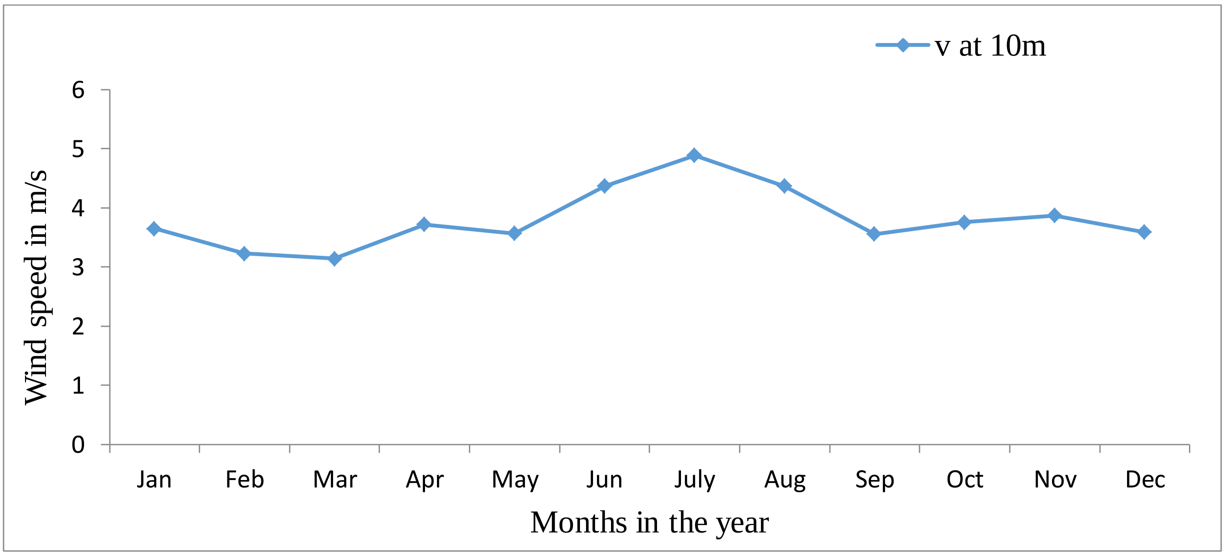

Figure 3. 5 Average wind speed of village understudy

The highest wind speed was observed in July while lowest in March at all the heights of wind speed measurements. To estimate the wind speed at the selected turbine hub height (50m), the following equation has been used.

$$V_H \times ln\frac{H_{ref}}{H_o} = V_{ref} \times ln\frac{H}{H_o} \qquad (3.4)$$

$$V_H = V_{ref}\left[\frac{\ln(H/H_o)}{\ln\left(H_{ref}/H_o\right)}\right]$$

Where

H → the hub height of the wind turbine[m]

H_{ref} →the anemometer reference height [m]

H_o →the surface roughness length [m]

V_H →wind speed at the hub height of the wind turbine [m/s]

V_{ref} →wind speed at the anemometer height [m/s]

The surface roughness length is a parameter that characterizes the roughness of the surrounding terrain. Table 3.8 contains the representative surface roughness length (Mathew, 2006). H_o is the roughness length, which is 0.1–0.25m for cropland and a value of 0.15 has been used in the calculation since the site is located in a semi-desert area.

Table 3. 8 Terrain description for surface roughness (Mathew, 2006).

Terrain Description	H_o
Very smooth, ice or mud	0.00001 m
Calm open sea	0.0002 m
Blown sea	0.0005 m
Snow surface	0.003 m
Lawn grass	0.008 m
Rough pasture	0.010 m
Fallow field	0.03 m
Crops	0.05 m
Few trees	0.1 m
Many trees, some building	0.25 m
Forest and woodlands	0.5 m

Wind speed varies from day to day as well from hour to hour, and also from month to month as indicated in the above figure according to data collected from AMS. The following result shows an hourly basis of wind speed at the hub height of 50m. Since calculating wind speed for every 365 days of the year is difficult manually, by taking the representative days of the month let look at the variation of the hourly wind speed of each month in the year.

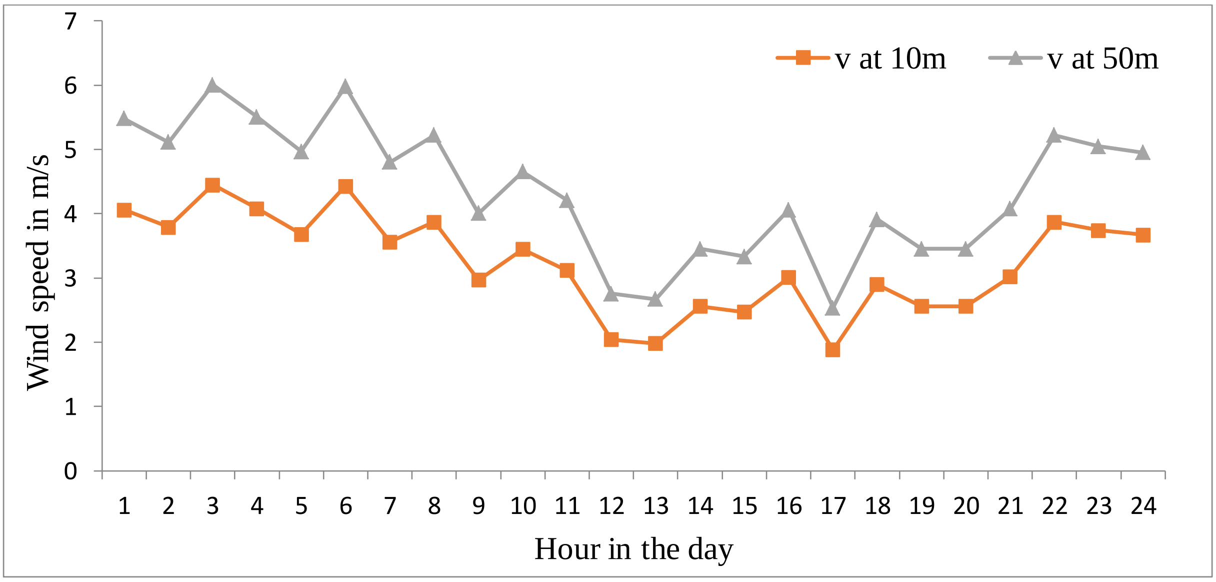

Figure 3. 6 March 15 Minimum potential of wind speed based daily of the site

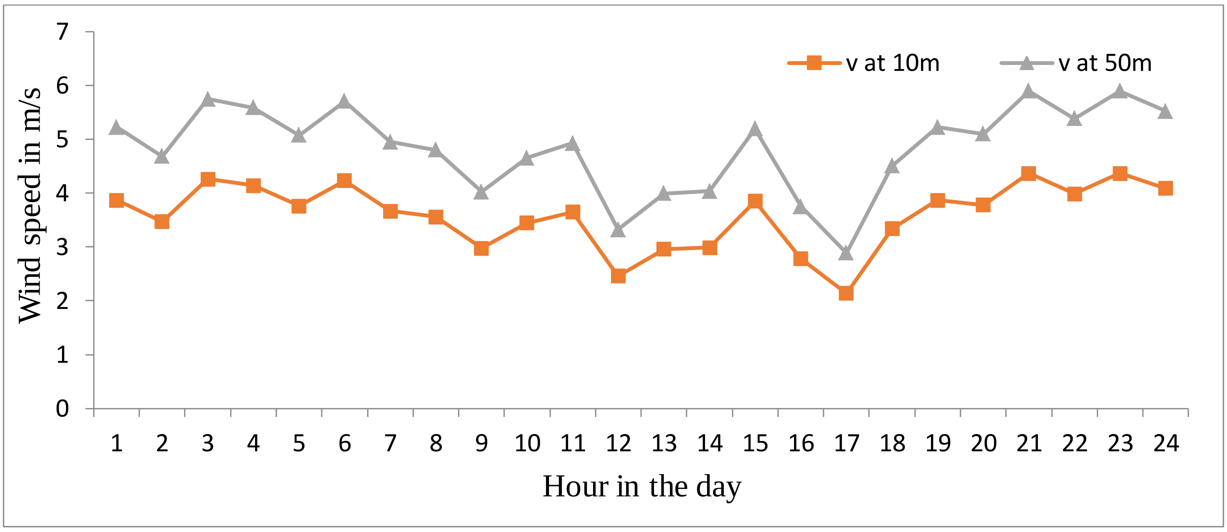

Figure 3. 7 July15 Maximum potential of wind speed based daily

The above two figure 3.6 and figure 3.7 shows that the months with minimum and maximum wind speed respectively. The figure may aslo show that wind speed is varying from hour to hour and maximum wind speed is recorded during the night time on daily basis status. Even though wind speed and wind direction are varying from day to day and from hour to hour, to extract power from wind turbines it is necessary to maintain (yaw) wind as required means wind turbines were always facing the headwind and incurred no losses due to lagging dynamic yawing control. There are two mechanisms for controlling wind speed and direction as needed. Weibull and Rayleigh's functions appear to accurately reflect the wind speed probability datasets (Nielsen, 2011). Weibull and Rayleigh distributions measure how much time of the year (in percent) that each wind speed occurs. The Weibull distribution is the most widely used probability density function

Table 3. 9 Average monthly wind speed at reference height and required hub height

Months	Jan	Feb	Mar	Apr	May	Jun	July	Aug	Sep	Oct	Nov	Dec	Ave.
V at 10m	3.65	3.23	3.14	3.72	3.57	4.37	4.46	4.37	3.56	3.76	3.87	3.59	3.85
V at 50m	5.35	4.78	4.66	5.44	5.24	5.79	6.44	5.98	5.48	5.59	5.75	5.26	5.46

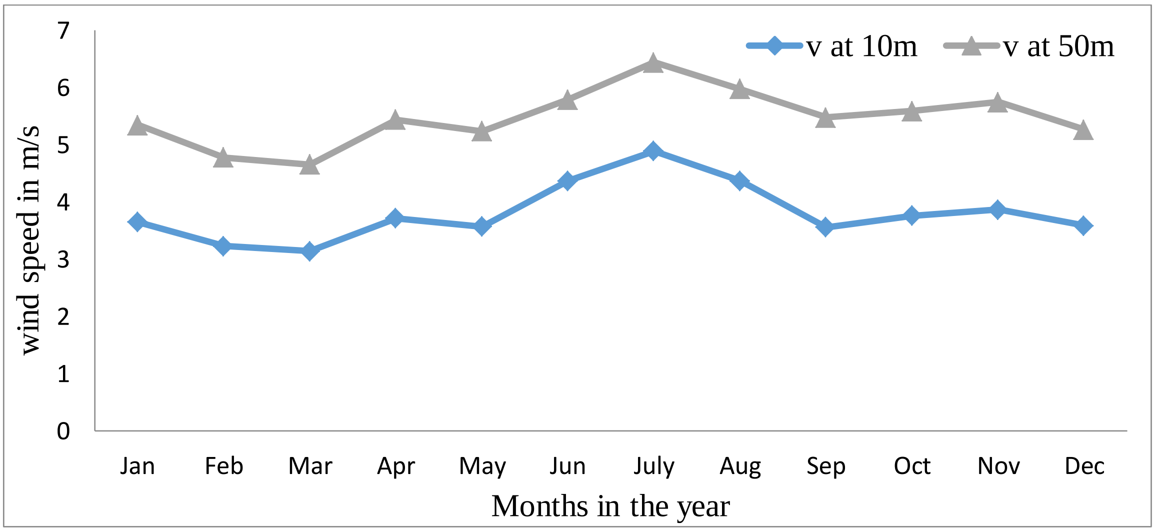

Figure 3. 8 Average monthly wind speeds at 10m and 50m height of the site

The above figure 3.8 clearly demonstrate average win d speed of the site under at refence height of 10m and at corresponding hub height 50m of the wind turbine. Maximum wind speed is recorded on rhe july months while the lowest wind speed is on march as calculated early.

3.5 Load Estimation of the Village

Loads in this case study are divided into two according to their nature, primary and deferrable. A primary load is an electrical load that must be met immediately and a deferrable load is an electrical load that must be met within some period, but the exact time is not important. All considered loads are primary except water pumping. Water pumping is a deferrable load.

Primary load: the primary load is the electrical demand that the power system must meet; the system electrical demand associated with lights, radio, TV, household appliances, computers, and industrial processes is typically modeled as the primary load. If electrical demand exceeds supply, a deficit is recorded as an unmet load [HOMER user manual].

The user specifies an amount of primary load in kW for each hour of the year, either by importing and file containing hourly data or by allowing HOMER to synthesize hourly data from average daily load profiles. When synthesizing load data, HOMER creates hourly load values based on user-specified daily load profiles. Different profiles for different months and different profiles for weekdays and weekends are specified. A specified amount of randomness can be added to synthesize load data so that every day's load pattern is unique. In this thesis, 15% hourly and 10% daily load, noise is assumed to account for the variability of load demand.

According to (Bekele, G. and Tadesse, G., 2012) the Electric load in the rural villages of Ethiopia can be assumed to be composed of lighting, radio receiver, television set, water pumps, health posts, and primary school load. In this study, flour mills, milk processing, and 'Injera Mittad' are added to the load together with previously mentioned loads. As introduced earlier, the community under study, which equipped with two primary schools and a health post, has 740 households with an average of six members per family and with a total number of 4,440 is living in the village according to data obtained from Chole Woreda Administration.

Table 3. 10 Households Electricity Consumption Features

Appliance type	Number of appliance	Rating (W)	To number of customers (740)	Operating hours (hr)		Power (kw)	Energy (kwh/day
				h/day	period		
CFL	4	11	150	6	18:00-0:00	6.60	39.61
	3	11	234	5	18:00-23:00	7.72	38.61
	2	11	356	4	18:30-22:30	7.82	31.33
Television	1	100	150	5	19:00-00:00	15.34	75.00
	1	100	234	3	19:00-22:00	23.42	70.20
Refrigerator	2	120	95	24	All day	22.81	273.60
Radio	2	20	360	8	8:00-10:00	14.44	83.20
	1	20	150	4	18:00-22:00	3.56	12.00
Charger	4	10	250	8	23:00-7:00	2.57	80.00
	2	10	350	6	7:00-13:00	7.45	42.00
	1	10	650	4	10:00-14:00	6.55	26.90
Coffee	1	600	350	1	7:00-8:00	210.3	210.56

machine	1	600	90	0.5	20:00-20:30	54	165.00
Stove	1	2500	260	2	19:00-21:30	325	650.00
	1	2500	134	1	11:00-12:00	335	335.00
Enjera mittad	1	3000	134	1.30	9:00-10:00	402	522.60
	1	3000	90	1	9:00-10:00	270	270.00
Total						1712.	2396.00

Public service and commercial load								
Types	No of user		Appliance type	Rating	No of appliance	Operating hours		kW/day
						h/day	Period	
School	High school	1	Scanner	100	1	1	9:00-10:00	0.1
			Printer	100	2	2	9:00-11:00	0.4
			Speaker	15	1	1	For 5 minute every period	0.015
			TFL	11	15	4	18:00-22:00	0.66
			Fax machine	100	1	0.5	14:30-15:00	0.05
			Total Kwh/day					1.12
	Prepa Ratory	1	CLF lamp	11	20	3	18:00-21:00	0.66
			Computer	10	30	6		1.8
			Television	100	8	4	8:00-12:00	3.2
			Microscope	20	2	3	9:00-12:00	0.12
			Total kWh/day					5.78
Mosque	4		CLF lamb	11	6	2	18:00-20:00	0.132
			Megaphone	15	2	1	For10 minut every pray	0.03
			Total kWh/day					0.648
Clinic	2		CLF lamb	11	12	12	18:00-6:00	1.584
			Vaccine refrigerator	120	2	24	All day	5.76

		Lab equipment	150	6	5		4.54
		Television	100	12	6		7.22
		Microscope	20	3	4		0.24
		Total kWh/day					19.31
Other		Water pump	2000	1	3	14:00-17:00	6.65
		Flour mill	7500	2	3	13:00-16:00	45.87
		Razor	150	10	8	9:00-17:00	12.57
		FTC office	200	2	3	8:00-11:00	1.22
		Total kWh/day					64.21

The above table 3.10 indicates that different households have different daily energy consumption from each other depending upon their income. A large number of households uses mobile charger, CFL and radio while, the other few houses hold also use Injera mittad and LED television also. Hence the amount of total energy consumed by 740 households of the village is about 2396.58 kWh/day and the total energy consumption of one high school and one preparatory school is 6.9 kWh/day. Finally, the total energy consumption of different community services such as the clinic, religious station, flour mill, and FTC are together approximated to be 66.24 kWh per day. By considering 5kW energy for excess, the total energy demand for the village per day is 2470 kWh/day. HOMER software needs hourly load as input for simulation. To get the hourly load of the village, the above loads are distributed in the EXCEL spreadsheet program from the knowledge of load usage time, which is gained from the Electrified village of the same socio-economic condition. For instance, lighting loads are switched on from 18:00-23:00 on average, grinding mills are operated during daytime and the entertainment devices usually switched on when required. There is no education during the winter season especially during July and August as well as during the break time of the school no need for energy consumption except for special cases.

3.5.1 Load Curve Estimation

The load on power stations varies from time to time. These variations during the whole day (24 hours) are recorded hourly and plotted against time on the graph. The load curve is a graphical representation between load in kW (or MW) in proper time sequence and time in hours. It shows the variation of load on the power station. The highest point on the load curve represents the maximum demand (peak demand) on the station on that day. The area under the load curve gives the total energy supplied on that day and if this area is divided by the number of hours gives the average load (power) on the station. several family is assumed to use an electric stove of 3 kW rating for baking a local bread, ‘‘Injera’’, for 40 min every fourth day. The timing for baking is assumed to be in either of 6:00–9:00, 11:00–14:00, or 15:00– 18:00. Each household is to be installed with three CFLs of 11 W rating to be lit from 18:00 to 23:00. Additionally, a CFL of 11 W is also considered for external lighting. A water storage capacity of 4 days is suggested requiring a storage capacity of 1188 kWh for the community and 60 kWh for primary school and health centers. The peak deferrable load is 3.75 kW for primary school and health center and 49.5 kW for the community. At the weekend, mills are not working and evening classes are conducted in the day time. TV and radio are used from 10:00 to 17:00.

Table 3. 11 Daily Load profile of Magna Lege Buna village

Time (hr)	1	2	3	4	5	6	7	8	9	10	11	12	13
Household	2	1.2	1.12	1.54	1.9	0.89	2.43	65	120	135	115	98	88
School	0.08	0.05	0.09	0.04	0.1	0.01	0.1	0.32	0.43	0.45	0.56	0.5	0.07
Clinic	0.04	0.67	0.98	0.98	0.67	0.78	0.34	0.23	0.36	0.88	0.56	0.6	0.12
Other	0.23	0.34	0.45	0.6	0.8	0.6	0.6	2.3	4.4	5.8	6.8	3.7	1.1
Total	2.35	2.26	2.64	3.2	2.7	2.35	3.53	52.3	110	121	123	103	90

Time [hr]	14	15	16	17	18	19	20	21	22	23	24
House hold	75	97	120	135	125	140	166	170	145	65	36
School	0.08	0.98	0.47	0.07	0.43	0.05	0.03	0.02	0.08	0.07	0.06
Clinic	0.11	0.21	0.23	0.29	0.34	0.65	0.76	0.79	0.45	0.23	0.89
Other	0.98	3.56	4.32	4.78	4.78	3.21	3.65	3.12	2.1	1.2	1.9
Total	76	101	125.4	140	130	143	170	173	147	66.7	38.9

From the above table 3.11 of daily load distribution, it is possible to develop a daily load duration curve using Microsoft excel and its output becomes as shown in figure 3.10.

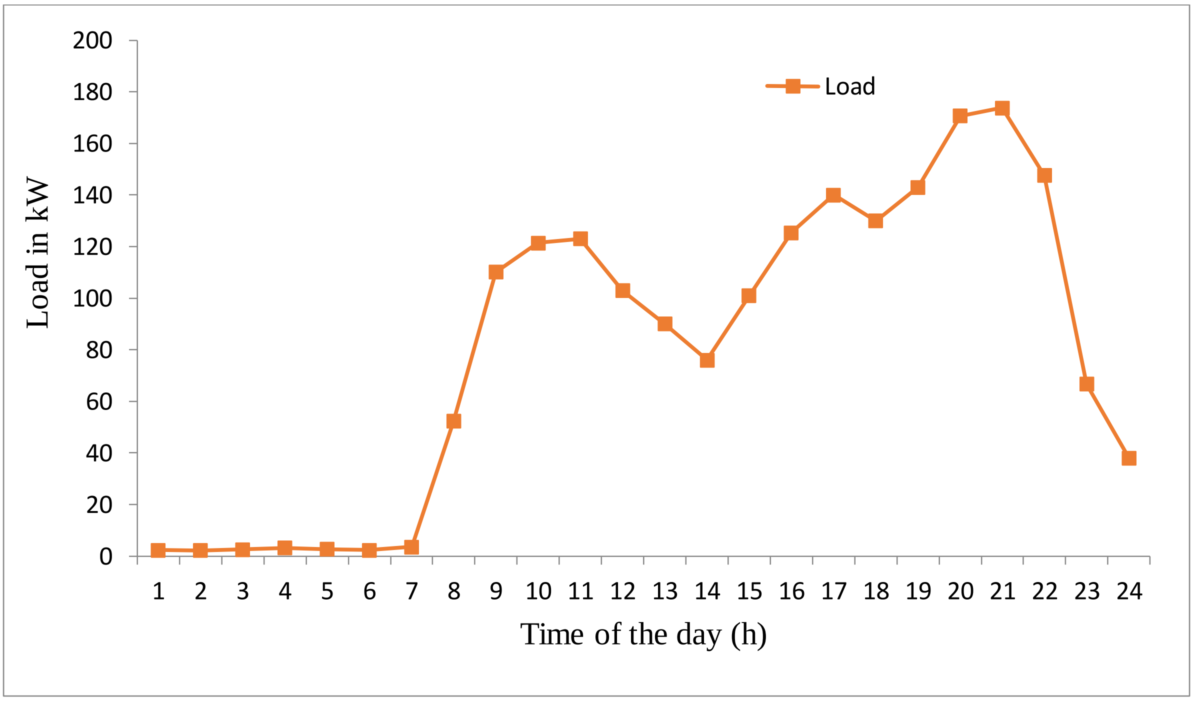

Figure 3. 9 Daily Load curve for Magna Lege Buna Village

CHAPTER FOUR

RENEWABLE ENERGY RESOURCES ANALYSIS OF THE STUDY SITE

4.1 Solar Potential Analysis

4.1.1 Solar radiation assessment of the village

Monthly average solar radiation is one of the principal parameters used by HOMER software as input. Unfortunately, there is no properly recorded solar radiation data and, what is available is sunshine duration data from Adama meteorological station for the site under study. However, given knowledge of the number of sunshine hours and local atmospheric conditions, sunshine duration data can be used to estimate monthly average solar radiation, with the help of an empirical equation.

Monthly average, Daily global Radiation

$$\mathrm{H} = \left(\mathrm{a_s} + \mathrm{b_s}\frac{\mathrm{n}}{\mathrm{N}}\right) H_o \text{---(4.1)}$$

where H is monthly average daily radiation on horizontal surface (kWh/m^2).

H_o is monthly average daily extraterrestrial radiation on a horizontal surface (kWh/m^2).

N is the maximum possible daily hours of bright sunshine,

n is the monthly average daily number of hours of bright sunshine,

$a_s and\ b_s$ are regression coefficients and has been calculated from the relationship given by (Duffie and Beckman, 2006).

$$a_s = -0.11 + 0.235\cos\varphi + 0.323\left(\frac{n}{N}\right)$$

$$b_s = 1.449 - 0.533\cos\varphi - 0.694\left(\frac{n}{N}\right)$$

Extraterrestrial solar radiation (H_o)

Now let explain about the amount of solar radiation reaching the top of the atmosphere over a particular point on the earth's surface. To calculate the extraterrestrial normal radiation defined as the amount of solar radiation striking a surface normal (perpendicular) to the sun's rays at the top of the earth's atmosphere. Solar radiation outside the earth’s atmosphere is called extraterrestrial radiation. Daily extraterrestrial radiation on a horizontal surface for each day of the year and different latitudes can be estimated from the solar constant, the solar declination, and the time of the year (Duffie and Beckman, 2006) as follows.

$$H_o = \frac{24\times3600}{\pi} G_{sc} \times d_r \times \left\{\frac{\pi}{180} \times \omega_s \times \sin(\varphi) \times \sin(\delta) + \cos(\varphi) \times \cos(\delta) \times \sin(\omega_s)\right\}$$

(4.2)

where G_{sc} is the solar constant (which is equal to 1367w/m2);

d_r the inverse relative distance Earth-Sun;

ω_s the sunset hour angle($radian$);

δ declination angle

φ the latitude ($radian$)

The latitude of a location is the angle made by the radial line, joining the given location to the center of the earth, with its projection on the equatorial plane. Note: the latitudinal and longitudinal location of the Magna Lege Buna Village is 8° 9' 60" and 39.5° 49' 59.99'' respectively in the northern hemisphere.

Earth-sun distance (d_r)

$$d_r = 1 + 0.033cos\left(\frac{360 \times n_d}{365}\right)$$ ---(4.3)

where n_d is the number of days in the year between 1 (January 1) and 365 or 366 on December 31. The relative earth-sun distance for every critical month is calculated from the above equations.

solar declination angle (δ)

The declination angle is the angular position of the sun at solar noon, concerning the plane of the equator. Its value in degrees is given by Cooper's equation (Duffie and Beckman, 2006).

$$\delta = 23.45\sin\left(\frac{360}{365}(284 + n_d)\right)$$ --(4.4)

Hence, the solar declination angle at mid of each month (for the recommended average value of moth) is calculated from the above equation 4.4.

Sunrise and Sunset Hour Angle (ω_s)

It is the hour angle at the time of sunrise (or sunset). Or it is the hour angle when the latitudeangle is zero. The sunset hour angle (ω_s) is given by

$$\omega_s = \cos^{-1}[-\tan(\varphi) \times \tan(\delta)]$$ --(4.5)

where φ is the Latitude of location and δ is the declination angle calculated above.

Daylight hours (N)

The daylight hours, N, are given by [2, 9]:

$$N = \frac{24}{\pi} \times \omega_s \text{--} (4.6)$$

π = 180°, therefore, Daylight Hours, N, for the critical months can be calculated as follows

$$N = \frac{24}{\pi} \times \cos^{-1}[-\tan(\varphi) \times \tan(\delta)]$$

Where

$$\delta = 23.45\sin\left(\frac{360}{365}(284 + n_d)\right)$$

The value of n or sunshine hours for the recommended date of the months is taken from Appendix B. monthly solar radiation data calculated through the above progress from daily sunshine hours is summarized in the following table.

Table 4. 1 Monthly average solar radiation of site of study

Mid of months	n_d	n	N	n/N	φ	δ	ω_s	H_o $kWh/m^2/day$	H $kWh/\frac{m^2}{day}$
Jan 15	17	9.2	11.58	0.79	8.09	-20.91	86.89	8.88	7.23
Feb 14	47	8.86	11.75	0.75	8.09	-12.95	88.13	9.59	6.89
Mar 15	75	8.19	11.95	0.69	8.09	-2.417	89.66	10.24	6.64
Apr 15	105	7.22	12.18	0.59	8.09	9.414	91.35	10.57	6.46
May 15	135	7.66	12.37	0.62	8.09	18.79	92.77	10.52	6.58
Jun 15	162	7.04	12.46	0.56	8.09	23.08	93.47	10.40	5.60
July 15	198	6.54	12.42	0.53	8.09	21.18	93.16	10.46	5.05
Aug 15	228	6.99	12.26	0.57	8.09	13.45	91.95	10.57	5.43
Sep 15	258	7.08	12.04	0.59	8.09	2.216	90.32	10.41	5.97
Oct 15	288	7.35	11.82	0.62	8.09	-9.599	88.62	9.82	6.16
Nov 15	318	7.95	11.63	0.68	8.09	-18.91	87.21	9.06	6.78
Dec 15	344	8.97	11.54	0.78	8.09	-23.04	86.53	8.65	6.67
Average									6.31

As someone can understand from above table 4.1 Magna Lege Buna has a monthly average solar radiation potential of 6.31 kWh/m^2. This value is related to the studies of (Tesema, S. and Bekele, G., 2014) on International Journal of Energy and Power Engineering publication confirms the study by SWERA for the solar radiation potential of the Somali region which is the highest potential value of 7.5 kWh/m^2 in Ethiopia for Werder Zone.

4. 1.2 Components of solar radiations

Calculating solar radiation that arrives earth's surface is not easy, because it is influenced by different factors such as air molecules, the temperature of the air, cloudy, and another particle in the atmosphere. The scattered solar radiation that reaches the ground is known as diffuse irradiation and where some of the radiation is reflected from the ground onto the receiver; this is named reflected irradiation. The radiation that is not reflected or scattered and reaches the surface directly is called direct irradiation. Then, the summation of these three components is the total (or global) irradiation that strikes the absorber unit (Keller & Costa, 2011).

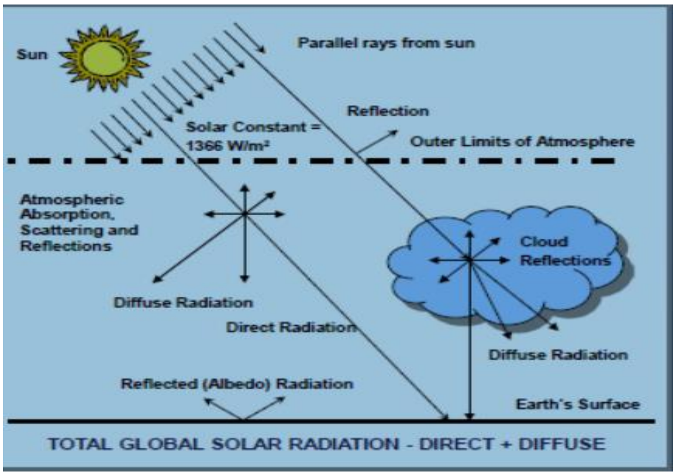

Figure 4. 1 Component of solar radiation on the surface (Duffie and Beckman 200).

Table 4. 2 Monthly Average daily global radiation($kWh/m^2\ /day$) on horizontal surface

Month	Jan	Feb	Mar	Apr	May	June	July	Aug	Sept	Oct	Nov	Dec
Ave.	7.23	6.89	6.64	6.46	6.58	5.60	5.05	5.43	5.97	6.16	6.78	6.67

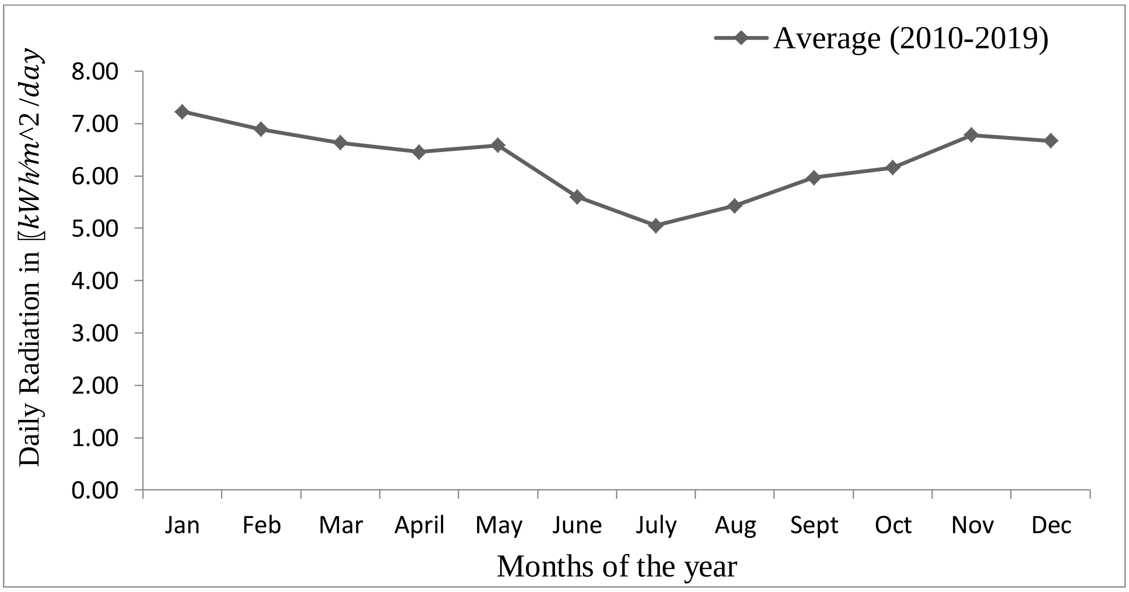

Figure 4. 2 Monthly Average daily global radiation of Magna Lege Buna village' on horizontal surface`

4.1.3 Monthly average daily diffuse radiation of the site

Diffuse solar radiation is a part of the sunlight that passes through the atmosphere and is consumed, scattered, or reflected by water vapor, dust particles, or pollution (Erbs *et al.*,1982). In contrast to beam radiation, which has a well-defined direction, diffuse radiation originates from all over the skydome. Although diffuse radiation is most intense near the Sun, a good approximation is to assume that it is isotropic, i.e., uniformly distributed in all directions. The proportions of diffuse and beam radiation are strongly dependent on weather conditions. In sunny weather with clear skies, some 10- 20% of the radiation is diffuse. In cloudy weather with a lack of bright sunshine, most of the incident radiation is diffuse. The hourly diffuse radiation on a horizontal plane correlated to the hourly clearness index (K_t). Diffuse radiation can be determined from the product of clearness index and global radiation, and the equation for the correlation is given by (Erbs *et al.*, 1982).

$$\overline{H}_d = \overline{H}_g \begin{Bmatrix} 1.0 - 0.249K_t & for & K_t < 0.35 \\ 1.557 - 1.84K_t & for & 0.35 < K_t < 0.75 \\ 0.177 & for & K_t > 0.75 \end{Bmatrix} \text{-----------------(4.7)}$$

Where $\overline{H}_d$ = monthly average, daily diffuse radiation on a horizontal surface at a location

$\overline{H}_g$ = monthly average daily global radiation

$\overline{K}_t = \frac{\overline{H}_g}{\overline{H}_o}$, Known as monthly average daily clearness index

Table 4. 3 Monthly Average daily diffuse radiation ($kWh/m^2/day$) on horizontal surface

Month	Jan	Feb	Mar	Apri	May	June	July	Aug	Sept	Oct	Nov	Dec
$\overline{H}_d$	1.78	1.97	2.23	2.52	2.44	2.55	2.66	2.58	2.49	2.2	1.98	1.75

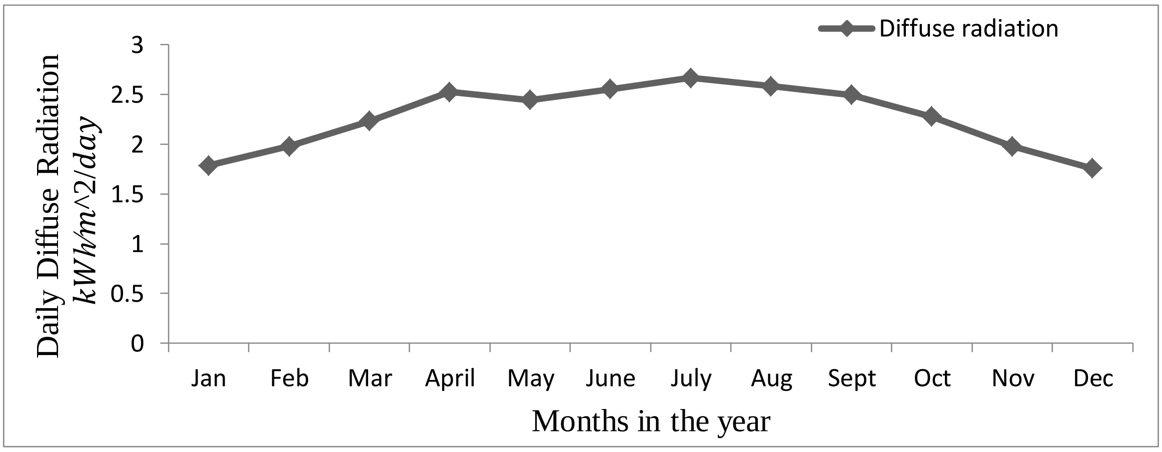

Figure 4. 3 Daily diffuse radiations on the horizontal surface of the site understudy

Hour Angle (ω)

The concept of hour angle is used for describing the rotation of the earth around its polar axis which is equivalent to +15 per hour during the morning and -15 in the afternoon. It is the angular distance between the observer's meridian and the meridian whose plane contains the sun. The following equation can be used to calculate the hour angle in degrees. It should be noted that afternoon the hour angle (ω) is zero.

$\omega = 15(12 - ST)$--(4.8)

4.1.4 Hourly Extraterrestrial Radiation on the horizontal surface

Extraterrestrial radiation is defined as the incidence of solar radiation outside the earth's atmosphere and is computed with the following equation: The Hourly Extraterrestrial Radiation, (I_o) on a horizontal surface at the specific location at a particular hour is may be obtained in (KJ/m^2h) by multiplying instantaneous radiation (Kw/m^2) by 3600.

$I_o = \frac{12\times3.6}{\pi} I_{sc}E_o \times \left((\sin\varphi\cos\delta) \times (\sin\omega_2 - \sin\omega_1) + \frac{\pi(\omega_2-\omega_1)}{180}(\sin\varphi\sin\delta)\right)$------(4.9)

where I_{sc} is a solar constant (1367 W/m2); E_o is the eccentricity correction factor; δ is the declination angle; φ is the latitude of location; ω_1 and ω_2 are the hour angle at the beginning and end of the time interval, where all angles are given in degrees. The eccentricity correction factor E0 can be calculated according to Spencer. The following series gives the equation for time (in minutes). For most engineering and technological applications, however, a very simple expression used by Beckman may be employed:

$E_o = 1 + 0.0033\cos\left(\frac{2\pi n}{365}\right)$--(4.10)

4.1.5 Hourly Global Solar Radiation on Horizontal Surfaces

The monthly average hourly global radiation for the representative days of the month on a horizontal surface can be calculated from the monthly average daily global radiation on a horizontal surface by using formulae from Collares-Pereira and Rabl for global irradiance.

$\frac{\bar{I}_g}{\bar{H}_g} = (a_1 + b_1\cos\omega)\frac{\bar{I}_o}{\bar{H}_o}$--(4.11)

Where

$\bar{I}_o$ & $\bar{H}_o$ are monthly average, hourly, and daily extraterrestrial radiation respectively that would fall at the location on the horizontal surface

$\bar{I}_g$ →Monthly average hourly global radiation on the horizontal surface

$\bar{H}_g$ → Monthly average daily global radiation on the horizontal surface

The value of a_1& b_1 may be calculated as follow

$$a_1 = 0.409 + 0.5016\sin(\omega - 60^\circ)$$

$$b_1 = 0.6609 - 0.4767\sin(\omega - 60^\circ)$$

ω →Hour angle at a particular time

$$\omega = (ST - 12)15^\circ$$

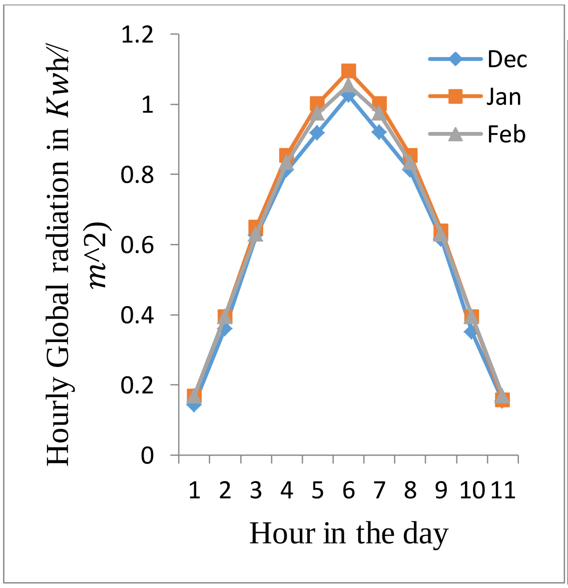

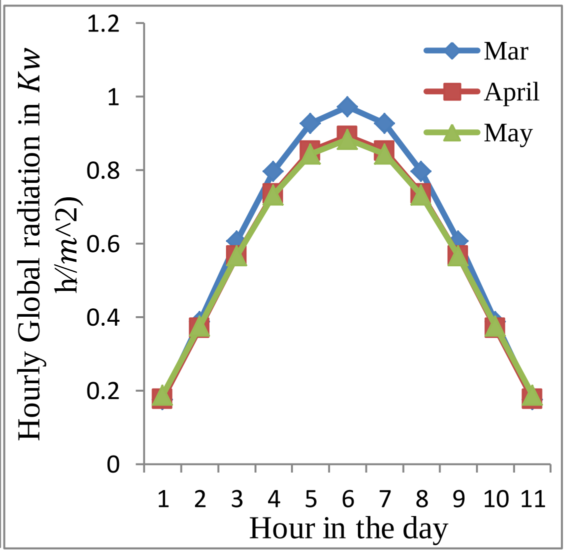

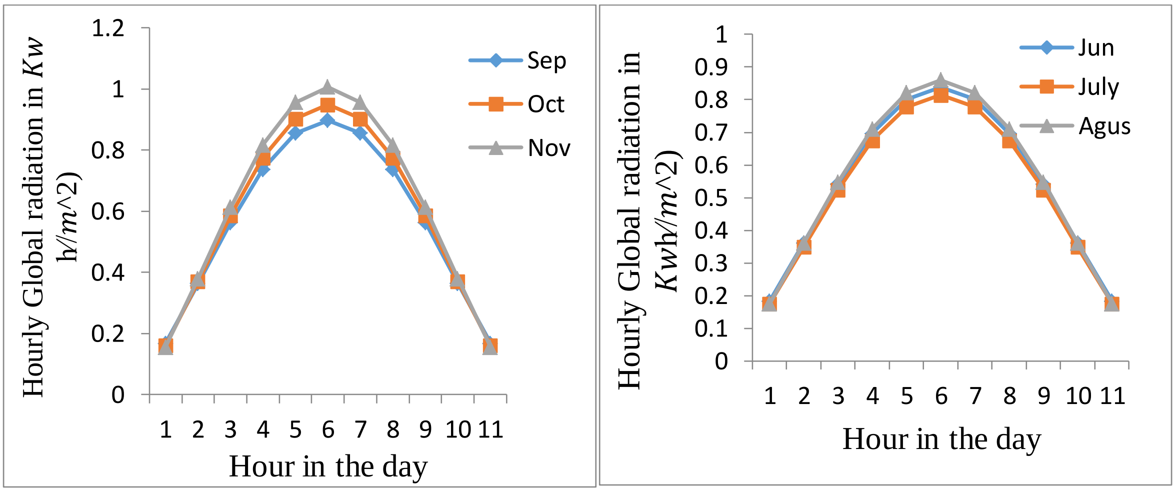

Figure 4. 4 Monthly averages, hourly global radiation of the village on the horizontal surface

From this figure 4.4, it's possible to conclude that hourly global irradiance is gradually increased from morning to its maximum value at midday and decreases to its minimum value in the afternoon. These figures also indicate that hourly irradiance is maximum during December, February, and January and minimum during the winter season, especially in July and August. Daily radiation can be obtained by adding hourly radiation each day in months.

4.1.6 Hourly Diffuse Radiation on Horizontal Surface

Diffuse solar radiation is a part of the sunlight that passes through the atmosphere and is consumed, scattered, or reflected by water vapor, dust particles, or pollution. This type of radiation cannot throw sharp shadows and therefore cannot be focused. Large numbers of meteorological/radiometric stations normally measure the received global irradiation on horizontal surfaces. It is not an easy task to collect such measurements, mainly due to the high price of the measuring equipment. For this reason, several mathematical models have been defined to estimate diffuse radiation on horizontal surfaces. The models that can determine diffuse radiation on horizontal surfaces can be classified into two types as follows:

$\bar{I}_d = (1 - 0.09K_t)\bar{I}_g \quad$ for $0 < K_t \leq 0.22$

$\bar{I}_d = \left(0.9511 - 0.1604K_t + 4.388{K_t}^2 - 16.638{K_t}^3 + 12.36{K_t}^4\right)\bar{I}_g$ for $0.22 < K_t \leq 0.8$

$\bar{I}_d = 0.165\bar{I}_g$ for $0.8 < K_t < 1$

Hourly clearness index (K_t) during a particular hour is the ratio of the hourly global radiation on the surface to the hourly extraterrestrial radiation on the surface during the same time.

$$K_t = \frac{I_g}{I_o} \text{---} (4.12)$$

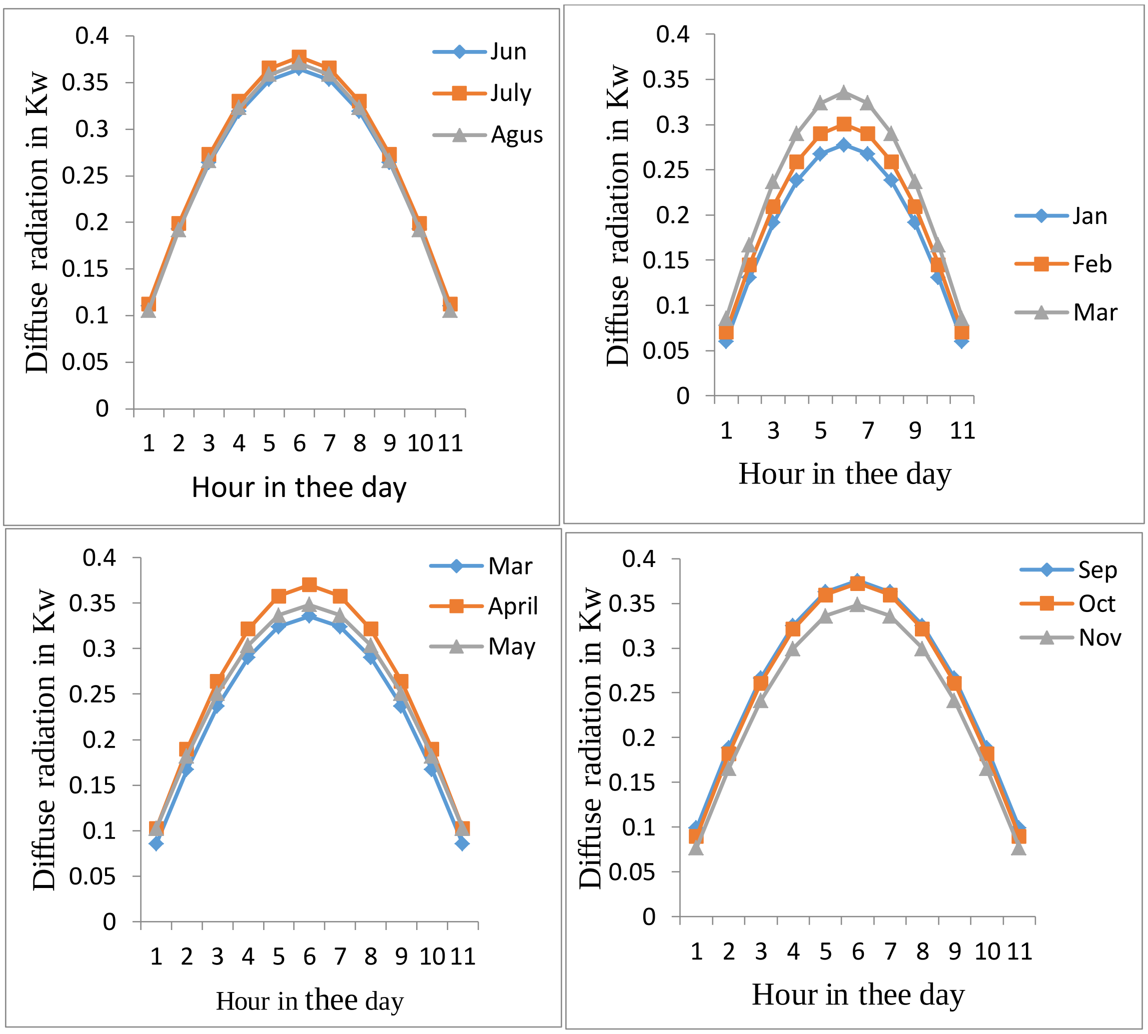

Figure 4. 5 Seasonally average hours diffuse ration on the horizontal surface of the site

Seasonally average hourly diffuse radiation is maximum in winter (June, July, and August) because these three months is a rainy month of the year. Hence maximum hourly diffuse solar radiation is absorbed by the cloud. In contrast to this summery season (sunny three months) have a minimum of diffuse radiation because during these three months the sky remains clear.

4.1.7 Determination of Incident Solar Radiation on PV Array

Once the radiation on the horizontal surface is known let calculate the global radiation striking the tilted surface of the PV array. The total radiation received by the PV module surface consists of direct radiation, diffuse radiation, and reflected radiation. The diffused radiation is a combination of three components (isotropic, circumsolar, and horizon brightening) and the reflected radiation is the radiation reflected from the surrounding ground or any other surfaces if exists. For this reason, different models had been proposed in the literature for estimating the total solar radiation incident on the PV module surfaces. One of the models has been proposed by Hay and Davies, Klucher and Reindl (HDKR model) and HOMER uses this model for simulation.

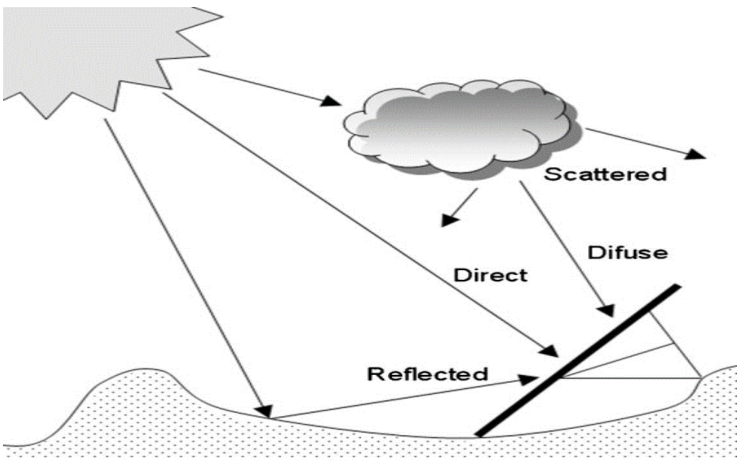

Figure 4. 6 Components of the solar radiation on the tilted surface (Keller and Costa, 2011).

4.1.8 Optimum Tilt Angle

The tilt angle is the angle between the south-facing solar panel and the horizontal line. To harvest maximum energy from the sun, solar panels must be inclined at ideal angles to gather the most extreme solar energy accessible in particular locations. This angle varies between $0\leq \beta \leq 180$. Tilt angle oriented south in the northern hemisphere and oriented north in Southern Hemisphere (Sunderan *et al.*, 2011). Estimating the solar radiation on inclined surfaces is a compulsory aspect in the tilt angle selection, which consequently determines the amount of solar radiation received by the PV module surfaces. Each location has a specific tilt angle that differs from other locations because one of the factors that highly affect tilt angle values is the latitude of the location. When a plane is rotated about the horizontal east-west axis with a single daily adjustment, the tilt angle of the surface will be fixed for each day and is calculated by the following equation. (Karafil *et al.*, 2016)

$\beta = |\varphi - \delta|$---(4.13)

The tilt angle of the summer season is found to be minimum and the tilt angle of the winter season is found to be maximum according to the seasonal optimum tilt angle calculation depending on solar angles. (Karafil *et al.*, 2016)

Table 4. 4 Monthly optimal tilt angle for panel

Months	Jan	Feb	Mar	Apr	May	Jun	Jul	Au	Sep	Oct	Nov	Dec
Tilt (β)	29.0	23.0	15.8	11.4	10.7	14	13.	9.8	10.7	17.6	27.0	31.1
Ave.	$17.8333 \approx 18^0$											

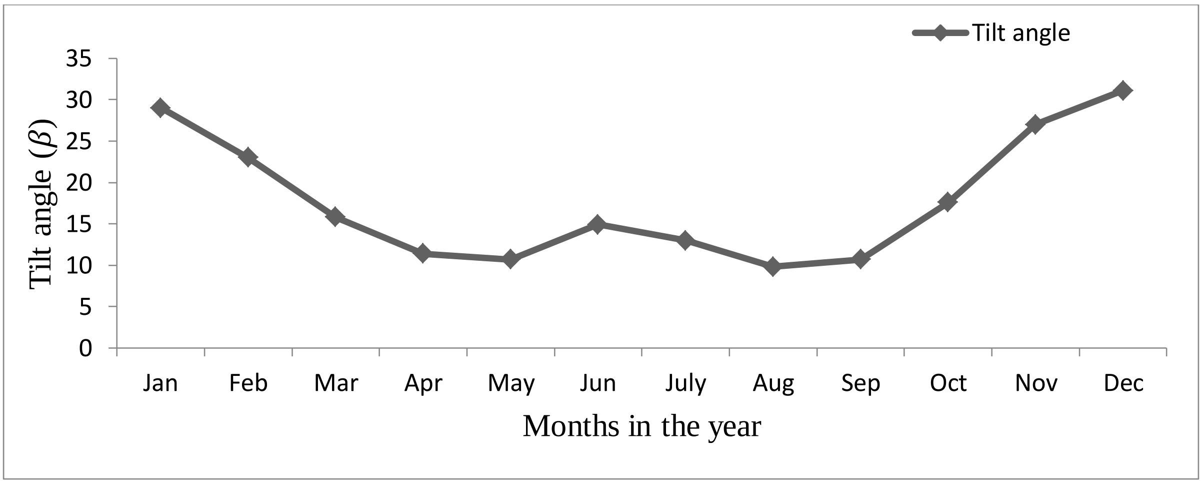

Figure 4. 7 Monthly optimal tilt angles for panel

4.1.9 Hourly Global Solar Radiation on an Inclined Surface

Beam radiation ($I_{b\beta}$), reflected radiation (I_r), and diffuse radiation ($I_{d\beta}$) are the three components of the global solar radiation incident on an inclined surface (I_β). The fraction of incident radiation reflected by the ground is called reflected radiation.

$I_\beta = I_{b\beta} + I_{d\beta} + I_r$--(4.14)

Generally, diffuse radiation models for inclined surfaces can be classified into two groups: Isotropic and anisotropic models. They differ in the division of the sky into regions with normal and elevated diffuse radiation intensities. Isotropic models assume there is uniformity in the distribution of diffuse radiation intensity over the sky. Anisotropic models include appropriate modules for representing areas of elevated diffuse radiation.

4.1.10 Hourly Diffuse Radiation on Inclined Surface

Another anisotropic model is the one proposed by Hay and Davies, which is commonly referred to as the Hay model. Two primary sources are assumed to be the origins of sky diffuse radiation, namely the disc of the sun disc and the rest of the sky with isotropic diffuse radiation Klein, 1997). The two components are described by the anisotropy indexf_{Hay}:

$$f_{Hay} = \frac{I_b}{I_o} = \frac{I - I_d}{I_o}$$

Based on the Hay model, the equation for the intensity of diffuse radiation on an inclined plane has the form.

$$I_{d\beta} = I_d \left[f_{Hay} \left(\frac{\cos\theta}{\cos\theta_z} \right) + \left(\frac{1+\cos\beta}{2} \right) \left(1 - f_{Hay}\right) \right] \text{--}(4.15)$$

4.1.11 Estimating Hourly Ground-Reflected Radiation on an Angled Surface

Part of the global solar radiation that is reflected by the earth's surface and any other intercepting An object is called ground-reflected radiation.

$$I_r = I_g \rho \left(\frac{1-\cos\beta}{2} \right) \text{---}(4.16)$$

Determining the appropriate ground albedo is the main concern of users modeling this component, where ρ is the ground albedo (Gueymard, 1987). Throughout the day, the ground albedo varies due to several factors, such as deviations from Lambert's law of isotropy and variations in ground properties (e.g., snow cover or soil water content).

Finally, total hourly irradiance in the plane of PV array tilted with the tilt angle of (β) can be calculated as

$$I_\beta = r_b I_b + I_d \left[f_{Hay} \left(\frac{\cos\theta}{\cos\theta_z} \right) + \left(\frac{1+\cos\beta}{2} \right) \left(1 - f_{Hay}\right) \right] + I_g \rho \left(\frac{1-\cos\beta}{2} \right) \text{-------------------}(4.17)$$

Where $r_b = \frac{\cos\theta}{\cos\theta_z} = \frac{\sin\delta\sin(\varphi-\beta)+\cos\delta\cos(\varphi-\beta)\cos\omega}{\sin\delta\sin\varphi+\cos\delta\cos\varphi\cos\omega}$.

The following graph shows hourly solar radiation on a tilted surface for the representative days of each month seasonally for better clarity and annual hourly solar radiation is shown below

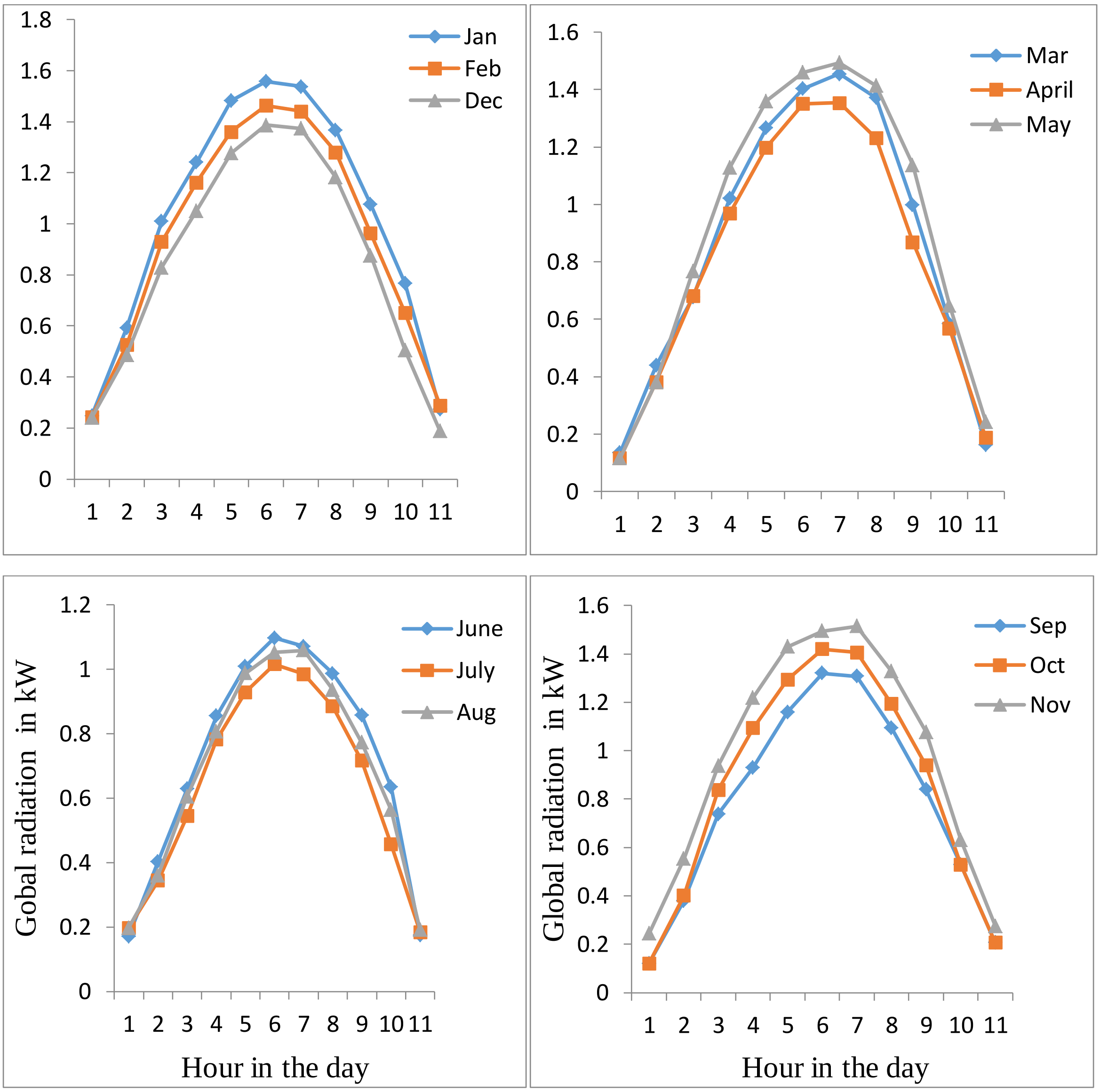

Figure 4. 8 Hourly global radiation reach on tilt surface Vs hours of the day.

Figure 4.8 and 4.9 below shows months with maximum and minimum hourly solar radiation of the site for the recommended day of the months respectively

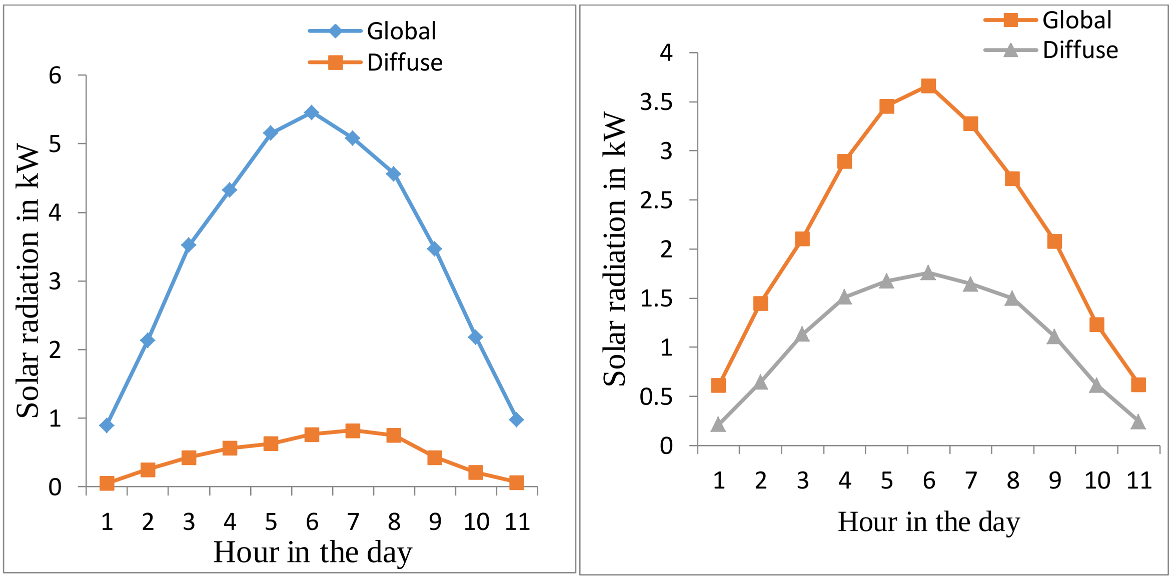

Figure 4. 9 January 17 and July 17, hourly solar radiation on the tilted surface of the site respectively

The above two figures indicate that hourly solar global and diffuse radiation for maximum and minimum sunshine duration of the month respectively. As it's observed from the figure global solar radiation is maximum in January and minimum in July (rainy month) of the year, while diffuse radiation is maximum in July month and minimum in January. This shows that July is cloudy months thus why most of the radiation is diffuse radiation.

4.1.12 Average Solar Power Potential of the Site

Once tilted irradiances for all hours of the day are computed, the daily total H_β obtained by summing values for individual hours. . The maximum daily global radiation on the horizontal surface and the tilted surface is 7.23(kWh/m^2) and 10.5 (kWh/m^2)as shown in figure 4.2 and figure 4.10 on January 17 respectively and this value confirms with maximum sunshine duration is recorded in January. Minimum sunshine duration 6.54 h is recorded on July 17 and total daily global radiation on a horizontal surface is 5.05(kWh/m^2) and 7.03 (kWh/m^2) on the tilted surface as shown in the below figure 4.2 and 4.10.

Table 4. 5 Total daily solar radiation in (kWh/m^2) reaching tilted surface

Month	Jan	Feb	Mar	April	May	June	July	Aug	Sep	Oct	Nov	Dec
Tilt Rad.	10.5	10.2	9.36	8.19	8.23	7.13	7.03	7.5	8.62	9.43	10.0	9.4

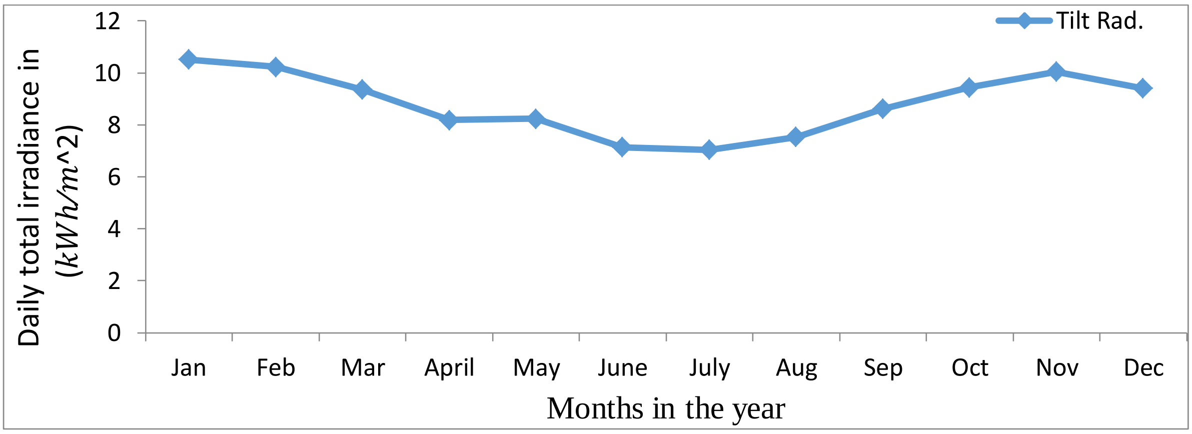

Figure 4. 10 Monthly mean daily solar irradiances in the plane of PV for the site of the study

As calculated in chapter four the site understudy has a very huge potential of annual average solar radiation of 6.31 kWh/m^2 /day and the average clearness index was found to be 0.519. From the above figure 4.10, it's possible to conclude that daily solar radiation of the site is maximum during the summery season especially during January, February, December, and November, and minimum during the winter (rainy) season of the country and in contrast, this site is blessed with rain which in turn there is the maximum water flow rate of the river.

4.2 Wind Potential Analysis

4.2.1 Wind System Energy Productivity

The wind energy is extracted by using an appropriate wind turbine and wind turbine then converts the kinetic energy of moving air into rotational mechanical shaft energy. The rotational energy of shat is then converted into electrical energy through the transmission system. The transmission system consists of the rotor shaft with bearings, brake(s), an optional gearbox, as well as a generator and optional clutches (Lackner *et al.*, 2010). The energy available in the wind can be expressed using the equation.

$$P_w = {}^{1}/_{2}\,\rho A V^3 \text{---} (4.18)$$

where P_w is extracted wind power(W)

ρ =Density of air $({}^{kg}/_{m^3})$

A= the swept area (m^2)

V=instantaneous wind velocity (m^3)

Energy conversion from free-flowing fluid streams is limited because full energy extraction implies a decrease of fluid velocity (decrease of the kinetic energy of the stream), down to zero which is impossible. Some fluid may not pass through the turbine and may simply flow around it (bypass it). This limitation is expressed in terms of the Betz limit defined by the power coefficient C_p and it is defined as the ratio of actual power developed by the rotor to the theoretical power available in the wind and it is given by the equation:

$C_p = \frac{2P_T}{\rho A_T V^3}$---(4.19)

where, C_p= power coefficient

P_T= the actual power developed by the turbine

A_T= Area of turbine

4.2.2 Rotor Swept Area

The area over which the sweeping blades can capture the wind is known as the rotor area of the wind turbine. The rotor area decides how much energy a wind turbine is capable to produce from the wind. Since the rotor area increase with the square of the rotor diameter, a turbine that is twice as large will receive four times much energy. Besides, the energy on the wind is proportional to the cube of the wind speed.

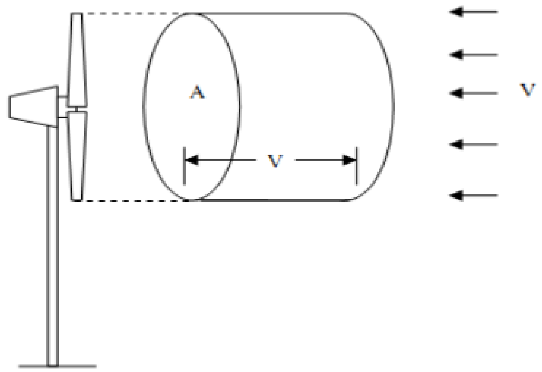

Figure 4. 11 Rotor swept area and Air parcel moving towards a wind turbine (Muralikrishna et al., 2008)

Rotor swept area is given by

$$A = \frac{\pi D^2}{4} = \pi r^2$$

Where r is the radius of the rotor and D diameter of the rotor;

To generate electricity from the wind the load is the transmission load (gearbox) and electrical generator load

$P_{Tout} = \eta_t C_p \, {}^1\!/_2 \, \rho A V^3$---(4.20)

where: P_{Tout}= output power of wind turbine

η_t =Overall efficiency (transmission system/power train and generator efficiency)

C_p=the power coefficient

Where $C_p = \left(1 + \frac{v_o}{v}\right)\left(1 - \frac{v_o}{v}\right)$and it is known as the power coefficient of the motor or rotor efficiency. The value depends on the ratio downstream to the upper stream wind speed. v and $v_o$are upstream and downstream wind velocity respectively. It is the entrance of the rotor loaded and downstream wind velocity at the exit of the rotor blades respectively (Erich Hau, 2006).

The power coefficient and efficiency of wind turbines vary greatly from manufactures to manufacturers. As a result, the power output of wind turbines varies from the turbine to the turbine and is given by a power curve that plots the output power of a turbine against wind speed. The wind speed at which the wind turbine starts generating electrical power is called the cut-in wind speed. The rated wind speed is the wind speed at which the turbine operates at its maximum efficiency of energy conversion. Rated power is the power output at equal to, or above, the rated speed.

$P_{Eout} = C_p \eta_g P_{wT}$---(4.21)

4.2.3 Site Selection for Wind Power

The power extracted from the wind turbine has a direct relationship with wind speed; hence selecting a suitable location for installation of the wind turbine is must be located at an area with strong and constant wind speed. Even though daily wind speed is changing from time to time, its monthly or year output may remain constant over the selected area. Nevertheless, the most suitable site for wind turbines would be found in areas where the annual average wind speeds are known to be moderately high and Some of the main consideration (Technical, Economic, Environmental, social and other factor are examined before a decision made to erect a generating plant on specific).

High annual average wind speed is the most basic requirement for the successful use of wind energy conversion systems. The wind velocity is the critical parameter. Anemometer data is normally based on wind speed measurement from a height of 10m. For the most accurate assessment of wind power potential, anemometer data must be obtained at the precise site and hub height for any proposed wind energy conversion system.

Altitude It affects the air density and thus power in wind turbine and hence the useful wind energy conversion system electric power output. Also, as it well knows, the wind tends to have higher velocities at a higher altitude as it has discussed in the previous section.

Distance to road and load Center. This is another factor the system engineer must consider for heavy machinery, structure, material, blade, and other apparatus will have to travel into any chosen wind farm project site. Similarly, the nearness of the site to the local center has a vital role in choosing the most likely wind farm site. The near to local center has advantages and minimizing transmission line length and at the same time minimize both transmission cost and transmission power loss.

Visual Aspect One of the more obvious environmental effects of wind turbines is their visual aspects. This is more important when concern more for visual value. From Experience most of wind turbine has good design and the use of subdued neutral colors "off white" is popular to minimize this effect. Thus, even if it has less impact on the aesthetic view it should need to give attention while selecting wind farm projects.

4.3 Micro-hydropower Potential Analysis

To determine the power potential of water in a stream it is necessary to know the flow quantity of water available from the stream and the available head. Head is the vertical difference in level (in meters) through which the waterfalls. The theoretical power (p) available from a given head of water is in exact proportion to the head and the quantity of water available. As in the case of solar and wind the steam flow rate of the river is not varying from hour to hour or even though it changes from day to day the change is small. So the daily power out from micro-hydro power remains constant for each day of the while it varies from month to month.

4.3.1 Theoretical Power of Hydropower

Theoretically, the power output of the micro-hydro is expressed by considering head and steam flow, the magnitude of the hydropower can be expressed in an equation as follows:

$$P_{theo} = \rho g Q h_g \text{--} (4.22)$$

where, P_{theo}=theoretical power output, ρ= density of water (kg/m^3), Q flow rate (m^3/s), h_g=gross head (m). Using collected data from chapter three (gross head and flow rate)

$$P_{theo} = 1000\,Kg/m^3 * 9.81m/s^2 * 15m * 0.21\,m^3/s$$

$$P_{theo} = 30.974 \text{ kW.}$$

This indicates that micro-hydropower is not sufficient to satisfy the electricity demand of the village under study which requires 3211 Kwh per day energy consumption. For micro-hydro power potential analysis 15m height head of river is used. Because of 30m head is far away from the village, the location of river is not suitable for installation of turbine and its water flow rate is not high as that of 15m head run of river.

4.3.2 The Efficiency of the System

The overall efficiency of the micro-hydro power system is the product of turbine efficiency η_t , drive system (gear) efficiency and generator efficiency η_g . The recommended efficiency of the hydro turbine, gearbox, and generator efficiency is presented in the following table. It's known that the efficiency of a selected turbine (crossflow turbine) is in the range of 65-85 % and whiles the efficiency of the gearbox also varies from 85-95 % for better performance of hydropower production.

Pelton 5-30 kW: 70-80%, Pelton above 30 kW: 75-85%, Cross-flow 5-30kw: 60-70, Cross-flow above 30 kW: 65-85%

Table 4. 6 Overall efficiencies of the micro-hydro power system (ESHA, 2007)

No	Type of components		Efficiency (%)
1	Crossflow turbine	5-30kw	60-70
		More than 30kw	65-78
2	Gearbox		95
3	Generator		93

Overall efficiency the hydropower system

$$\eta = \eta_{chanal} * \eta_{penstock} * \eta_{turbine} * \eta_{generator} * \eta_{gear\ ratio} * \eta_{transmission\ line} \text{-------(4.23)}$$

$$\eta = 0.95 \times 0.9 \times 0.68 \times 0.95 \times 0.93 \times 0.9 = 0.5778$$

CHAPTER FIVE

SIZING AND MODELING OF HYBRID ENERGY SYSTEM COMPONENTS

System design is the process of determining the size of each component of a standalone photovoltaic, wind turbine and micro-hydropower system to meet the load requirement. System design the system shall not either oversized or undersized.

Total Load of Magna Lege Buna Village, $Total\ Load = 2470\ KWh/day$

Assuming 30% for losses and reserve capacity in case of a sudden load increase in the future. Then total energy from all sources (i.e. solar PV, wind and Micro-hydro).

$$Total\ Load = 2470\ KWh/day * 1.3$$

$$Total\ Load\ = 3211\ KWh/day$$

The use of three renewable sources causes the energy generation to be divided into three parts. Let's assume 45% of the daily energy demand is to be contributed by solar panels, 35% from the wind turbine and the remaining 20% from micro-hydropower generation of the system. Then the total energy demand is 3211 KWh/day and 45% of total energy become 1445 KWh/day; have to supplied by solar and 35% of total energy demand is 1123.85 KWh/day that required to be obtained from the wind while the remaining 20% of total energy demand is from micro-hydro and its value is 642.2 KWh/day. The basis for assumption is availability of potential of resources in the village and cost of installation and maintenance. The parameter for percentage of assumption is initial capital cost of installation and available potential of renewable energy resources in the village as per data collected and analyzed.

5.1 Mathematical Modeling and Sizing of PV System for the Site

PV system design methods are procedures, techniques, aids, or tools for designing. In this study, all the steps required for designing and sizing of the stand-alone PV system is considered. For this PV system design solar panel, solar charge controller, solar battery, and solar inverter were chosen from the market as a reference which used in sizing our system.

5.1.1 Site Inspection

Site inspection is the most predetermined case of the design because it helps to determine whether a stand-alone system is viable or not. The factors influencing power generation from the PV system are irradiation, PV material, size and capacity of module and temperature. At constant temperature power generation from PV System increases with increasing irradiation. So, the site location should be inspected to know the number of sun days per year.

5.1.2 Load Requirements

Determining the load of the village is also an important point in designing a PV system because it helps to know how powerful a PV system required for satisfying clients' demands. The load is determined by listing all appliances with their power ratings and operation hours then summing it to obtain the total average energy demand in watt-hours or kilowatt-hours. Table 3.10 gives ideas of how to estimate the load and since the daily energy required from the solar photovoltaic array is 1445 Kwh/day.

$$Eeq = 1445\ Kwh/day$$

5.1.3 Solar System Module Sizing

The minimum number of PV modules required is equal to the total of energy required from the PV module divided by the product of power fact generation and watt-peak of PV module available for you. Several PV modules for the system is the ratio of total watt-peak rating requires operating the appliance to the watt-peak of the PV module available for you.

$$Nm = 1module \times \frac{watt\ peak\ rating}{rated\ out\ put\ of\ the\ PV\ available} \text{--}(5.1)$$

The total watt-peak rating required to operate the appliances is equal to the total PV energy required from the panel divided by the worst month of sunshine hours and correction factor (f_t) since the temperature of PV is not constant. Hence the worst month sunshine hour is 6.54 h/day and the correction factor$(f_t = 0.89)$.

$$P_{peak} = \frac{daily\ energy\ required}{minimum\ sunshine\ hours \times correction\ factor} \text{--}(5.2)$$

$$P_{peak} = \frac{1445\ \text{Kwh/day}}{6.54\ \text{h/day} \times 0.89}$$

$$P_{peak} = 248kW.$$

Table 5. 1 The specification of Selected PV panel (Alibaba supermarket.com)

Solar PV Panel Specification	
Manufacturer	Sun power

Model Name	Sun power X21-335-BLK
Cell Type	Mono-crystalline Silicon
Numbers of Cell	72 Cells
Maximum Power Rating STC	335w
Open Circuit Voltage VOC	47.2 V
Short Circuit Current ISC	9.76A
Maximum Power Voltage Vm	38.9V

Since wattage power output of solar panel mostly varies between 250w and 400w for the more efficient module, Let select panel with a rated output of the panel is 335W [Rajput and Sudhakar, 2013].

$$Nm = 1module \times 248kw/day/360w$$

$$Nm = 741 \ \ panels.$$

The minimum number of PV panels required is 741 PV panels. If more PV modules are installed, the system will perform better and battery life will be increase. So, this system should be powered by at least 741 modules of 335Wp PV module. Based on system demand Solar PV module can be connected either in series, in parallel, or both. This mainly depends on the desire voltage or current. The number of the series module can be determined by dividing system DC voltage by solar PV module rated voltage and computed as follows,

$$N_{series} = \frac{system\ Dc\ voltage}{rated\ module\ voltage} \text{--(5.3)}$$

$$N_{series} == \frac{96v}{24v} = 4 \text{ Panels}$$

$$N_t = N_s \times N_p \text{---(5.4)}$$

$$N_p = N_t/N_s = 741/4 = 185.25 \approx 186 \text{ Panels}$$

$$N_p = 186 \ \ panel\ required\ in\ parallel$$

Hence,

$$P_{array} = N_s \times N_p \times P_{module}$$

$$P_{array} = 4 \times 186 \times 335w \times 6.54h = 1630.03\frac{\text{kWh}}{\text{day}}.$$

Since the designed PV array output is greater than the daily energy demand of the village from the solar panel the calculated number of panels is safe**.**

5.1.4 Battery Bank Sizing

Battery bank sizing is one of an important parameter in designing the standalone solar system because during the night (no sunshine) and cloudy day energy must be supplied to the appliance to perform its activity so, it’s used as a backup in the system and to maintain a constant voltage during peak loads or a shortfall in generation capacity. An off-grid hybrid system requires a storage (backup) system to store energy for later usage when there is no supply of energy from renewable energy resources. Back up energy utilization and maintaining the constant voltage of the system during peak load and shortage of energy is the primary function of the battery. There are two types of battery primary battery and secondary battery. Primary batteries are used and throw batter or battery used for one time only and the secondary battery is a rechargeable battery of renewable energy system as in case of this study. The voltage of the battery may not maintain constant during the charging and discharging process.

The battery bank system voltage can be 12volts, 24 volts, 48 volts or 96 volts depends on the amount of voltage your solar system produces. The desired battery capacity depends on the total energy that the battery bank must supply to loads, Maximum power demand, maximum depth of discharge, System voltage and Charge current and recharge time. The amount of energy required to be stored by the battery is the product of energy that must be delivered by PV array and the maximum autonomy days.

$$E_{sb} = E_{req} \times n \text{--(5.5)}$$

Autonomy is the number of days that you need the system to operate when there is no power produced by the PV panel as a result of rainy or cloudy days. It means back up the storage of the system.

$$Battery\ size\ = \frac{energy\ required \times autonomy\ day}{batter\ losses \times DoD \times voltage\ of\ system} \text{--(5.6)}$$

$$Battery\ size\ with\ 3\ days\ of\ autonomy = \frac{E_{req} \times n}{0.85 \times 0.6 \times V_{system}}$$

Where;

0.85= battery loss

0.6=depth of discharge

V_{system} = Our system voltage i.e. 96v

C = Battery bank capacity or energy required per day from PV panel in wh.

n =Autonomy days

$$Battery\ size\ with\ 3\ days\ of\ autonomy = \frac{1445000wh/day \times 3day}{0.85 \times 0.6 \times 96v}$$

But in electrical terms $1w = 1vA$

$$size\ of\ batter = 88541.66\text{Ah}$$

This is the amount of energy that a battery can store and the major specification to determine how a big batter is required to run the system. Now let calculate the number of batters required for the system. If the capacity of our battery system is 1000A

$$Number\ of\ batter\ required = 1\ battery \frac{battery\ bank\ capacity}{nominal\ capacity\ of\ selected\ battery} \text{--------(5.7)}$$

$$N_b = 1\ battery \frac{88541.66Ah}{1000Ah}$$

$$N_b = 88.9 \approx 89 \text{ batteries.}$$

These batteries are connected either in series or parallel connection to store the required energy for the appliance for later usage.

$$N_{bs} = \frac{V_{syst}}{V_{bat}} \text{--(5.8)}$$

$$N_{bs} = \frac{96v}{12v} \approx 8batteries$$

$$N_{bp} = 1battery \frac{N_{bt}}{N_{bs}} \text{--(5.9)}$$

$$N_{bp} = 1battery \frac{89}{8} \approx 12batteries$$

The battery chosen from the HOMER storage tool for this study is Iron Edison LFP 1400Ah -48V. It is a 48V battery with a nominal capacity of 1400 Ah (67.2KWh). Iron Edison LFP 1400Ah was chosen for its highest capacity and availability in the local market.

5.1.5 Hourly Energy Storing Capacity of the Battery

Because of the random behavior of PV panels, the battery bank capacity constantly changes correspondingly in the hybrid system. In such a system, the state of charge of the battery is acquired as follows: When the total output of PV panels, wind generators, and micro-hydro is greater than the load energy, the battery bank is charging state (Maleki and Askarzadeh 2014). The charge quantity of the battery bank at time t can be obtained by

$$E_{Ba(t)} = E_{Ba}(t-1) \times (1-\delta) + \left[E_{PV}(t) - \frac{E_{load}(t)}{\eta_{inv}}\right] \times \eta_{Ba} \text{-----------------------------(5.10)}$$

Where $E_{Ba(t)}$ *and* $E_{Ba}(t-1)$ are the charge quantities of battery bank at time t and t-1, δ is the hourly self-discharge rate, η_{inv} denotes the inverter efficiency, $E_{load}(t)$ is the load demand at time t, and η_{Ba} is the charge efficiency of the battery bank.

When the total output of PV panels, micro-hydro and wind generators is less than the load demand, the battery bank is discharging. For this thesis, the discharge efficiency of the battery bank is assumed to be 1.

$$E_{Ba(t)} = E_{Ba}(t-1) \times (1-\delta) - \left[\frac{E_{load}(t)}{\eta_{inv}} - E_{PV}(t)\right] \text{------------------------------------(5.11)}$$

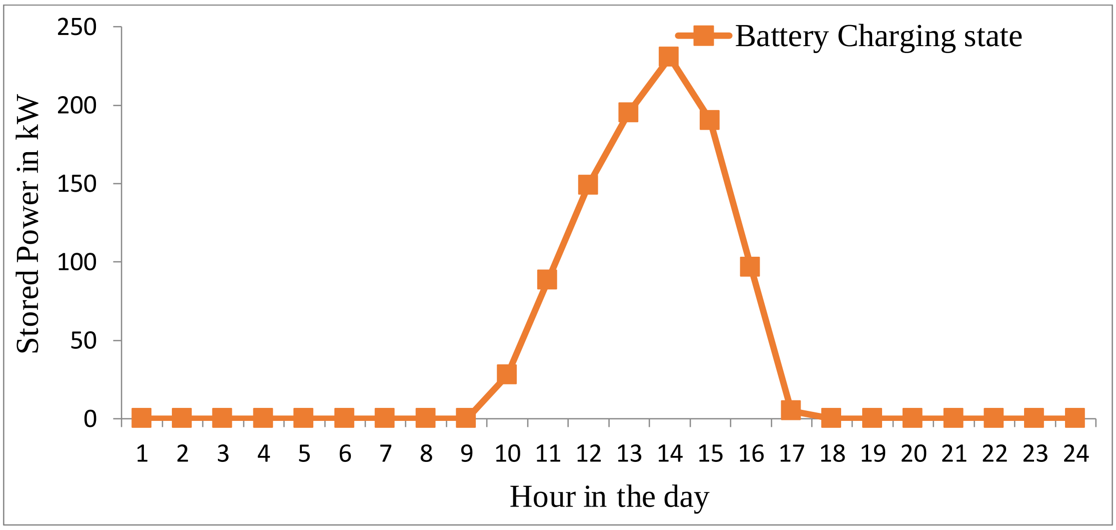

Figure 5. 1Energy storing potential of the battery

5.1.6 Sizing of Charge Controller

Selecting appropriate charge controller to match the voltage of the PV array and the battery is very important. Its known that function of a charge controller is to regulate the charge going into battery bank from solar panel array and prevent overcharging and reverse current flow at the night. The charge controller rating is equal to the product of several batteries in parallel, the short circuit current of the PV module available and the safety factor. Where safety factor 1.3.

$$I_{rated} = \left(N_{bp} \times I_{sec}\right) \times 1.3 \text{--(5.12)}$$

Where I_{rated} solar charge control rating

N_{bp} Number of battery in parallel

I_{sec} Short circuit current

$$I_{rated} = 12 \times 9.76A \times 1.3$$

$$I_{rated} = 152.25A$$

Number of controllers required for the system

$$N_{controller} = \frac{I_{rated}}{amper\ of\ each\ controller} \text{--} (5.13)$$

By assuming the ampere of single charge controller to be is to be 10 since its ranges between 1 to 60 amperes, then

$$N_{controller} = 15.22 \approx 16 \text{ controller}$$

5.1.7 Sizing of Inverter

The primary function of the inverter is to convert DC electricity of solar panels to clean AC electricity for running various appliances or local transmission of electricity. If the power rating of the inverter is less than the total power of the electrical load our system will be overloaded so the inverter rating should be 25%-30% greater than the power of appliances. Input rating of inverter should never be lower than a total watt of power consumed by the appliance and it must have the same nominal voltage as that of system battery. The size of the inventor on market is range from 500w-10kw for domestic application. Investors may also be classified based on the input they accept as 12v Dc, 24v DC, 48v Dc, and even 96v Dc. From this, the widely used inventor is 48v Dc inventors.

$$I_{size} = \frac{Total\ power\ of\ appliance \times 130}{100} \text{--} (5.14)$$

$$I_{size} = \frac{1445kw \times 130}{100} = 1878.5kw$$

So the required inverter size equals 1878.5k W or a little bit greater than 1878.5 kW.

5.1.8 Sizing of Cable

Cable sizing is important to match the type of wire need to use with the current which will pass through it. That is why cable sizing is a very important. For this thesis its proposed that copper wire is the selective cable for transmission line. The cables cross-sectional are determined by the following equation:

$$A_w = \frac{\rho \times L \times I}{V_d} \text{--} (5.15)$$

Where, A_w the cross-sectional area of the wire

ρ resistivity of the wire

L length of wire

I rated current of the wire

V_d voltage drop

Table 5. 2 Results obtained from the sizing of the proposed standalone PV system

Components	**Description of components**	**Result**
Site inspection	Installation must around area free from tree shadow	50m away from sinkile river
Load estimation	Total energy required from PV panel	1445Kw/day
PV array	array capacity	335w
	Number of modules in series	4
	Number of modules in parallel	186
	Total number of modules	741
	Module area	1.26 m^2
	PV module installation area	932 m^2
	Operation Temperature Range-Charge	0-45
	Efficiency	21 %
Battery sizing	Battery bank capacity	88541Ah
	Number of batteries in series	8
	Number of batteries in parallel	12
	Total number of batteries required	89
	Efficiency of battery	95%
Invertor	Capacity of inventor	1878
	Efficiency	94%

5.1.9 Overall Efficiency of PV System

The overall efficiency of the PV system is affected by all components of the PV assembly since power is absorbed by the PV module and when the conversion process of DC into AC for a domestic appliance. The overall efficiency of the panel is the product of the efficiency of the module, efficiency of the controller, the efficiency of the inventor, and efficiency of the battery.

$$\eta_{pv} = \eta_m \times \eta_c \times \eta_i \times \eta_b \text{-----------------(5.16)}$$

Where η_{pv} is the overall efficiency of the PV panel

η_m is the efficiency of the module

η_i is the efficiency of the inventor

η_c is the efficiency of controller and η_b is the efficiency of battery storage

5.1.10 Determination of Selected PV Array Power Output

The PV module generating electrical power depends on the total solar radiation G_T incident on the PV surface, which in most cases is not horizontal but inclined to have higher energy production, better condition for module cooling. Power out from solar PV panels depends on the type of material from which the module is made, light intensity (sunshine duration), temperature of the location, area of PV panel and other many environmental factors such as shading, accumulation of dust and cable losses of the circuit.

Photovoltaic panels convert solar radiation to electricity with efficiencies in the range of 5% to 20%, depending on the type of the cell. The power out of the PV system at each hour is calculated by

$$P_{pv} = Y_{pv} f_{pv} A_{array} [1 + \alpha_p (T_c - T_{c,stc})] \left(\frac{G_T}{G_{T,stc}}\right) \text{---(5.17)}$$

where Y_{pv} is the rated capacity of the PV module (power output under STC conditions).

f_{pv} is the PV derating factor introduced taking into account additional factors affecting PV (soiling, losses, shading, snow cover)

α_p is the PV temperature coefficient for the power (%/°C).

T_c is the PV module instantaneous temperature.

$T_{c,stc}$ is the PV module temperature (°C) at STC.

G_T is incident solar radiation

$G_{T,stc}$ is the incident radiation at standard test conditions.

Standard Test Conditions (STC) properties (solar radiation of 1000 w/m^2, PV cell temperature of 25°C, and no wind). Further when information about PV module temperature is not known (if the effect of module temperature is neglected).

$$P_{pv} = Y_{pv} f_{pv} A_{array} \left(\frac{G_T}{G_{T,stc}}\right) \text{---(5.18)}$$

Table 5. 3 Total solar panel output of the site (W)

Jan	Feb	Mar	Apr	May	Jun	July	Aug	Sep	Oct	Nov	Dec
306.7	298.1	288.8	280.8	274.7	272.8	274.6	278.5	285.3	293.3	302.0	308.5

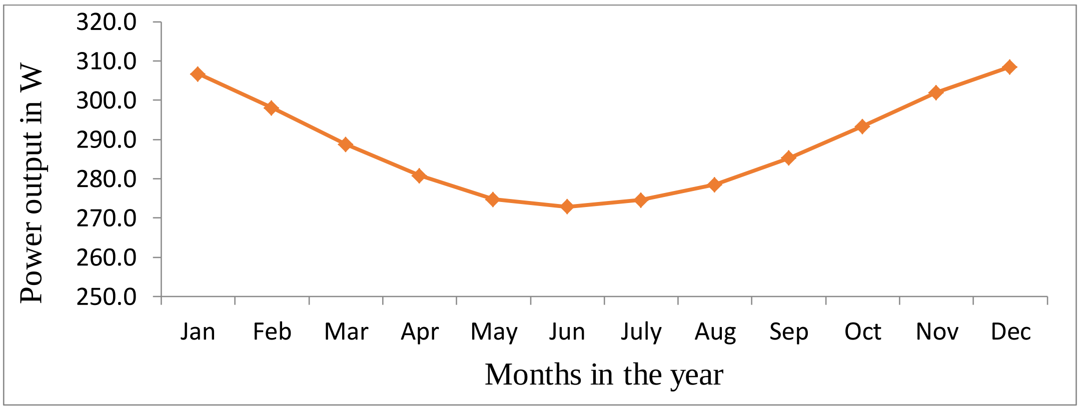

Figure 5. 2 Monthly average PV panel power output of the selected module

The above figure 5.2 indicates that power produced by PV panel is minimum especially during the winter season (June, July, and August) but in contrast, the water flow rate is maximum during this time since its rainy season as a usually in every side of our country. So using a hybrid system of energy supplying methods is the crucial way of supplying continuous electricity for the end-users. Hourly usable output energy from Solar panel is given by the following equations

$E_{PV} = A_{PV} \times r_{PV} \times H_{\beta} \times P_R$--(5.19)

Where E_{PV} is energy in kWh

A_{PV} total solar panel area m^2

r_{PV} The efficiency of PV module

H_{β} Hourly solar radiation on the tilted surface (kWh/m^2)

P_R Performance ratio (losses due to inventor, battery, charge regulator,temperature, shading, accumulation of dust and snow, cable loss and any other losses.

The hourly power out from PV panel for the site by considering all above factor is attached to the end of documents in appendix F.

5.2 Mathematical Model of Wind Energy Components

5.2.1 Wind Turbine Sizing and Selection

Power can be extracted by the wind turbine through the following sequences.

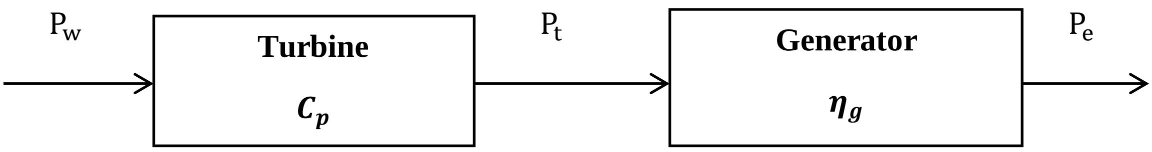

Figure 5. 3 Wind electric systems

$\text{Pwind} = {}^{1}/_{2}\,\rho A V^3$--(5.20)

Where $Pwind$ is the power extracted by the wind turbine, V is the average wind speed of the site, A is the swept area of the rotor diameter, ρ is the air density and its value at sea level is 1.225 kg/m^3 at normal atmospheric pressure. The swept area of the rotor diameter can be obtained from equation 3.10 which is shown below.

$$A = \pi r^2 = \frac{\pi D^2}{4}$$

$P_{turbine} = C_p \times P_{wind}$---(5.21)

$$P_{turbine} = \frac{1 * C_p \rho A v^3}{2}$$

Finally, Hourly electrical power output by wind generator with rated power output is defined by the following expression:

$P_{electical} = \eta_g * P_{turbine}$--(5.22)

$$P_{electical} = \frac{1}{2}\rho_{wind} A v^3 C_p * \eta_g$$

Where

ρ_{wind} - is the density of air in 1.22 kg/m^3

A - is the swept area (m^2).

v - is the wind speed (m/s)

Cp - is the coefficient of performance which has equal to 0.593,

η_t - is the wind turbine efficiency

ηg is the efficiency of the generator. Since power to be dileverd by PV system is known, the next stage is determining the power supplied by wind turbine and its fundamental dimension such as rotor diameter. Known that wind turbines produce instantaneous power, wind turbine size will be determined using average power of daily energy demand from wind. Hence average power demand from wind turbine of Magna Lege Buna village is 1123 kW. Thus the electrical power required from wind turbine output is 1123KW.

$$P_{elecical} = 1123\ KW$$

Usably electrical power extracted from wind turbine is smaller than that of power harvested by wind turbine. This is due to Betz law limit (means that wind turbines can never be better than 59.3% efficient) and inefficiency in the generator. Then its possible to develop an inequality equation.

$$P_{wind} > P_{turbine} > P_{electical}$$

Having the above inequality equation, it possible to develop an equality equation as;

$$P_{turbine} = P_{wind} \times C_p$$

$$P_{electical} = P_{turbine} \times \eta_g$$

Taking the coefficient of performance value as 0.593 and assuming good quality generators may have full load efficiency of 0.87. Known that, $Pelectrical$ = 1123 KW

The other two, wind power and output power from the turbine can be obtained as follows

$$P_{turbine} = \frac{P_{electrical}}{\eta_g} = \frac{1123Kw}{0.87} = 1293Kw$$

$$P_{wind} = \frac{P_{turbine}}{C_p} = \frac{1293Kw}{0.593} = 2181Kw$$

To extact this amount of energy from the wind its reuired to determining the suitable number of blade turbines, appropriate tower height, power controlling system and type of generator used for assemble.

5.2.2 Turbine Blade

Wind turbines may use two, three, four, or even more number of the blade to extract power from moving air. Selection criteria for the proper number of the blade are either depend on the amount of power required to be extracted, developed momentum, etc. As the number of the blade is increased the range of the torque which causes the blade to rotate is increased. But obviously, as the number of the blade is increased the weight and overall cost is increased. Hence the turbine with four blades is ignored due to the high capital cost and that of the two-blade turbine has the advantage of cost but, it's spinning faster. spinning faster has its demerits it may cause more noise and failure. Thus for this thesis three-blade design is selected and it can generate more power at a lower rotational speed than the two-blade and more cost-efficient than a four-blade design.

5.2.3 Power Regulation Systems

The power produced by wind turbine is required to be controlled within allowable fluctuations for avoiding turbine damage and stabilizing the power output. If it does not regulated to the the manufacture rated level, the power would increased with wind speed and causes damage to components. When wind velocity is higher than cut off limit, the wind turbine is not allowed to produce any power to make turbine safe. But in many case as well in case of this thesis the probability for such high wind velocities is very low in most of the wind regimes, so its not economical to design strong transmission lines and larger generators to accommodate higher level of power. There are three commonly used types of power control in the industry (Ahmad *et al.*, 2018). These controlling mechanisms are Stall Control, Pitch Control, and Active Stall Control.

In enegral, all control methods have their advantages and disadvantages but most modern wind turbines are pitch or active-stall controlled since simplicity of construction is not an issue for the big machines, where output optimization and power quality are the ultimate goals.

5.2.4 Tower Height Approximation

Appropriate tower height is required to get wind speed away from the ground which may be distributed by ground turbulence such as trees. A wind machine tower should be at least 10m higher than any obstruction in the surroundings such as larger buildings and trees in the forest. A small wind machine tower is tied into the ground typically by truss design or by guy wires. Guy wire is a cable attached to the tower and anchored to the ground so that it prevents falling and shaking of a tower under high forces moving winds. The large wind machine is usually made up of steel and its great majority is tubular or conical type in cross-section as observed in the case of Adama wind turbine (Ahmad *et al.*, 2018). Special consideration should be given to the possibility of destructive vibration caused by natural frequency mismatching between wind machine and tower. So that based on the above information and considering the height of trees under the site of study which is approximately about 15m on average the desired tower height for this case study is 50m.

5.2.5 Generator type

Wind turbine energy conversion system consists of a rotor shaft with bearing, brakes, an optional gearbox and clutches and generator. From these components, the generator is the main component of the wind turbine power conversion system and proper selection of the generator is required. For the case of this thesis Synchronous generator with 24 RPM and 440V is selected. The selected wind turbine generators must be operated under fluctuating power output levels and variation in wind velocity.

Table 5. 4 Wind turbine technical parameter (Alibaba super market.com)

Wind Turbine Specification		
Company	Manufacturer	Enercon
	Model	E-48
Power	Rated power	800kW
	COP	0.45
	Cut-in wind speed	3.5 m/s
	rated wind speed	12.0 m/s
	Cut off wind speed	25 m/s
Rotor	Diameter	48 m
	Swept Area	1810 m^2
	Number of blades	3
	Rotor speed	5-10 RPM
	Type	AERO-48
	Material	GFK/Epoxy
	Distance between the neighboring turbine	100 m
Generator	Type	Synchronous generator
	Maximum speed	24.0 RPM
	Voltage	440.0v
	Grid frequency	50 Hz
Tower	Hub height	50 m
	Type	Steel tower
	Shape	Conical
	Corrosion protection	Painted

5.2.6 Selected Wind Turbine Power Curve

The power production of a wind turbine (WT) has a range of intervals in which the speed of the wind is working. This means, too small and too much wind speed doesn't correspond to any wind power extraction due to the following cases

Too small wind speed-: have no capability of rotating turbine blade example if it's less than 3m/s and too high wind speed-: if it's greater than the amount of wind speed that can be handled by generator performance V> 25 m/s.

The power curve of the selected wind turbine for power extraction of the site may have four distinct regions based on the available range of wind speed. The power output of this turbine is expressed by the piecewise function for these sections.

$$P_w = \begin{cases} 0 & , v < cut\ in\ wind\ speed \\ \frac{1}{2}\rho A v^3 C_p * \eta_t * \eta_g & , cut\ in\ wind\ speed \le v \ \wedge P_{wind} < rated\ power \\ rated\ power & , P_{wind} \ge rated\ power \\ 0 & , v \ge cut\ out\ wind \end{cases} \quad \text{---(5.23)}$$

The fraction of power extracted from a practical wind turbine is usually given the symbol, standing for the coefficient of performance. The coefficient of performance is not a constant but varies with wind speed, the turbine rotational speed, and turbine blade parameters (like the angle of attack and pitch angle). For a practical wind turbine, the maximum value is in the range of 0.2 to 0.45. The pitch is varied to hold at its largest possible value up to the rated speed of the turbine and then is varied to reduce while continues to increase with wind speed, to maintain output power at its rated value.

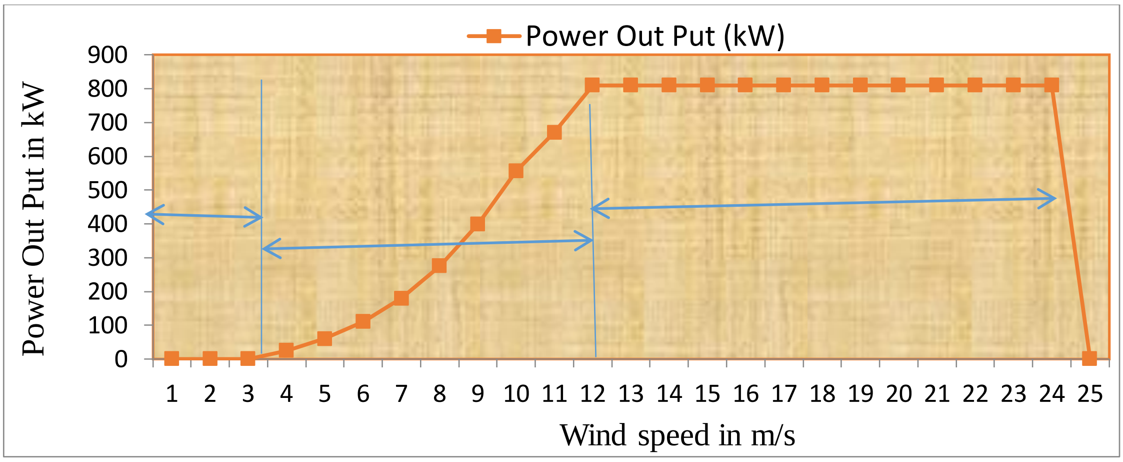

Figure 5. 4 Wind turbine power curve of E-48

In the first region when the wind speed is less than a threshold minimum, known as the cut-in speed typically about 3.5 m/s, the power output is zero. In the second region between the cut-in and the rated speed, there is a rapid growth of power produced. In the third region, a constant output (rated) is produced until the cut-off speed is attained. Beyond this speed (region 4) the turbine is taken out of operation to protect its components from high winds and turbine blade from damage even from falling of turbine and causing firing effect; hence it produces zero power in this region.

To harness this amount of power from the wind turbine, let assume 30 wind turbine then power output required from each of wind turbine is about 88 kW. The corresponding rotor diameter to achieve this amount of power is 48m with an 1810 m^2 swept area. Any wind turbine with a rotor diameter of above value or more could be the best wind turbine for this system design.

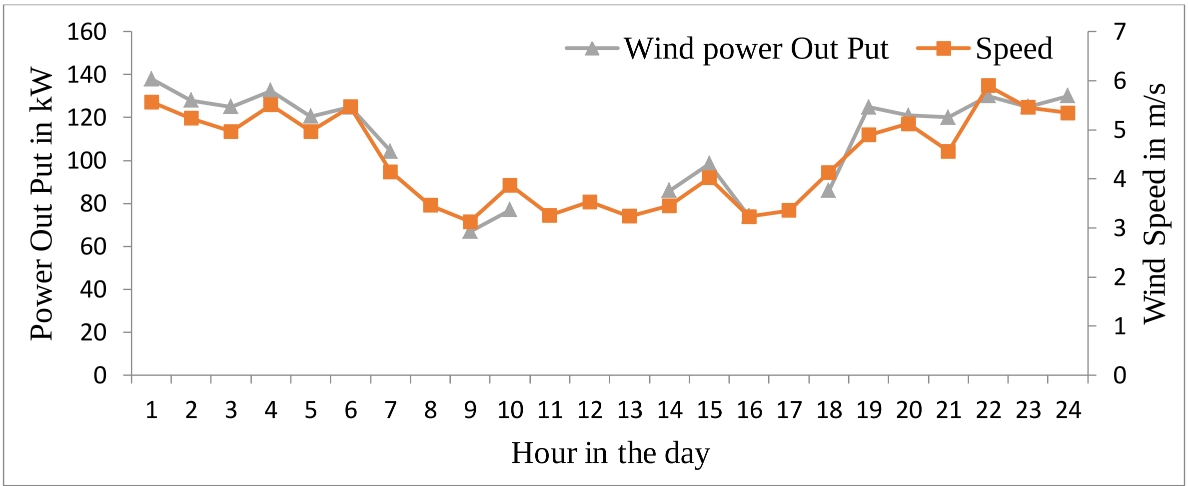

Figure 5. 5 March 16 Daily Power out put and corresponding wind speed

The above figure 5.5 shows daily power out and corresponding wind speed for critical months on daily basis. The daily power out and wind speed on daily basis for the remaining months of the year is attached to appendix H.

5.3 Modeling of Micro-hydropower Plants

The main components of a micro hydropower plant are electromechanical components (hydro turbine and generator) and civil components. Here a selection of generators and designing of civil work components is not the main target of this work, because it's directly related to other departments means electrical and civil engineering departments respectively.

5.3.1 Mechanical Components (hydro turbine)

A hydro turbine is a rotating machine that converts the potential energy of the water to mechanical energy. Hydro turbines can be of either impulse or reaction types the difference being the manner of head/energy conversion. In an impulse turbine, the potential energy of water is converted into kinetic energy in the nozzle before reaching the turbine. The high velocity flowing jets from the nozzle strikes the buckets of the turbine thereby transferring the kinetic energy of water in the jet to the mechanical/rotational energy of the turbine using the principle of Newton's Second Law. Turbines that fall under this category are Pelton, Turgo, and cross-flow turbines.

5.3.2 Hydro Turbine Selection and Selection Criteria

The type and size of a turbine for a hydropower system are different from one project to another project and there are various types of hydro turbines. The best selection criteria of turbine type depend upon the site data (particularly available head, the speed at which it is desired to run the generator or other devices loading generator and power required) and another technical parameter likewise of affordable, quality of machine or cost of the machine, appropriate equipment to operate for local people, etc. Referring to the required output, available net head and water flow (discharge) from table 2.3 suitable turbine type for this site is an impulse turbine typically a cross-flow turbine (Harvey *et al.*, 1998). Based on the data gathered from the site, head, h_g=15m and discharge rate, Q=0.21 m^3/s both H_{net} and Q is within the limits, the intersection point on the figure.5.2 below lies inside the white, non-dotted field.

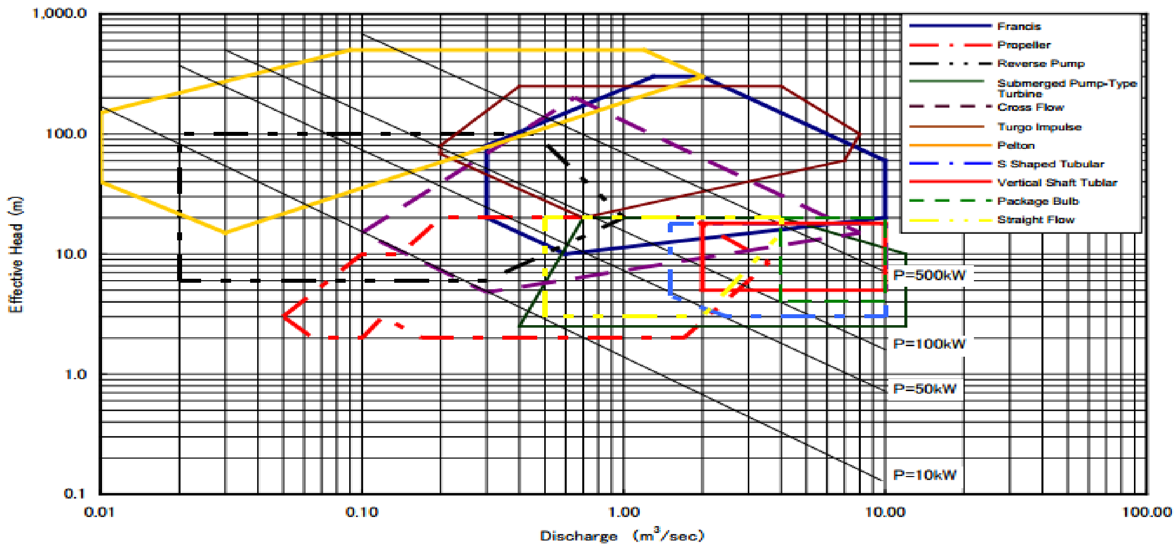

Figure 5. 6 Turbine selecting chart (Penche, 1998).

5.3.3 Power Out of Micro Hydro with Cross-Flow Turbine

The power exploited from hydropower at a particular site is proportional to the product of flow rate and net head of water falling above the ground.

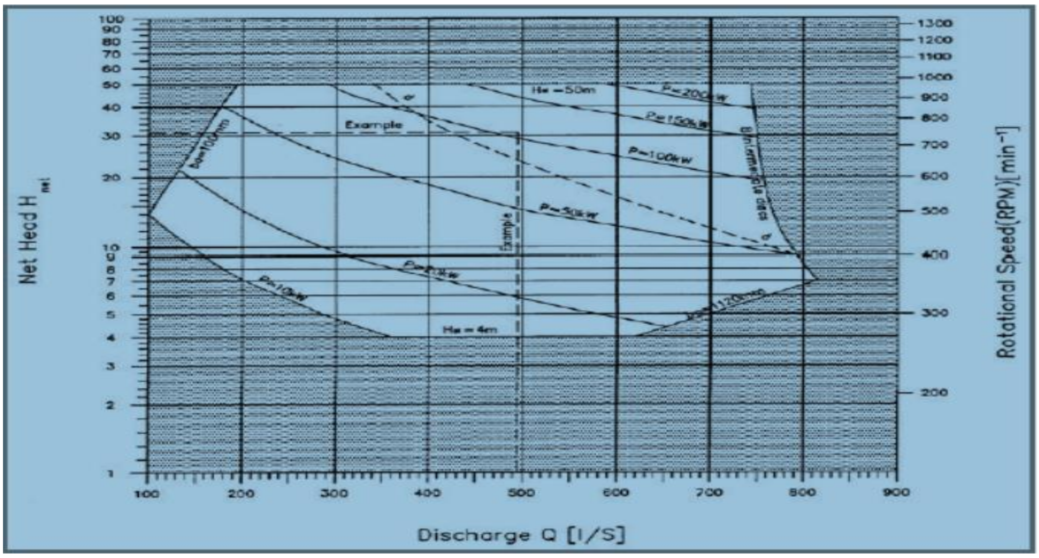

Figure 5. 7 Crossflow turbine design, power output, and rpm (Manual for micro hydropower development)

From the above figure 5.7 the intersection point of net head and discharge flow, turbine output power is approximately equal to 20 kW and the rotational speed of the turbine is 500 RPM. Turbine efficiency can be calculated by the following turbine output power:

Turbine output power (P_T , kW)

$P_T = \rho g \eta H_{net} Q \ (Kw)$---(5.24)

Where,

P_T- Turbine output power in kW

ρ- Density of water ($1000 kg/m^3$)

g- Gravity ($9.81 m/s^2$)

H_{net}- Net head in meter (m)

Q - Flow rate (m^3/s)

η-Turbine Efficiency (%)

$$\eta = \frac{P_T}{\rho g Q H_{net}}$$

$$\eta = \frac{20kw}{1000\,kg/m^3 \times 9.81\,m/s^2 \times 0.2\,m^3/s \times 15m}$$

$$\eta = 0.68$$

5.3.4 Sizing of the Cross-Flow Turbine

Once specific speed of turbine, power out put of turbine and net head are known, its possible to the calculate the fundamental dimension of the turbine. Hence for sizing of cross-flow turbine, the dimension of interest is the runner length (L_{runner}), diameter (D_{runner}) and jet thickness (t_{jet}). Assuming generator input shaft speed (N_a) 1500 RPM and from figure.5.7, the approximate turbine rotational speed (N_t) read is equal to 500 RPM. Therefore, the speed (gear) ratio (I) will be:

$$I = \frac{N_a}{N_t} = \frac{d_L}{d_s} = \frac{1500}{500} = 3.0$$

$$D_{runner} = \frac{40\sqrt{H_{net}}}{N_t} \text{ ---(5.25)}$$

Where:-

$$H_{net} = H_g - H_{hdry},\ H_{hdry} \text{ is usually 2 to 7\% of } H_g$$

$$= H_g - 7\%\ of\ \ H_g = 15\text{-}1.05\text{=}13.95 \text{ m}$$

$$D_{runner} = \frac{40\sqrt{13.95}}{500} = 0.298 \text{ m}$$

Having t_{jet}, the approximate runner length L_{runner} can be obtained from the orifice discharge equation. The runner length will be equivalent to the jet width.

$$L_{runner} = \frac{0.81 \times Q}{D_{run} \times \sqrt{H_{net}}} \text{---(5.26)}$$

$$L_{runner} = 0.1524 \text{ m}$$

The jet thickness is calculated from the following coerretion (Nasir. 2013).

$$t_{jet} = \frac{0.233 \times Q}{L_{run} \times \sqrt{H_{net}}} \text{---(5.27)}$$

$$t_{jet} = 0.0859 \text{ m}$$

5.3.5 Sizing of Penstock

Penstocks (pipes) are used to conveying water from the intake to the powerhouse. They can be installed over or under the ground, depending on factors such as the nature of the ground itself, the penstock materials, the ambient temperature, and the environmental requirements. The internal penstock diameter (D_p) can be estimated from the flow rate, pipe length and gross head (CelsoPenche. 1998). The diameter of penstock can be calculated from discharge and head of the river

$$D_p = 2.69 \times \left\{ {n_p}^2 \times Q^2 \times {L_p}/{H_g} \right\}^{0.1875} \text{--}(5.28)$$

Where n_p= Manning's coefficient.

Q= water flow rate (m^3/s).

L_p = penstock length in (m).

H_g = Gross head in (m).

The value of manning coefficient for mild steel penstock material is 0.012. The length of the penstock can be approximated from the layout of the scheme.

$$L_p = 24m$$

Then according to above equation (5.28) the internal diameter of penstock is approximated to be ($D_p = 0.315\ m$). The wall thickness of the penstock depends on the pipe materials, its tensile strength, pipe diameter and the operating pressure. The minimum wall thickness is recommended as:

$$t_p = \frac{D_p + 508}{400} + 1.2 \text{--}(5.29)$$

Where D_p= penstock diameter in mm.

t_p= minimum penstock thickness in mm.

Hence, t_p =2.47 mm.

The pipe should be rigid enough to be handled without danger of deformation in the field.

Table 5. 5 Micro hydro Power results

Features	Preliminary Survey data
River Source	Sinkile river
Net Head	13.95 m
Least measured Flow and Date	0.204 m3/s (May 2012)
Power	21000Watts/ 21kW
No of the households demanded	740 households
Generator	25 kVA,3 Phases, Synchronous, Brushless
Load Controller	ELC 21 kW with Ballast tank 30 kW
Penstock Type and Length	Mild Steel Type, 66.0 m
Type of Turbine	Cross flow 20 kW shaft output

5.4 Hybrid Energy System Modeling

5.4.1 Hybrid Power Generation Modeling

Total hybrid power generated at any time t is given by:

$$P_t = \sum_{pvg=1}^{N_p} P_{pv} + \sum_{wg=1}^{N_w} P_w + \sum_{ht=1}^{N_{HT}} P_h \text{---(5.30)}$$

Where, N_p is the number of PV cells unit, N_w is the number of wind generators unit and N_{HT} is the number of hydro turbine generator units. This generated power will feed to the loads. When this generated power exceeds the load demand then the surplus of energy will be stored in the battery bank. This energy will be used when a deficiency of power occurs to meet the load demand. Proposed solar, wind and Micro-hydropower hybrid schematic diagram and HOMER simulation of the required system is indicated in the figure 5.8 and 5.9 below respectively. There are numerous of hybridization of renewable energy sytem, such as AC coupled, DC coupled and AC/DC coupled. In this study AC/DC coupling system is used.

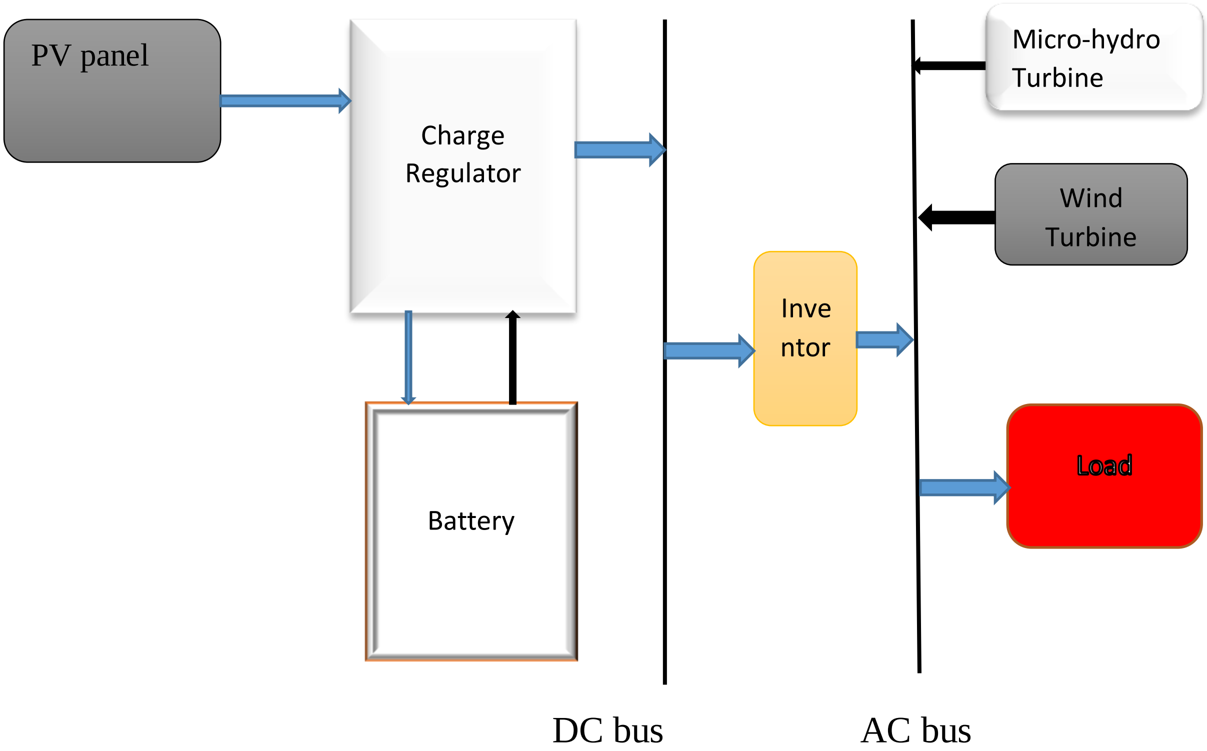

Figure 5. 8 Schematic diagram of the proposed hybrid system

5.4.2 Introduction to HOMER Software

Hybrid Optimization Model for Electric Renewable (HOMER) is computer software developed by the US National Renewable Energy Laboratory (NREL) in 1992 (Gilman, 2006). It is a micropower optimization model and simplifies the task of evaluating designs of both off-grid and grid-connected power systems for a variety of applications. In designing power systems different decisions can be made about the configuration of the system, such as; what components to include in the system, the size and the quantity of the components, and the cost of each component. Incorrect power system design can lead to a shorter life of the battery, increase the cost of energy production, an insufficient supply of electricity demand. HOMER models the power system's physical behavior and its life cycle cost (Net Present Cost). That is the total cost of installing and operating the system throughout its life cycle. HOMER allows the modeler to compare many design options based on their technical and economic inputs (Gilman, 2006).

A hybrid energy system is an excellent solution for electrification of remote rural areas where the grid extension is difficult and not economical. Among these main renewable energy resources used in this study are: small/micro hydropower, wind, and photovoltaic

(PV). Those energy resources when used in a hybrid system using energy-producing components such as the PV module, hydro and wind turbines and other components to make the flow of energy complete (battery, inverter, etc…), provide smooth, reliable, uninterruptable, and cost-effective electrical energy to the end users than if any of the systems were used independently. This is because each system does not depend on the other to produce its energy.

HOMER performs simulation, optimization, and sensitivity analysis in a single power system configuration. In a simulation process, HOMER simulates the operation of a system by making energy balance calculations for each of 8,760 hours in a year. For each hour, HOMER compares the electric demand in the hour to the energy that the system can supply in that hour, and calculates the flows of energy to and from each component of the system.

The following major inputs are given to the HOMER software, all in regarding windows.

- The un-gauged river's flow rate data and head height in meters.
- Ten years monthly average wind speed at required hub height of the tower.
- Monthly averaged radiation incident on PV panel which tilted at angle β.
- Primary and deferrable loads as per calculated.

To perform optimization process HOMER require the following input of the cost.

Table 5. 6 Additional input to HOMER (Alibaba supper market.com)

Specification	PV module (SPR-X21)	Wind turbine (E-48)	Micro-hydro	Inventer (Dyn-500)	Battery (Iron-49000)
Size (kW)	1	10	98	500	8541Ah
Capital ($)	2000	70000	150,000	3000	15,000
Replacement cost ($)	2000	70000	120,000	2500	10,000
O and M cost ($/yr)	20	3400	3500	250	450

5.4.4 Homer Simulation set up

The DC power generated by PV array is converted in AC bus by inverter and fed into AC bus. Wind turbine and micro hydro provide AC power and fed into AC bus. Excess power is stored by battery and used when there is deficiency of supply.

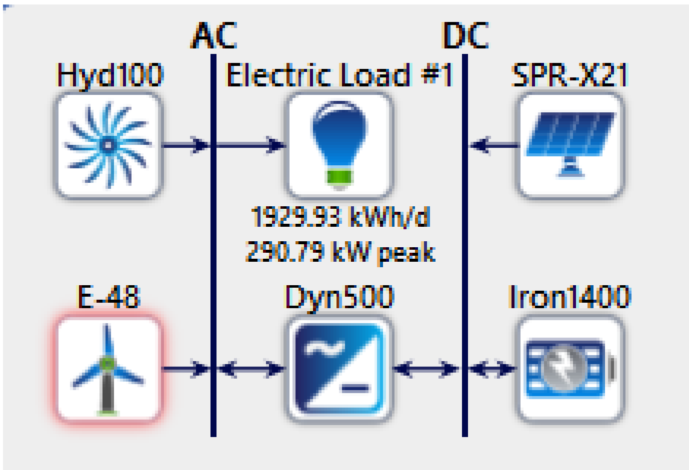

Figure 5. 9 HOMER software simulations of hybrid system components

From the above hybrid HOMER system components, the peak load (maximum energy consumption per day) is about 290.79 kWh/day. Since converter sizing is at least 25-30% much more than the daily energy consumption of the community load the selected converter size is about 363.5kW. The selected PV panels are PV panels of mono-crystalline silicon flat plate type with a lifetime of around 25 years and maximum efficiency of 21%. Since HOMER performs simulation and optimization process it decides how many solar panels are required to satisfy power energy required from the solar system.

CHAPTER SIX

RESULTS AND DISCUSSIONS

6.1 Simulation Results of the Site

6.1.1 Hourly Load profile of the site

Overall simulation of monthly and yearly load profile of the site under study is indicated by different color codes to distinguish the load difference between each time of the day. As indicated in the following table during night time means from 19:00 t0 21:00 o'clock the energy demand of the village is maximum which is coded by yellow color and also during lunchtime it's relatively maximum where from 0:00 to 7:00 nearly no energy demand since the time is midnight any operation is do not performed as obvious and it's colored by black color.

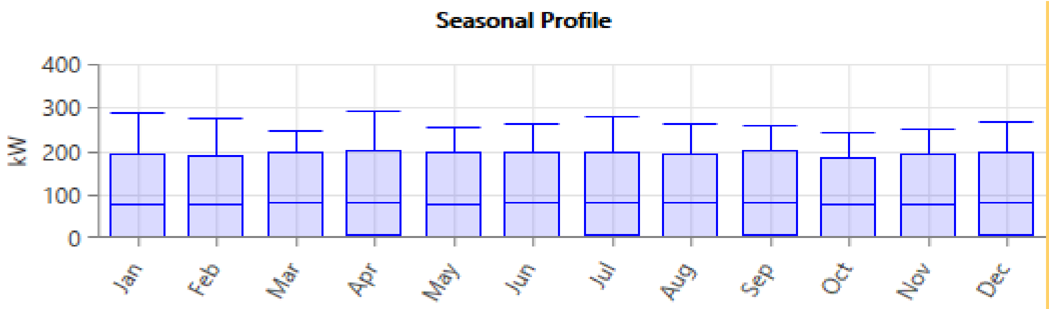

Figure 6. 1 Seasonal load profile of the site understudy

6.1.2 Hourly usable power output of selected PV panel

Usable energy is energy feed into the grid for end appliance uses after a drop over different components such as module, inventors, battery, and temperature effect. The usable energy from the panel is affected by panel efficiency, daily sunshine duration, the temperature of the site, and to which direction your panel is facing or average tilt angle which is 18° in the case of this study. It's known that the rating power of panel designed by manufacturer is at STC which assume there is $1000W/m^2$ the area is a module at the temperature of 25°C. But this is not always true. So rating or module wattage indicates what solar panel capable of producing at ideal condition while solar efficiency tells how much sunlight is converted into electricity for usage at home. The efficiency of a solar panel is affected by its solar cell construction (based on their reflectivity), less reflective cells can collect more sunlight and use it rather than bouncing it back to the atmosphere. The efficiency of a solar panel is also affected by an environmental effect such as shading from nearby trees or other buildings, excessive cloud coverage, excessive dirt, dust and pollution. Energy loss occur in case of PV panel power production is inverter loss (4% to 10 %), battery loss (10% to 15%), temperature loss (5% to 20%), Dc cable loss(1% to 3%), AC cable loss(1% to 3%), loss due to weak radiation(3% to 75) and loss due dust, snow is 2% (Sunderan *et al.*, 2011).

The following two figures show maximum and minimum hourly usable power extracted from solar radiation by considering all factor minimizing the efficiency of a solar panel for the month of maximum and minimum sunshine duration.

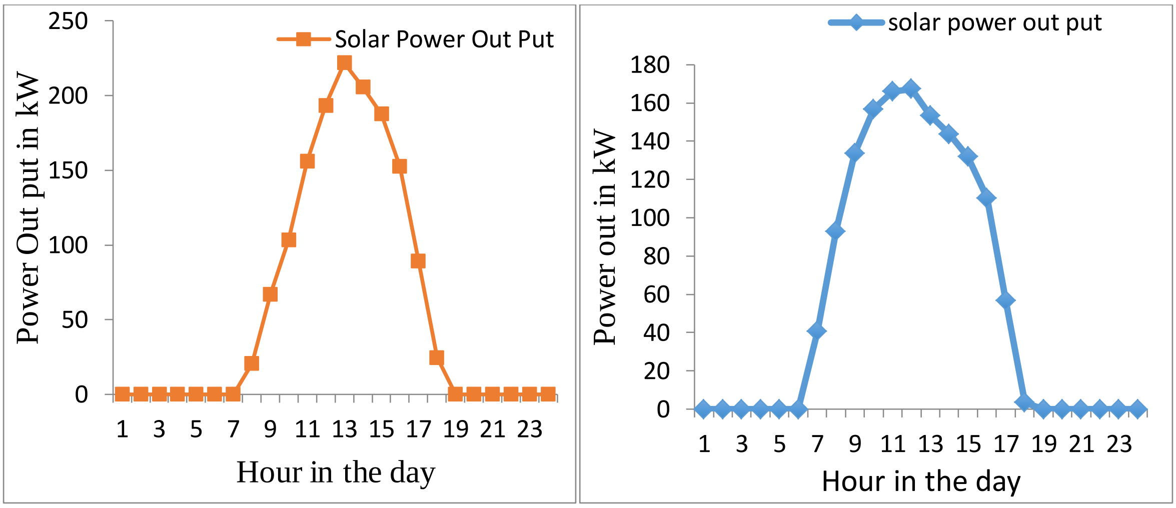

Figure 6. 2 January 17 and July 17, Maximum and Minimum hourly usable power output from solar radiation respectively

The above figure 6.2 shows that the power output produced by the PV system usually increases during mid-day hours. The maximum power produced by this PV system is 222.1 kW at hour 12 of January 17.

6.1.3 Hourly Power out of wind speed

Average monthly wind speed variation of the site at 50 m heights where the average wind speed found to be 5.46 m/s. The highest wind speed was observed in July while lowest in March at all the heights of wind speed measurements. For energy yield estimation, a three-bladed wind turbine of 800kW rated power with a rotor diameter of 50m from Enercon was chosen. There will be certain times when the wind turbine will have zero output when hourly wind speed is less than cut-in wind speed of the selected wind turbine.

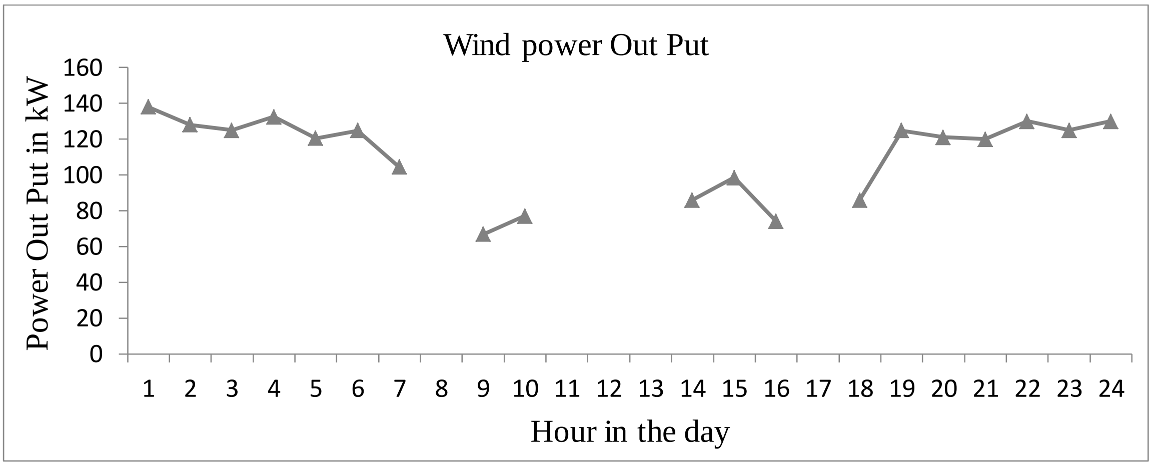

Figure 6. 3 March 16, Minimum hourly usable power output from wind turbine

6.2 Hybrid Result of the Study

A hybrid off-grid energy supplying system is a suitable solution for solving the problem of discontinuous energy supply for the user. Here as indicated in the following figure usable energy from solar is maximum during the mid-day and no energy supply at night from solar energy. But the energy demand of the village is maximum at 19:00 to 21:00 as calculated in chapter three of this thesis. The best solution for such type of problem is either using a hybrid system or storage battery as a case of this study. In another word, the usable energy from wind is somewhat maximum during the night time when compared to day time.

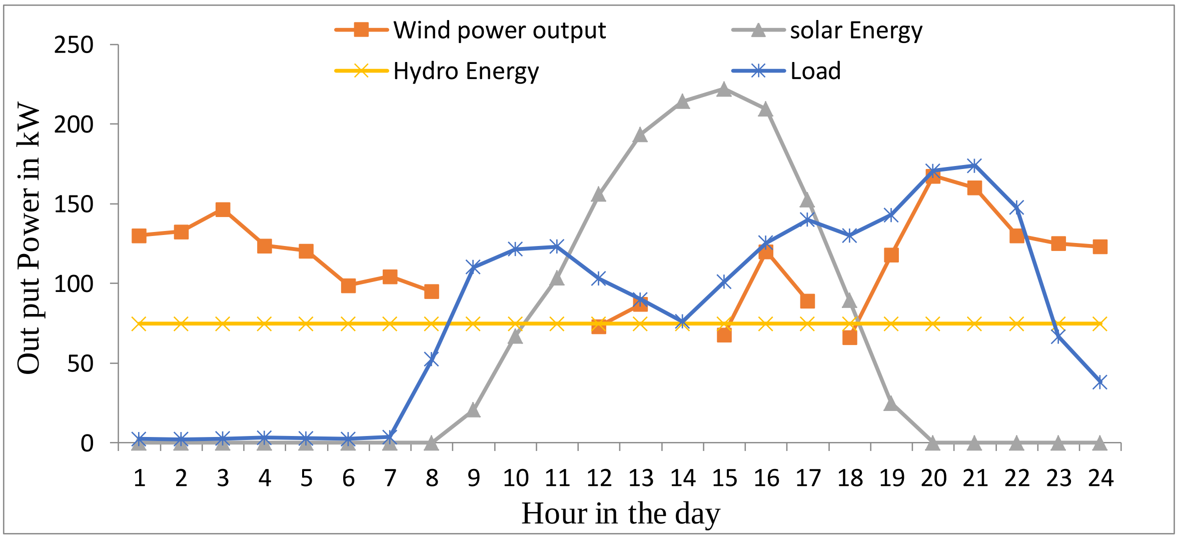

Figure 6. 4 January 17, hybrid energy supply vs energy demand of the site

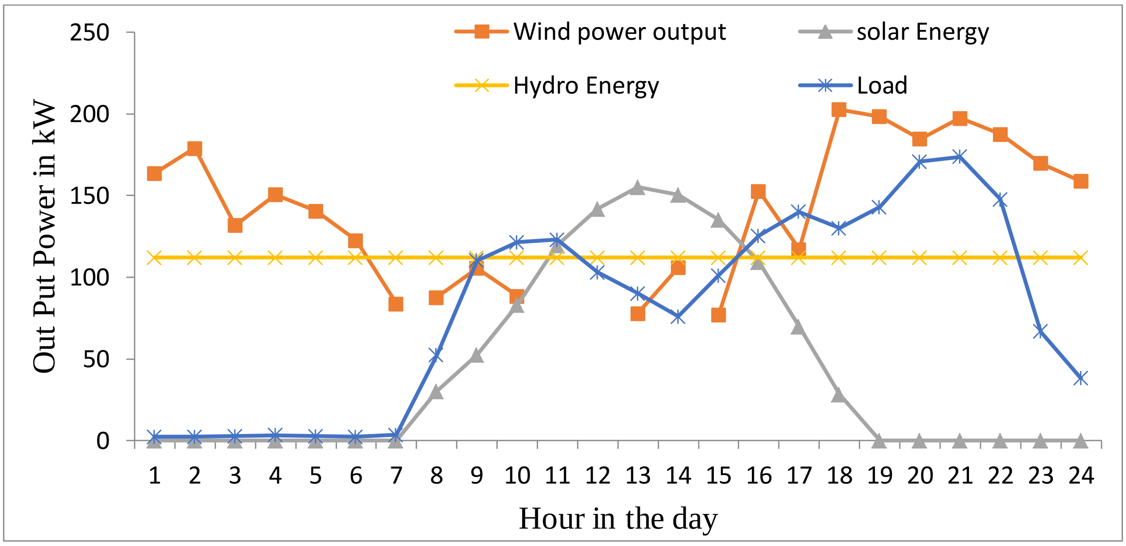

Figure 6. 5 July 17, Hybrid energy supplying configuration

The above two figure shows the months with maximum and minimum solar radiation and the integration of energy from wind and hydro turbine respectively.

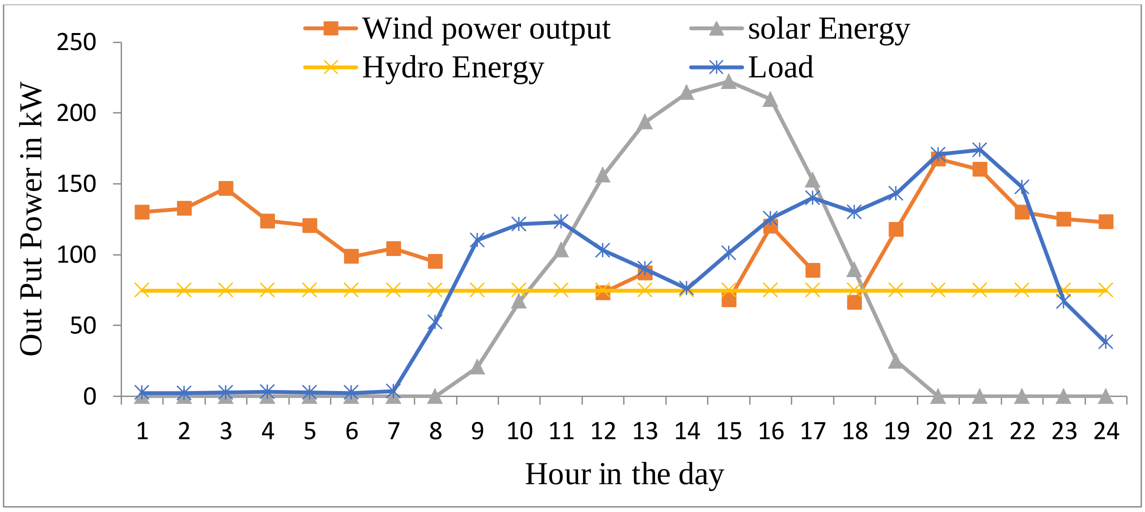

Figure 6. 6 March 16, Hybrid energy supplying configuration

From the above figure 6.6 it's obvious to understand that power extracted from wind is maximum during the night time due to wind blows more at night than during the day time and even though there is no power output from solar radiation at night, there is excess power from wind and micro-hydropower. In addition to this, there is a storage battery bank with three autonomy days if there is a sudden failure of one system is occur unexpectedly. Energy stored by battery is excess energy is the difeerence of energy between over all energy produced by three renewbale eneegy source and energy utilized by appliance.

Hence the following figure shows that over all enegy produced and excess energy stored by batter.

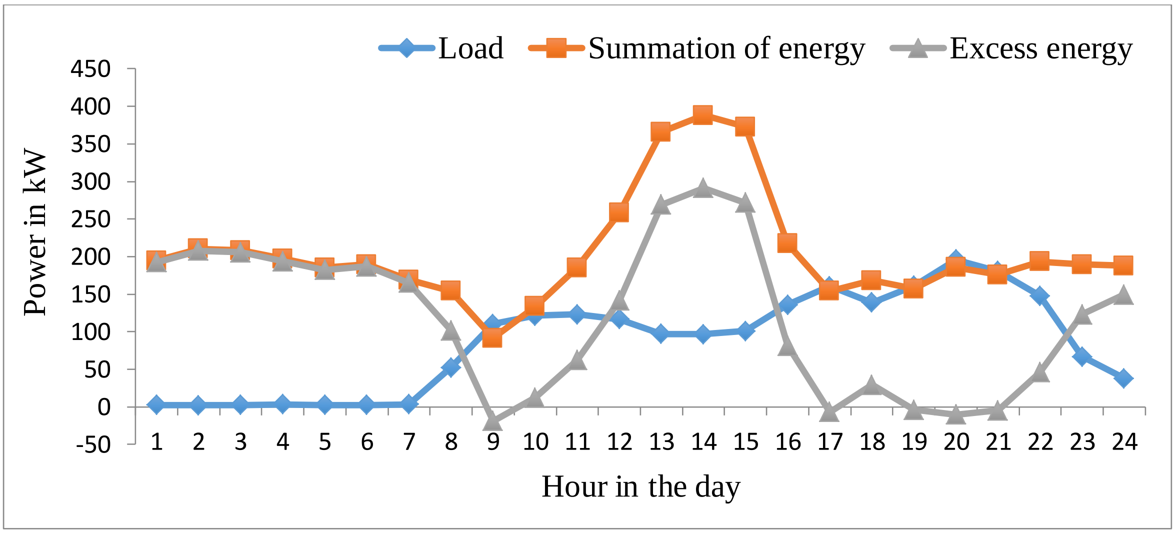

Figure 6. 7 Overall energy produced and excess energy after utilization

As seen in the figure above there is excess (safe) power from hybrid integration of the resources during each time of the day. Finally, one thing to be known is the proposed hybrid off-grid system simulation is based on critical recommended days of the months. For example, hourly usable power out of the solar panel is based on the worst months of sunshine duration in July with the value of 6.54h and that of the wind turbine is for the recommended day of the month march because as data calculated from NMS this month noted the smallest wind speed of 4.24m/s at the hub height of 50m. In other words, the ungagged water flow rate of the river under study is measured in May. This is due to as everyone understood mostly in Ethiopia this month is the worst because it’s a sunny month and the flow rate of the river much small than any months of the year.

6.3 HOMER Optimization Result

Homer pro software performs three main tasks, Such as simulation, optimization and sensitivity analysis of the raw data. HOMER optimizes the raw data input to find the least cost feasible hybrid system for the study according to the input data for simulation and optimization. The following table 6.1 shows that the optimization results of the software are progressing and when it is completed the result is displayed in two forms as categorized and overall forms. In categorized form, only the least cost system displays while in the overall form they ranked at the top according to the least cost to the highest initial capital and replacement costs.

Table 6. 1 The catagorized optimization results of HOMER

Rank	PV module	Wind turbine	Micro-hydro	Battery	Inventer	Generator	Dispatch stategy	Initial capital	Total NPC	Operating cost	COE	refraction	Diesel	Gene
1	0	13	49	194	8	0	CC	172739	222,816	38	0.346	1	0	0
2	260	10	49	196	9	0	CC	174791	225,203	3900	0.365	1	0	0
3	377	0	49	245	23	0	CC	966542	1.13M	12345	0.467	1	0	0

Optimization of software shows that the least cost-effective hybrid system is labeled at the top of the table. The optimization result indicates the integration of the solar, wind and hydro with inventor and storage battery is feasible to load the community. One can observe from optimization result of the software size of a different configuration of the system and their representation, net percent cost, operational cost, initial capital cost and required number of different components for the selected size of each component. The battery chosen for this study is 96v with a nominal voltage of 1400 Ah (67.2 kWh) as calculated in the previous section.

Displaying complete overall optimization result of the software in this section impossible, so only the most feasible configuration of the system is labeled. From the optimal simulation result table the most cost-effective system, i.e. the system with the lowest net present cost, is the PV, wind, micro-hydro, and battery converter configuration. Monthly electric production of wind energy and micro-hydro energy is indicated in the following figure. Hence from this result simply one can understand that maximum energy is delivered by wind energy when compared to micro-hydro based on the water flow rate of the river understudy.

CHAPTER SEVEN

CONCLUSIONS AND RECCOMENDATION

7.1 Conclusion

The overall result briefly indicates that the site under study is blessed with a considerable amount of annual solar radiation 6.23 kWh/m^2/day on a horizontal surface, annual wind speed of 5.46 m/s at 50m and 0.21 m^3/s a water flow rate of an ungagged river. Therefore, there is site potential for installation of the hybrid system configuration of solar, wind and micro-hydro power for the remote area of Magna Lege Buna village electrification. Magna Lege Buna village one of the villages in Chole kebele and its 95km far away from the extended electric grid, so grid extension to this village is not advantageous due to different factors such as topographic location (terrain) and transmission line costs since its distance dependent.

Grid-tied and standalone electrification system has its advantage and disadvantage. For example, a Grid electrification system has a financial problem if it is far away from the main grid extension and the main problem of the stand-alone system such as solar, micro-hydro and as well as wind is the fluctuation of energy supply, causing intermittent delivery of power and causing the problem if continuous energy supply is required. So such problem and other problem related to this is solved by using a hybrid off-grid electrification system.

As calculated previously, the daily energy demand of the village and the potential of each standalone renewable energy resource are not balancing each other. That means electrifying the village either by solar, wind, or micro-hydro separately is impossible concerning available potential and also due to intermittency of the resources. So developing the hybrid energy supply or integrating the three renewable energy resources is one of the ways to solve the energy demand problem of the village and a way of increasing the living standard of the people living in that area. This hybrid energy supplying system (Solar/wind and micro-hydropower) have the advantage of producing uninterruptable, smooth, most cost-effectively, free pollution, it's friendly to the environment and reliable electrically energy supplying system than if any system may use independently.

The crucial objective of this thesis was to access the energy demand of the village and to find the best way of an off-grid power system supplying to a rural area in Magna Lege Buna Village with optimum and economical ways. In the design of solar PV, wind turbine and micro-hydro turbine for Magna Lege Buna village, the thesis arrived at 8.69 kWh/m^2/day scale annual average daily solar radiation on a perfectly tilted surface and 5.46m/s scale annual average wind speed at 50m above the ground and $0.21 m^3/s$ water flow rate for a household with a total number of 740 households and the total average energy demand was about 2470 kWh/m^2/day with a maximum daily load of 297 kW/day. Off-grid renewable energy-based power systems cannot provide a continuous supply of electricity without a storage medium. Consequently, storage battery banks were added to the hybrid system. After selecting the appropriate components and studied their characteristics, the hybrid system has been modeled in HOMER software and simulations have been made to determine the best system which can supply the village load with the required level of availability. The usefulness cost of all hybrid structure that can fulfill the continuous load demand has been calculated to determine the system which provides the lowest cost.

Finally from this thesis, it’s possible to conclude that an off-grid standalone hybrid of micro-hydro, solar PV and wind turbine system is economically feasible and more even environmentally friendly to replace the existing nonrenewable energy supplying system for the proposed village.

7.2 Recommendation

Furthermore, investigations need to be carried out to modify this thesis work the following recommendations are given by the author of this thesis.

- This thesis was deal to solve the electricity problem in the Magna Lege Buna village found in the east Arsi zone/ Oromia region, Ethiopia. Others may work optimize to this system for rural electrification as well by integrated or substituting the lowest energy potential (micro hydro-power) with biomass in the future if the number of livestock is increased further than the current number of livestock which very minimum as data obtained from village FTC and also extend the electrification to another area which was detached from the main grid.
- This thesis mainly deal only on a preliminary study in order to estimate the Potential of solar, wind and micro hydro power producing and energy demand of the village. But it does not include environmental, economic and financial issues. For a comprehensive study prior to construction and installing solar, wind and micro hydro energy conversion systems, a detail environmental, economic and financial feasibility analysis for the proposed solar, wind and micro hydro farm should be performed.
- A major limitation to the use of renewable hybrid energy systems was the high initial capital cost. so, the governmental and non-governmental organizations should work to motivate and increase the interest of their community to use electricity.
- As far as the environmental aspects are concerned, these kinds of renewable hybrid systems have to be widespread to cover the energy demands of rural areas and used to apply green energy policy, by reducing the greenhouse gas emission and environmental pollutions were an important point taken to account.
- This study shows only two selected sites of the village in Chole kebele and it doesn't represent all villages of the kebele. So, future researchers should expand this research work to other sites and make rural people beneficial.

REFERENCE

Bekele, G. and Tadesse, G., 2012. Feasibility study of mini Hydro/PV/Wind hybrid system for off-grid rural electrification in Ethiopia. Applied Energy, 97, pp.5-15.

Duffie,J.A.,andBeckman, W.A.(2006)SolarEngineeringofThermalProcesses,3rdedn.JohnWiley&Sons, Inc.,New York.

Bekele, G. and Palm, B., 2010. Feasibility study for a standalone solar–wind-based hybrid energy system for application in Ethiopia. Applied Energy, 87(2), pp.487-495.

Tesema, S. and Bekele, G., 2014. Resource assessment and optimization study of efficient type hybrid power system for electrification of a rural district in Ethiopia.International Journal of Energy and Power Engineering, 3(6), pp.331-340.

Emebet, T., 2016. Design of Standalone (PV/Micro-Hydro/DG) Hybrid Power Supply for off Grid Rural Community–A Case Study of Maji District (Tum) in South Nation Nationality People Region (SNNPR) (Doctoral dissertation, AAU).

Somano, G.Z. and Shunki, G., 2017. Design and modeling of hybrid PV-micro hydropower generation case study Jimma Zone. American Journal of Electrical Power and Energy Systems, 5(6), p.91.

Tesfa, A., 2015. Feasibility Study of Off-Grid Hybrid Systems: Mini-Hydro, PV, and Wind Power Systems for Rural Electrification in Ethiopia (Study Area: Mojana Wodera District, North Shewa, Amhara Regional State, Ethiopia (Doctoral dissertation, Addis Ababa University).

Tamirat B., Comparative Analysis of Feasibility of Solar PV, Wind and Micro-hydropower Generation for Rural Electrification in the Selected Sites of Ethiopia. MSc. Thesis, Addis Ababa University, 2007.

Becker, C., Amkreutz, D., Sontheimer, T., Preidel, V., Lockau, D., Haschke, J., Jogschies, L., Klimm, C., Merkel, J.J., Plocica, P. and Steffens, S., 2013. Polycrystalline silicon thin-film solar cells: Status and perspectives. Solar Energy Materials and Solar Cells, 119, pp.112-123

Maleki, A. and Askarzadeh, A., 2014. Optimal sizing of a PV/wind/diesel system with battery storage for electrification to an off-grid remote region: A case study of Rafsanjan, Iran. Sustainable Energy Technologies and Assessments, 7, pp.147-153.

Bhattarai, D. N. (2005). Hydropower Development in Nepal: A study of Demand for Electricity and Financial Requirement up to 2030. Devi Kumari Bhattarai.

John Tewidell and Tony Weir, 2006. Renewable Energy Resource: second Edition: Tylor &Francis Group, London and New York:

Nasir, B.A., 2013. Design of micro-hydro-electric power station. International Journal of Engineering and Advanced Technology, 2(5), pp.39-47.

WMO No. 1029, 2008, Manual on Low-Flow Estimation and Prediction" Operational Hydrology Report No. 50.

Harvey, A., Brown, A., Hettiarachi, P., A (1998): Micro Hydro design manual, a guide to small – scale water power schemes, Intermediate Technology Publications

Simulation and Optimization of a Hybrid Renewable Energy System for application on a HOMER user manual NREL, 2008)

Berihun G. (2013) modeling and simulating of a micro-hydro wind hybrid power generation system for the rural area of Ethiopia. Master thesis at Addis Ababa University.

ESHA, 2 2007, Small Hydro Power Development in Africa „EIS Africa Issue. Guide on How to Develop a Small Hydropower plant. European Small Hydropower Association – ESHA-Esha @arcadis.de

Girma, Z., 2016. Techno-economic feasibility of small scale hydropower in Ethiopia: The case of the kulfo River, in Southern Ethiopia. Journal of Renewable Energy, 2016.

Hailu Kebede, M. and Bekele Beyene, G., 2018. Feasibility Study of PV-Wind-Fuel Cell Hybrid Power System for Electrification of a Rural Village in Ethiopia. Journal of Electrical and Computer Engineering, 2018.

Sathyajith Mathew, 2006, Wind Energy Fundamentals Resource Analysis and Economics, Netherlands, p61 – 95, *Sohoni, V., Gupta, S.C. and Nema, R.K., 2016. A critical review of wind turbine power curve modeling techniques and their applications in wind-based energy systems. Journal of Energy, 2016.*

Lackner, M.A., Rogers, A.L., Manwell, J.F. and McGowan, J.G., 2010. A new method for improved hub height means wind speed estimates using short-term hub height data. Renewable Energy, 35(10), pp.2340-2347.

Karafil, A., Ozbay, H. and Kesler, M., 2016. Temperature and solar radiation effects on photovoltaic panel power. Journal of New Results in Science, 5(12), pp.48-58.

Abdullah S, Jeanty PW. Willingness to pay for renewable energy: evidence from a contingent valuation survey in Kenya. Renew Sustain Energy Rev 2011; 15:2974–83

Geleta, G.T., 2019. Feasibility Study and Design of Solar PV-biomass Hybrid Power Generation Systems: A Case Study of Ilu Aba Bor Zone. Solar energy, 6(08).

Teferra, D.M., 2017. Potential and feasibility study of standalone solar PV/wind/biogas and biodiesel hybrid electric supply system in Ethiopia. International Journal of Energy Technology and Policy, 13(4), pp.368-377.

Obeng, G.Y. and Evers, H.D., 2009. Solar PV rural electrification and energy poverty: a review and conceptual framework concerning Ghana (No. 36). ZEF Working Paper Series.

Klein, S.A. Calculation of monthly average insolation on tilted surfaces. Sol. Energy 1977, 19, 325–329

Ahmad, J., Imran, M., Khalid, A., Iqbal, W., Ashraf, S.R., Adnan, M., Ali, S.F. and Khokhar, K.S., 2018. Techno-economic analysis of a wind-photovoltaic-biomass hybrid renewable energy system for rural electrification: A case study of Kallar Kahar. Energy, 148, pp.208-234.

Sigarchian, S.G., Paleta, R., Malmquist, A. and Pina, A., 2015. Feasibility study of using a biogas engine as a backup in a decentralized hybrid (PV/wind/battery) power generation system–Case study Kenya. Energy, 90, pp.1830-1841.

Kacira, M., Simsek, M., Babur, Y. and Demirkol, S., 2004. Determining optimum tilt angles and orientations of photovoltaic panels in Sanliurfa, Turkey. Renewable energy, 29(8), pp.1265-1275.

Sunderan, P., Ismail, A.M., Singh, B. and Mohamed, N.M., 2011. Optimum tilt angle and orientation of stand-alone photovoltaic electricity generation systems for rural electrification. JApSc, 11(7), pp.1219-1224.

Yadav, D.K., Girimaji, S.P. and Bhatti, T.S., 2012, December. Optimal hybrid power system design for rural electrification. In 2012 2nd International Conference on Power, Control and Embedded Systems (pp. 1-6). IEEE

Benti, N.E. and Tadesse, G., 2017. Feasibility Study of Solar Photovoltaic (PV) Energy Systems for Rural Villages of Ethiopian Somali Region (A Case Study of Jigjiga Zone). American Journal of Science, Engineering and Technology, 1(2), p.42.

Meri, y.t., 2018. assessment of solar energy potential and its economic feasibility to rural areas electrification of akaki kaliti, Addis Ababa, Ethiopia. MSc. Thesis

Muralikrishna, M. and Lakshminarayana, V., 2008. Hybrid (solar and wind) energy systems for rural electrification. ARPN Journal of Engineering and Applied Sciences, 3(5), pp.50-58.

Gebrehiwot, K., Mondal, M.A.H., Ringler, C. and Gebremeskel, A.G., 2019. Optimization and cost-benefit assessment of hybrid power systems for off-grid rural electrification in Ethiopia. Energy, 177, pp.234-246.

Abraha, A.H., Kahsay, M.B. and Kimambo, C.Z., 2013. Hybrid solar-wind-diesel systems for rural application in North Ethiopia: a case study for three rural villages using HOMER simulation. Momona Ethiopian Journal of Science, 5(2), pp.62-80.

Mandefro Bezie, Y., 2017. Feasibility Study of Small Hydropower/PV/Wind Hybrid System for Off-Grid Electrification of Liben and MedaWoulabu Villages

Schubel, P.J. and Crossley, R.J., 2012. Wind turbine blade design. Energies, 5(9), pp.3425-3449.

Mandelli, S., Barbieri, J., Mereu, R. and Colombo, E., 2016. Off-grid systems for rural electrification in developing countries: Definitions, classification, and a comprehensive literature review. Renewable and Sustainable Energy Reviews, 58, pp.1621-1646.

Nigussie, T., Bogale, W., Bekele, F. and Dribssa, E., 2017. Feasibility study for power generation using off-grid energy system from micro hydro-PV-diesel generator-battery for the rural area of Ethiopia: The case of Melkey Hera village, Western Ethiopia

Kusre, B.C., Baruah, D.C., Bordoloi, P.K. and Patra, S.C., 2010. Assessment of hydropower potential using GIS and hydrological modeling technique in Kopili River basin in Assam (India). Applied Energy, 87(1), pp.298-309.

Adaramola, M.S., Paul, S.S. and Oyewola, O.M., 2014. Assessment of decentralized hybrid PV solar-diesel power system for applications in the Northern part of Nigeria. Energy for Sustainable Development, 19, pp.72-82.

Paul Gilman, 2006, Micro-power system modeling with HOMER, National Renewable Energy Laboratory

Erich Hau, 2006, Wind Turbines, 2nd edition, Springer, UK

Goel, S. and Sharma, R., 2017. Performance evaluation of standalone, grid-connected and hybrid renewable energy systems for rural application: A comparative review. Renewable and Sustainable Energy Reviews, 78, pp.1378-1389.

APPENDIX

Appendix A. Table of Recommended Average days of the Months

Months	n_d for i^{th} day of months	For an average day (mid-day) of each month		
		Date	Day of the year n_d	Declination angle δ
January	i	17	17	-20.917
February	$31 + i$	16	47	-12.955
March	$59 + i$	16	75	-2.418
April	$90 + i$	15	105	9.415
May	$120 + i$	15	135	18.792
June	$151 + i$	11	162	23.086
July	$181 + i$	17	198	21.184
August	$212 + i$	16	228	13.455
September	$243 + i$	15	258	2.217
October	$273 + i$	15	288	-9.599
November	$304 + i$	14	318	-18.912
December	$334 + i$	10	344	-23.050

Appendix B. The actual average duration of sunshine hours (n) of chole village

Year	2010	2011	2012	2013	2014	2015	2016	2017	2018	2019	Ave.
Jan	7.66	9.59	9.84	9.17	9.65	9.80	6.90	10.10	9.30	10.20	9.20
Feb	5.23	9.53	9.85	9.85	8.77	10.20	9.10	7.90	8.56	9.60	8.86
Mar.	6.57	8.59	9.05	8.40	7.67	8.50	8.50	9.10	6.30	9.30	8.19
April	7.13	6.38	6.53	8.20	8.30	7.90	5.70	8.30	6.20	7.60	7.22
May	6.90	6.50	8.48	7.98	8.56	8.10	8.30	7.80	6.80	7.20	7.66
June	7.83	6.82	6.50	7.27	7.93	6.80	7.20	8.10	5.30	6.70	7.04
July	5.29	9.82	6.70	5.80	6.21	8.30	6.90	4.70	4.90	6.80	6.54
Aug.	7.67	8.30	6.45	6.02	7.10	8.70	7.20	6.10	6.90	5.50	6.99
Sept.	7.06	7.23	6.90	7.49	6.38	7.80	6.90	6.60	7.90	6.57	7.08
Oct.	6.77	10.10	7.65	6.70	7.54	6.40	7.60	6.90	6.35	7.40	7.35
Nov.	8.10	9.84	8.47	7.23	7.50	7.80	8.70	8.40	7.20	6.30	7.95
Dec.	8.90	9.85	8.99	8.60	9.37	8.20	9.40	9.97	8.20	8.30	8.97

Appendix C. Not electrified site of study population and number of community service

Study of site population and facility data of not electrified community from the Woreda administration office.

No	Kebele	Village	Number of Public and Public service		Quantity	specification
1	Chole	Magna Laga Buna	House holds	High income	150	
				Middle income	234	
				Low income	356	
			School	Primary	2	Gado Bille and Manya Lega Buna
				Secondary	1	Manya Lega Buna Villag
			Clinic and health post		2	Chole clinic Post.
			Mosque		4	Bilal, Abubaker
			Church		2	Mariam / Mikael
			Agricultural office and FTC		2	Manya Lega Buna FTC
			Flour mill		2	Dawud Abeba flour
			Water pump		1	
			Razor House		10	
2		Magna Oda Adi	House holds	High income	120	
				Middle Income	225	
				Low income	265	
			School	Primary	1	
				Secondary	-	
			Healthy extension		1	
			Mosque		5	
			Church		-	
			Agriculture office and FTC		2	
			Flour mill		2	
	Chole	Magna Derartu	House hold	High Income	123	
				Middle income	243	
				Low income	290	
			School	Primary	1	
				Secondary	2	
			Clinic		1	
			Mosque		5	
			Church		2	
			Agricultural office		2	
			Flour mill		1	
4		Magna Werqi	House holds	High income	96	
				Middle Income	178	
				Low income	246	
			School	Primary	1	
				Secondary	-	
			Clinic		1	
			Mosque		2	
			Church		-	
			Agricultural office		-	
			Flour mill			
5	Chole	Magna Adare	House holds	High income	167	
				Middle Income	235	
				Low income	296	
			School	Primary	1	
				Secondary	-	
			Clinic		1	
			Mosque		2	
			Church		1	
			Agricultural office		2	
			Flour mill		1	

Appendix D. Table of Solar Panel specification (Alibaba Super market.com)

Module Type	DHM72-345	DHM72-350	DHM72-355	DHM72-360	DHM72-365
Maximum Power(Pmax)	345W	350W	355W	360W	365W
Open-circuit Voltage (Voc)	46.7V	46.9V	47.02V	47.23V	47.42V
Maximum Power Voltage	38.41V	38.5V	38.73V	38.93V	39.14V
Short-circuit Current (Isc)	9.50A	9.60A	9.69A	9.76A	9.82A
Maximum Power Current	8.99A	9.09A	9.17A	9.26A	9.34A
Module Efficiency (%)	17.80%	18.06%	18.31%	18.57%	18.83%
Power Tolerance	0~+5W				
Standard Test Environment	Irradiance 1000 W/m^2, Ambient temperature 25°C.				

Appendix E. Hourly Global radiation on the tilted surface of PV array in kWh/$\mathbf{m^2}$/day

Hour	Jan	Feb	Mar	April	May	June	July	Aug	Sep	Oct	Nov	Dec
1	0.000	0.000	0.000	0.000	0.000	0.000	0.000	0.000	0.000	0.000	0.000	0.000
2	0.000	0.000	0.000	0.000	0.000	0.000	0.000	0.000	0.000	0.000	0.000	0.000
3	0.000	0.000	0.000	0.000	0.000	0.000	0.000	0.000	0.000	0.000	0.000	0.000
4	0.000	0.000	0.000	0.000	0.000	0.000	0.000	0.000	0.000	0.000	0.000	0.000
5	0.000	0.000	0.000	0.000	0.000	0.000	0.000	0.000	0.000	0.000	0.000	0.000
6	0.000	0.000	0.000	0.000	0.000	0.000	0.000	0.000	0.000	0.000	0.000	0.000
7	0.000	0.000	0.000	0.007	0.013	0.017	0.016	0.010	0.002	0.000	0.000	0.000
8	0.249	0.244	0.135	0.116	0.116	0.171	0.197	0.197	0.121	0.121	0.244	0.241
9	0.593	0.526	0.439	0.382	0.382	0.403	0.344	0.360	0.380	0.400	0.553	0.487
10	1.010	0.930	0.677	0.682	0.768	0.629	0.544	0.605	0.738	0.838	0.937	0.830
11	1.242	1.163	1.022	0.969	1.129	0.855	0.782	0.808	0.930	1.093	1.219	1.052
12	1.483	1.362	1.268	1.199	1.361	1.010	0.929	0.988	1.159	1.294	1.430	1.277
13	1.558	1.463	1.403	1.351	1.460	1.098	1.016	1.052	1.320	1.420	1.494	1.387
14	1.538	1.441	1.455	1.354	1.494	1.071	0.985	1.059	1.308	1.406	1.514	1.374
15	1.368	1.280	1.372	1.231	1.414	0.987	0.885	0.937	1.093	1.193	1.328	1.183
16	1.077	0.963	0.999	0.869	1.139	0.858	0.716	0.773	0.839	0.939	1.077	0.877
17	0.767	0.651	0.586	0.568	0.649	0.634	0.456	0.563	0.527	0.527	0.629	0.505
18	0.273	0.289	0.162	0.187	0.243	0.173	0.184	0.190	0.207	0.207	0.274	0.188
19	0.000	0.000	0.000	0.007	0.013	0.017	0.016	0.010	0.002	0.000	0.000	0.000
20	0.000	0.000	0.000	0.000	0.000	0.000	0.000	0.000	0.000	0.000	0.000	0.000
21	0.000	0.000	0.000	0.000	0.000	0.000	0.000	0.000	0.000	0.000	0.000	0.000
22	0.000	0.000	0.000	0.000	0.000	0.000	0.000	0.000	0.000	0.000	0.000	0.000
23	0.000	0.000	0.000	0.000	0.000	0.000	0.000	0.000	0.000	0.000	0.000	0.000
24	0.000	0.000	0.000	0.000	0.000	0.000	0.000	0.000	0.000	0.000	0.000	0.000

Appendix F. Hourly usable energy from solar energy kWh/day

Hour	Jan	Feb	Mar	April	May	June	July	Aug	Sep	Oct	Nov	Dec
1	0.000	0.000	0.000	0.000	0.000	0.000	0.000	0.000	0.000	0.000	0.000	0.000
2	0.000	0.000	0.000	0.000	0.000	0.000	0.000	0.000	0.000	0.000	0.000	0.000
3	0.000	0.000	0.000	0.000	0.000	0.000	0.000	0.000	0.000	0.000	0.000	0.000
4	0.000	0.000	0.000	0.000	0.000	0.000	0.000	0.000	0.000	0.000	0.000	0.000
5	0.000	0.000	0.000	0.000	0.000	0.000	0.000	0.000	0.000	0.000	0.000	0.000
6	0.000	0.000	0.000	0.000	0.000	0.000	0.000	0.000	0.000	0.000	0.000	0.000
7	0.000	0.000	0.000	3.123	4.345	1.468	3.794	2.976	1.477	0.000	0.000	0.000
8	38.019	37.186	20.591	17.702	17.702	26.061	30.042	30.098	18.459	18.459	37.186	36.820
9	90.519	80.303	67.076	58.369	58.369	61.528	52.506	54.938	58.013	61.078	84.404	74.285
10	154.156	141.919	103.379	104.050	117.268	95.954	83.047	92.419	112.730	127.996	143.106	126.653
11	189.625	177.533	156.009	147.861	172.307	130.473	119.406	123.292	141.960	166.858	186.153	160.570
12	226.434	207.868	193.516	183.000	207.737	154.128	141.818	150.806	176.990	197.486	218.248	195.010
13	237.826	223.391	214.225	206.287	222.861	167.584	155.113	160.608	201.496	216.762	228.062	211.720
14	234.823	220.047	222.101	206.716	228.088	163.504	150.363	161.657	199.622	214.664	231.138	209.778
15	208.821	195.449	209.447	187.984	215.827	150.640	135.162	142.997	166.835	182.101	202.739	180.569
16	164.369	147.035	152.510	132.697	173.807	130.945	109.322	117.968	128.139	143.405	164.369	133.837
17	117.144	99.432	89.399	86.756	99.060	96.842	69.615	86.003	80.498	80.498	96.087	77.125
18	41.696	44.094	24.784	28.585	37.145	26.477	28.154	29.076	31.564	31.564	41.872	28.668
19	0.000	0.000	0.000	3.257	3.577	4.377	2.897	2.900	2.679	0.000	0.000	0.000
20	0.000	0.000	0.000	0.000	0.000	0.000	0.000	0.000	0.000	0.000	0.000	0.000
21	0.000	0.000	0.000	0.000	0.000	0.000	0.000	0.000	0.000	0.000	0.000	0.000
22	0.000	0.000	0.000	0.000	0.000	0.000	0.000	0.000	0.000	0.000	0.000	0.000
23	0.000	0.000	0.000	0.000	0.000	0.000	0.000	0.000	0.000	0.000	0.000	0.000
24	0.000	0.000	0.000	0.000	0.000	0.000	0.000	0.000	0.000	0.000	0.000	0.000

Appendix G. Hourly wind speed at 50m of tower height in m/s**.**

Hour	Jan	Feb	Mar	Apr	May	Jun	July	Aug	Sep	Oct	Nov	Dec
0:00	5.708	6.936	5.600	5.384	5.101	5.560	7.179	5.857	5.249	5.249	5.236	5.857
1:00	7.247	6.302	5.371	5.857	5.384	7.206	6.005	6.909	5.857	5.546	5.857	5.546
2:00	5.560	5.735	6.842	6.774	5.452	6.896	7.179	6.005	6.005	6.005	7.058	5.384
3:00	3.873	5.249	5.506	6.127	6.599	6.572	5.587	7.206	7.206	7.166	5.857	5.708
4:00	5.223	5.465	4.966	5.236	7.058	5.371	5.074	7.476	5.330	5.708	5.371	5.830
5:00	5.560	6.127	6.572	4.021	5.722	5.870	5.708	5.384	5.857	6.154	5.560	5.708
6:00	4.075	4.804	4.804	5.708	4.872	5.371	4.953	4.359	4.953	5.384	5.209	5.371
7:00	3.752	4.021	4.359	4.804	4.021	4.953	4.804	4.021	3.455	4.359	4.656	4.359
8:00	2.982	3.131	4.008	3.630	3.833	5.560	4.021	4.656	4.359	4.804	3.981	4.494
9:00	4.062	2.402	3.873	2.685	3.576	4.345	4.656	5.249	4.021	4.035	3.455	3.900
10:00	2.793	2.766	2.146	3.428	3.725	4.507	5.371	5.560	2.672	4.278	4.345	3.455
11:00	1.457	3.603	2.753	4.332	2.672	4.035	4.926	5.506	2.982	4.656	3.455	4.494
12:00	3.117	2.820	2.672	2.551	3.900	4.926	3.994	4.953	4.480	4.035	4.359	2.672
13:00	3.576	2.645	3.455	3.131	2.820	3.752	4.035	4.021	4.656	4.804	4.656	4.332
14:00	2.551	2.766	4.021	4.062	2.672	3.873	5.195	4.197	4.008	4.035	3.967	4.008
15:00	3.725	3.455	4.062	4.021	4.210	4.359	3.752	5.101	4.237	4.210	4.359	4.939
16:00	2.874	2.672	2.537	2.524	2.551	4.035	5.870	4.008	4.480	4.359	4.953	4.507
17:00	2.753	3.158	3.914	3.873	2.820	5.223	5.371	4.656	4.804	3.900	3.617	5.101
18:00	3.698	3.320	2.402	4.170	4.656	4.359	6.451	5.155	3.833	4.480	4.197	3.846
19:00	4.656	3.900	3.455	4.156	4.345	5.236	7.503	5.857	4.494	4.953	4.359	4.656
20:00	4.804	4.413	4.075	3.900	4.008	4.507	5.897	7.206	4.953	5.209	5.708	5.236
21:00	5.830	5.249	4.035	4.197	4.399	5.560	5.384	6.909	5.371	5.074	7.058	5.695
22:00	5.223	5.452	4.129	5.411	5.870	5.384	5.897	5.438	5.857	5.857	5.708	5.384
23:00	5.749	5.384	5.749	5.115	5.884	7.058	5.519	6.154	5.978	5.695	5.452	5.506

Appendix H. Daily Power Out Put and corresponding Wind Speed of the Site

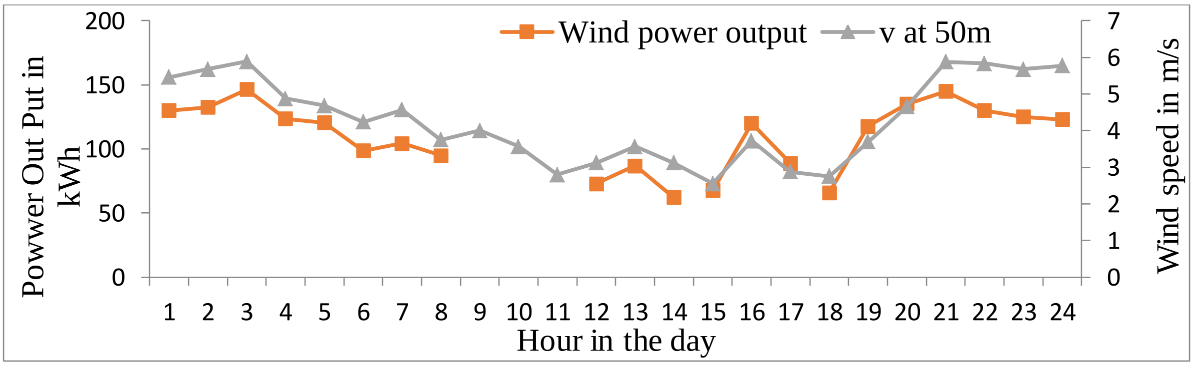

January 17, Daily Power out put and corresponding wind speed

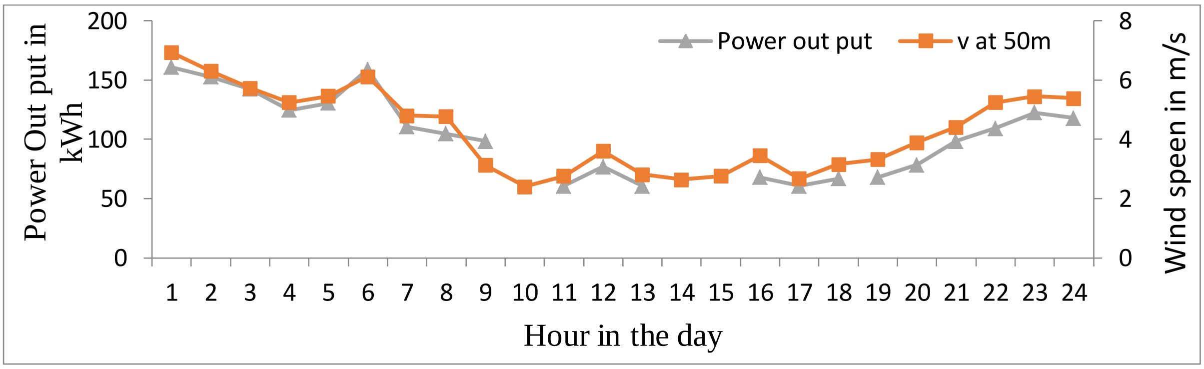

Febraury 16, Daily Power out put and corresponding wind speed

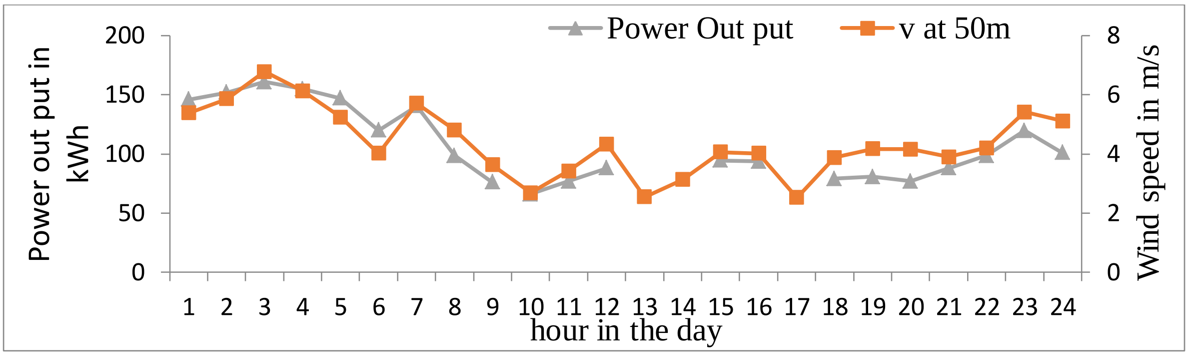

April 15, Daily Power out put and corresponding wind speed

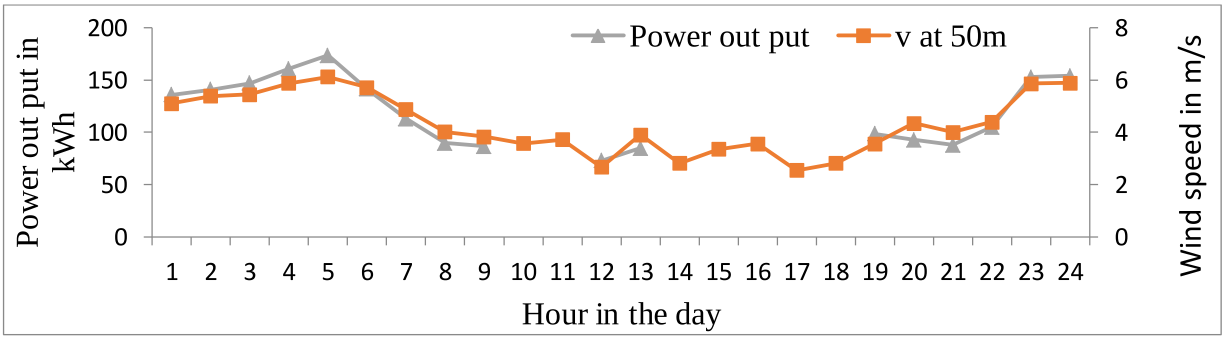

May 15, Daily Power out put and corresponding wind speed

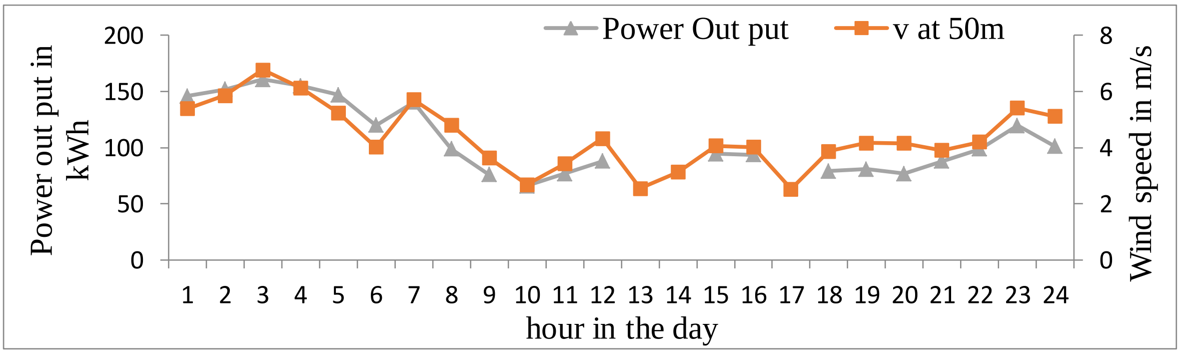

June 11, Daily Power out put and corresponding wind speed

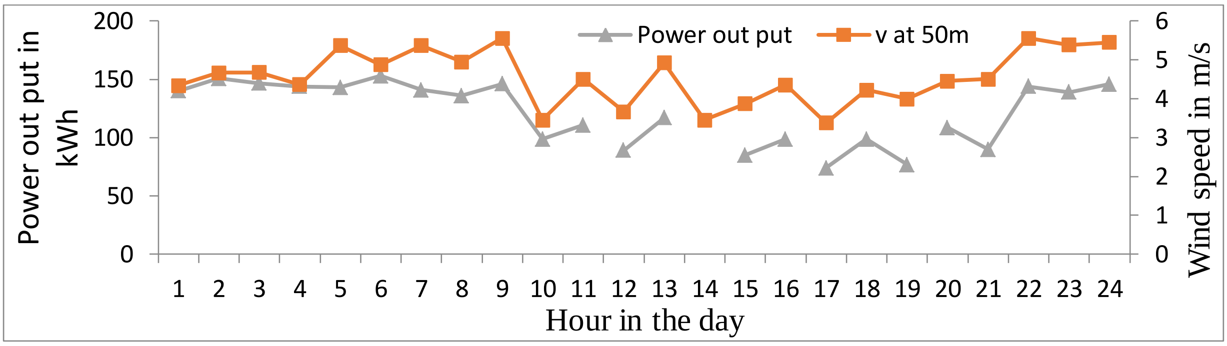

August 16, Daily Power out put and corresponding wind speed

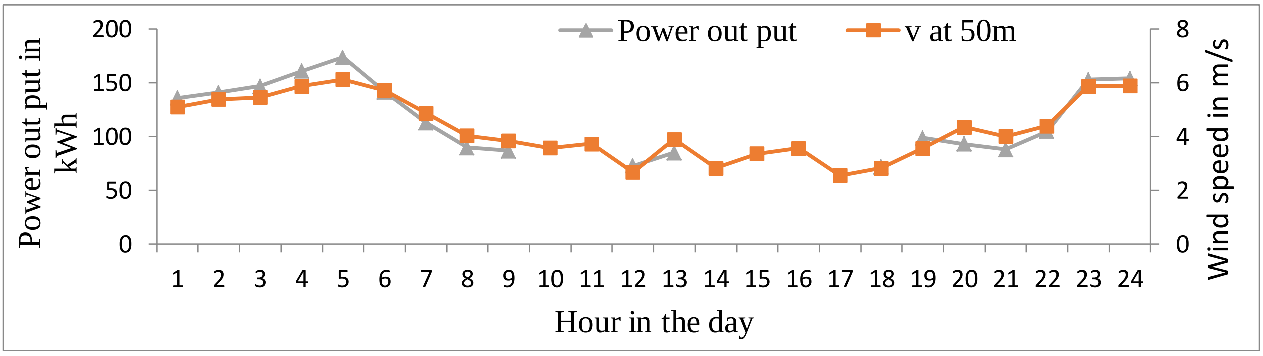

September 15, Daily Power out put and corresponding wind speed

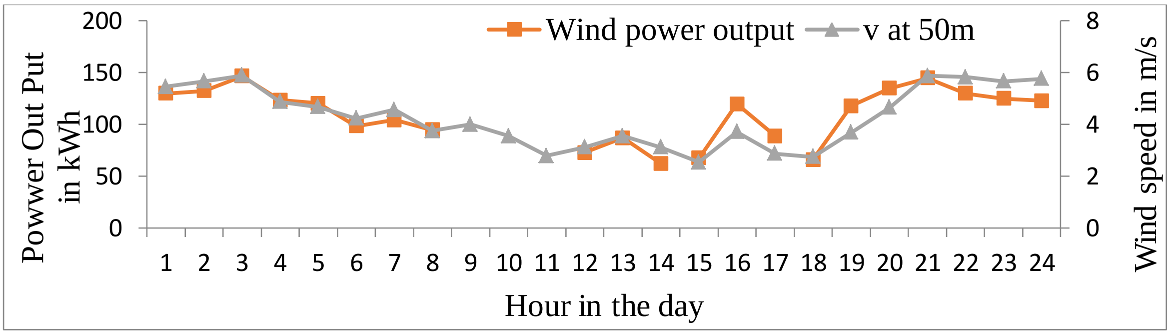

October 15, Daily Power out put and corresponding wind speed

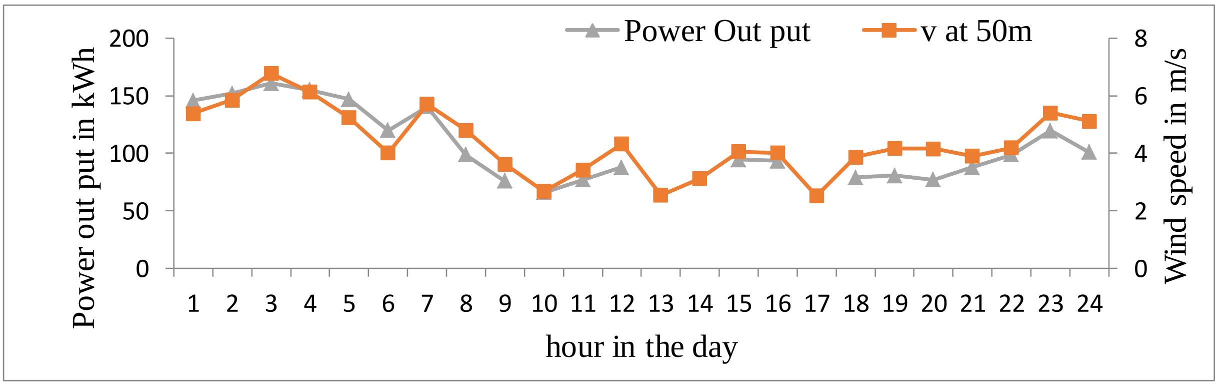

November 14, Daily Power out put and corresponding wind speed

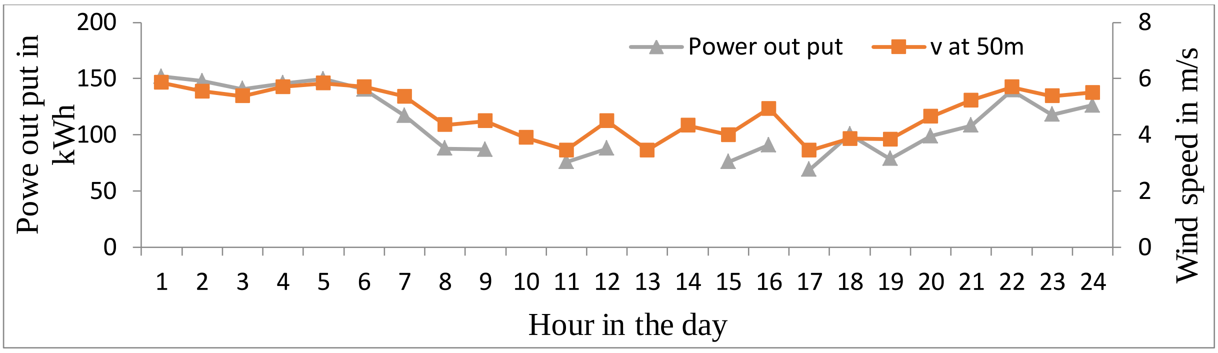

December 10, Daily Power out put and corresponding wind speed

Appendix I. Hourly usable energy from Wind energy in kWh/day

Hour	Jan	Feb	Mar	Apr	May	Jun	July	Aug	Sep	Oct	Nov	Dec
0:00	140.5445	252.1635	132.7202	117.9537	100.2913235	129.8627	279.5908	151.7949	109.3042	109.3042	108.4634	151.7949
1:00	287.5515	189.1226	117.069	151.7966	117.9523641	282.7591	163.6319	249.2286	151.7949	128.918	151.7949	128.918
2:00	129.8627	142.5475	242.0007	234.9113	122.4424633	247.7739	279.5908	163.6319	163.6319	163.6319	265.6397	117.9524
3:00	43.89737	109.3054	126.1169	173.7642	217.1273542	214.4765	131.7616	282.7559	282.7559	278.0171	151.7949	140.5429
4:00	107.6281	123.3553	92.54144	108.4646	265.6397296	117.069	98.70781	315.731	114.4404	140.5429	117.0677	149.706
5:00	129.8627	173.7642	214.4765	49.14073	141.5420667	152.8483	140.5429	117.9524	151.7949	176.0688	129.8613	140.5429
6:00	51.14623	83.78047	83.78047	140.5445	87.35938513	117.069	91.78805	62.57423	91.78805	117.9524	106.7947	117.0677
7:00	39.8958	49.14073	62.57493	83.78047	49.14018138	91.78907	83.77954	49.14018	31.15357	62.57423	76.25095	62.57423
8:00	20.04332	23.18765	48.64768	36.14512	42.53466171	129.8627	49.14018	76.25095	62.57423	83.77954	47.67097	68.56787
9:00	50.63983	10.47256	43.89737	14.63363	34.55616864	61.99553	76.25095	109.3042	49.14018	49.63654	31.15357	44.82099
10:00	16.47039	15.99758	7.464215	30.42944	39.04048544	69.18823	117.0677	129.8613	14.41397	59.1515	61.99484	31.15357
11:00	2.339182	35.34489	15.76461	61.41973	14.41396734	49.6371	90.29559	126.1155	20.04309	76.25095	31.15357	68.56787
12:00	22.8891	16.95242	14.41413	12.53655	44.82099477	90.2966	48.15741	91.78805	67.952	49.63654	62.57423	14.41397
13:00	34.55655	13.98173	31.15392	23.18765	16.95222942	39.8958	49.63654	49.14018	76.25095	83.77954	76.25095	61.41905
14:00	12.53655	15.99758	49.14073	50.63983	14.41396734	43.89737	105.9669	55.85591	48.64714	49.63654	47.18782	48.64714
15:00	39.04092	31.15392	50.63983	49.14073	56.39644711	62.57493	39.89536	100.2913	57.48796	56.39645	62.57423	91.03978
16:00	17.94451	14.41413	12.33861	12.14277	12.53641543	49.6371	152.8466	48.64714	67.952	62.57423	91.78805	69.18746
17:00	15.76461	23.79252	45.28838	43.89737	16.95222942	107.6281	117.0677	76.25095	83.77954	44.82099	35.74311	100.2913
18:00	38.19834	27.64382	10.47256	54.78583	76.25094812	62.57493	202.8017	103.509	42.53466	67.952	55.85591	42.98556
19:00	76.2518	44.82149	31.15392	54.25565	61.99484493	108.4646	319.1629	151.7949	68.56787	91.78805	62.57423	76.25095
20:00	83.78047	64.9286	51.14623	44.82149	48.64713978	69.18823	154.9645	282.7559	91.78805	106.7947	140.5429	108.4634
21:00	149.7077	109.3054	49.6371	55.85653	64.33403087	129.8627	117.9524	249.2286	117.0677	98.70781	265.6397	139.5485
22:00	107.6281	122.4438	53.20557	119.7363	152.8465829	117.9537	154.9645	121.5355	151.7949	151.7949	140.5429	117.9524
23:00	143.5561	117.9537	143.5561	101.0905	153.9031223	265.6427	127.0451	176.0688	161.4355	139.5485	122.4425	126.1155

Appendix J. HOMER optimization results

Export...

Optimization Results
Left Double Click on a particular system to see its detailed Simulation Results.

Categorized Ove

Architecture						Cost				System		SPR-X21		
SPR-X21 (kW)	E-48	Iron4900	Natel49 (kW)	Dyn500 (kW)	Dispatch	COE ($)	NPC ($)	Operating cost ($/yr)	Initial capital ($)	Ren Frac (%)	Total Fuel (L/yr)	Capital Cost ($)	Production (kWh/yr)	Capital Cost ($)
	10	9	49.0	196	CC	$0.0247	$224,751	$3,897	$174,371	100	0			2,339
	10	9	49.0	197	LF	$0.0247	$224,900	$3,900	$174,481	100	0			2,339
	10	9	49.0	197	CC	$0.0247	$224,900	$3,900	$174,481	100	0			2,339
	10	9	49.0	197	LF	$0.0247	$225,133	$3,905	$174,654	100	0			2,339
	10	9	49.0	197	CC	$0.0247	$225,133	$3,905	$174,654	100	0			2,339
0.260	10	9	49.0	196	LF	$0.0247	$225,203	$3,900	$174,791	100	0	521	504	2,339
0.260	10	9	49.0	196	CC	$0.0247	$225,203	$3,900	$174,791	100	0	521	504	2,339
	10	9	49.0	197	LF	$0.0247	$225,325	$3,909	$174,796	100	0			2,339
	10	9	49.0	197	CC	$0.0247	$225,325	$3,909	$174,796	100	0			2,339
0.0960	10	9	49.0	197	LF	$0.0248	$225,342	$3,906	$174,841	100	0	192	186	2,339
0.0960	10	9	49.0	197	CC	$0.0248	$225,342	$3,906	$174,841	100	0	192	186	2,339
	10	9	49.0	197	LF	$0.0248	$225,382	$3,910	$174,839	100	0			2,339
	10	9	49.0	197	CC	$0.0248	$225,382	$3,910	$174,839	100	0			2,339